



TALLINN UNIVERSITY OF TECHNOLOGY  
SCHOOL OF ENGINEERING  
Department of Electrical Power Engineering and Mechatronics

# **METHODOLOGY OF CROSS-SECTION SELECTION OF UPPER LIMB EXOSKELETON FOR INDUSTRY APPLICATIONS**

## **VÄLISSKELETI ÜLAJÄSEME TÖÖSTUSES KASUTAMISEKS RISTLÕIGE VAILMISE MEETODIKA**

MASTER THESIS

Student: ....Mohamed Abdelmomen.....  
/name/

Student code: 184581MAHM

Supervisor: Fjodor Sergejev, Professor  
/name, position/

Tallinn 2020

(On the reverse side of title page)

## **AUTHOR'S DECLARATION**

Hereby I declare, that I have written this thesis independently.  
No academic degree has been applied for based on this material. All works, major viewpoints and data of the other authors used in this thesis have been referenced.

"15" May 2020

Author: Mohamed Abdelmomen

*/signature /*

Thesis is in accordance with terms and requirements

"....." ..... 20....

Supervisor: .....

*/signature/*

Accepted for defence

"....." .....20... .

Chairman of theses defence commission: .....

*/name and signature/*

## **Non-exclusive Licence for Publication and Reproduction of Graduation Thesis**

I Mohamed Abdelmomen\_\_\_\_\_ (author's name) (date of birth: 23/06/1995)

1. grant Tallinn University of Technology free licence (non-exclusive licence) for my thesis

---

\_\_\_\_\_Methodology of Cross-section Selection of Upper Limb Exoskeleton for Industry Applications  
(*title of the graduation thesis*)

supervised by Professor Fjodor Sergejev  
(*supervisor's name*)

to be

- 1.1. reproduced for the purposes of preservation and electronic publication, incl. to be entered in the digital collection of TUT library until expiry of the term of copyright;
- 1.2. published via the web of Tallinn University of Technology, incl. to be entered in the digital collection of TUT library until expiry of the term of copyright.

2. I am aware that the author also retains the rights specified in clause 1.

3. I confirm that granting the non-exclusive licence does not infringe third persons' intellectual property rights, the rights arising from the Personal Data Protection Act or rights arising from other legislation.

Mohamed Abdelmomen (*signature*)

25/05/2020 (*date*)

**Department of Electrical Power Engineering and Mechatronics**

**THESIS TASK**

**Student:** Mohamed Abdelmomen, 184581 MAHM (name, student code)

Study programme, MAHM02/18 – Mechatronics (code and title)

main speciality:

Supervisor(s): Associate Prof. Fjodor Sergejev (position, name, phone)

Consultants: .....(name, position)

**Thesis topic:**

(in English) Methodology of cross-section selection of upper limb exoskeleton industry applications.

(in Estonian) Välisskeleti ülajäseme tööstuses kasutamiseks ristlõige vailmise meetodika

**Thesis main objectives:**

1. Define a methodology for cross-section selection of upper limb exoskeletons
2. Define best cross-sectional profile of the body components for the upper limb exoskeletons in mechanical behaviour aspect
3. Define best cross-sectional profile of the body components for upper body limb exoskeletons while maintaining cost and other non-mechanical aspects

**Thesis tasks and time schedule:**

No	Task description	Deadline
1.	Having formed the calculations and assumptions	Feb 2020
2.	Forming the correlation of dimensions and performance	Mar 2020
3.	Wrapping up the thesis	Apr 2020

**Language:** English **Deadline for submission of thesis:** "19" May 2020 a

**Student:** Mohamed Abdelmomen ..... "15" May 2020 a

/signature/

**Supervisor:** Fjodor Sergejev ..... ".....".....201....a

/signature/

**Consultant:** ..... ".....".....201....a

/signature/

**Head of study programme:** Mart Tamre ..... ".....".....201.a

/signature/

*Terms of thesis closed defence and/or restricted access conditions to be formulated on the reverse side*

# LIST OF CONTENTS

PREFACE .....	8
LIST OF FIGURES .....	9
LIST OF TABLES .....	16
LIST OF ABBREVIATIONS AND SYMBOLS .....	17
1 INTRODUCTION.....	18
2 LITERATURE REVIEW.....	20
2.1 History of exoskeletons.....	20
2.2 Exoskeleton types .....	21
2.3 Human augmentation .....	23
2.4 Application fields.....	23
2.5 Existing Solutions Analysis Including Industry and academic research.....	24
2.5.1 Introduction.....	24
2.5.2 Atoun (Model-A).....	24
2.5.3 Atoun (Model-Y).....	25
2.5.4 Innophys (Muscle Upper) .....	25
2.5.5 Exhauss (Worker).....	26
2.5.6 Ekso bionics – Ekso Vest .....	26
2.5.7 Analysis of recent research in the field .....	27
2.6 Conclusion of literature review, industry and academic research .....	31
3 METHODOLOGY .....	33
3.1 Introduction of methodology.....	33
3.2 Geometry.....	33
3.3 Manufacturing Process .....	38
3.4 Loads and Calculations .....	39
3.5 Kinematics of the draft model upper-body exoskeleton .....	42
3.6 Simulation setting .....	43
3.7 Results deriving .....	45
3.8 Selection criteria.....	47
3.9 Limitations .....	49
4 RESULTS .....	51
4.1 Shoulder Part Results .....	51
4.1.1 Tension Test .....	51
4.1.2 Bending test .....	52
4.2 Forearm Part Results .....	53
4.2.1 Tension Test .....	53
4.2.2 Bending test .....	54

4.3 Back Part Results .....	56
4.3.1 Compression test .....	56
4.3.2 Torsion test .....	57
4.3.3 Bending test .....	58
4.4 Back to Shoulder Connector Part Results.....	59
4.4.1 Bending test .....	59
5 DISCUSSION.....	61
5.1 General discussion .....	61
5.2 Discussion of the results .....	62
5.3 Methodology to be followed .....	64
5.4 Plans of the future.....	65
6 CONCLUSION .....	66
7 SUMMARY .....	68
8 KOKKUVÕTE.....	69
9 LIST OF REFERENCES.....	70
10 APPENDIX .....	75
10.1 Validation of tension test simulation .....	75
10.2 Test simulation for Shoulder part using different cross-section geometries .....	78
10.2.1 CISCOS cross-section geometry for shoulder part test simulations.....	78
10.2.2 RISROS cross-section geometry for shoulder part test simulations.....	79
10.2.3 EISEOS cross-section geometry for shoulder part test simulations .....	80
10.2.4 EISCOS cross-section geometry for shoulder part test simulations.....	81
10.2.5 CISEOS cross-section geometry for shoulder part test simulations.....	82
10.2.6 CISROS cross-section geometry for shoulder part test simulations.....	84
10.2.7 EISROS cross-section geometry for shoulder part test simulations.....	85
10.3 Test simulation for Forearm part using different cross-section geometries .....	86
10.3.1 CISCOS cross-section geometry for forearm part test simulations.....	86
10.3.2 RISROS cross-section geometry for forearm part test simulations.....	87
10.3.3 EISEOS cross-section geometry for forearm part test simulations .....	88
10.3.4 EISCOS cross-section geometry for forearm part test simulations.....	89
10.3.5 CISEOS cross-section geometry for forearm part test simulations.....	91
10.3.6 CISROS cross-section geometry for forearm part test simulations.....	92
10.3.7 EISROS cross-section geometry for forearm part test simulations.....	93
10.4 Test simulation for Back to shoulder connector part using different cross-section geometries .....	95
10.4.1 CISCOS cross-section geometry for Back to shoulder connector part test simulations .....	95

10.4.2 RISROS cross-section geometry for Back to shoulder connector part test simulations .....	96
10.4.3 EISEOS cross-section geometry for Back to shoulder connector part test simulations .....	97
10.4.4 EISCOS cross-section geometry for Back to shoulder connector part test simulations .....	98
10.4.5 CISEOS cross-section geometry for Back to shoulder connector part test simulations .....	99
10.4.6 CISROS cross-section geometry for Back to shoulder connector part test simulations .....	100
10.4.7 EISROS cross-section geometry for Back to shoulder connector part test simulations .....	101
10.5 Test simulation for Back part using different cross-section geometries .....	102
10.5.1 CISCOS cross-section geometry for Back part test simulations .....	102
10.5.2 RISROS cross-section geometry for Back part test simulations .....	103
10.5.3 EISEOS cross-section geometry for Back part test simulations .....	105
10.5.4 EISCOS cross-section geometry for Back part test simulations .....	106
10.5.5 CISEOS cross-section geometry for Back part test simulations .....	108
10.5.6 EISROS cross-section geometry for Back part test simulations .....	110
GRAPHICAL MATERIAL .....	112

## **PREFACE**

This master thesis is being done to be presented in Tallinn University of Technology. This presented master thesis topic is initiated by Department of Mechatronics in Tallinn University of Technology.

The major work of the presented thesis has been done in Tallinn University of Technology under the supervision of Associate Professor Fjodor Sergejev after agreement on the topic for the master thesis from Head of study programme Professor Mart Tamre.

I would like to express my gratitude to my supervisor Associate Professor Fjodor Sergejev for his amazing support and cooperation, the head of study programme Professor Mart Tamre for his cooperation and understanding. Moreover, I would like to thank my colleagues who helped me to gather a lot of information in this thesis by Eng. Fuat Ozan Dengiz, Eng. Hakan Demir, and Eng. Hoda Samir. Additionally, I would like to express my thankfulness for the teaching assistants who were always giving support and will to cooperate Eng. Even Sekhri and Eng. Dhanushka Chamara.

In the existing market of upper body exoskeletons, there is a lack of methodology that defines the best cross-section geometry of the parts that form the frame of the exoskeleton, and the existing exoskeletons in the market are using generic easy to form pipes to form the body.

In the presented thesis, a methodology has been formed for cross-section selection of the upper limb exoskeleton body while taking into consideration the profiles cross-section of the body components and manufacturing technology to be used. The ease of manufacturing is the first mesh of filtering the geometry of the shapes cross-section of the body components of the upper limb exoskeleton. Afterwards, the strength of the shape of the cross-section is the second filter of the profile of frame that forms the geometry of the upper limb exoskeleton. After the aforementioned filters of geometries, the best cross-section to be selected according to many parameters that will be considered while having the exoskeleton in the market.

Keywords: Cross-section, Static Solid Mechanics, Upper-limb, Exoskeleton, Master Thesis.

## LIST OF FIGURES

Figure 2.1 GE Hardiman Exoskeleton.....	20
Figure 2.2 Exhauss upper body exoskeletons in work .....	21
Figure 2.3 Lower body exoskeleton HAL of Cyberdyne .....	22
Figure 2.4 Full body exoskeleton Guardian XO of Sarcos Robotics .....	23
Figure 2.5 Atoun (Model-A).....	25
Figure 2.6 Atoun (Model-Y).....	25
Figure 2.7 Innophys (Muscle Upper).....	26
Figure 2.8 Exhauss (Worker).....	26
Figure 2.9 Exo bionics – Ekso Vest.....	27
Figure 3.1 Draft model of the exoskeleton using standard pipes .....	34
Figure 3.2 Cross-section for pipe with circular outer and circular inner shape .....	34
Figure 3.3 Schematic for extrusion.....	38
Figure 3.4 Scheme of loading kinematically to the exoskeleton in exploded view .....	42
Figure 3.5 Normal standard meshed unloaded pipe for back part .....	45
Figure 3.6 Stress-strain of tensile test for the standard pipe with yield line .....	47
Figure 4.1 Tension test stress-strain curves for all possible shapes for shoulder part .....	51
Figure 4.2 A zoom into the results shown in figure 4.1 .....	51
Figure 4.3 Force-Angle curves for bending test done for all shapes for shoulder part .....	52
Figure 4.4 Tension test stress-strain curves for all possible shapes for forearm part .....	53
Figure 4.5 A zoom into the results shown in figure 4.4 .....	53
Figure 4.6 Force-Angle curves for bending test done for all shapes for forearm part .....	54
Figure 4.7 A zoom into the results shown in figure 4.6 .....	55
Figure 4.8 Stress-strain curves for compression test simulation done for all shapes for back part.....	56
Figure 4.9 Force-angle curves for torsion test simulation done for all shapes for back part .....	57
Figure 4.10 Force-angle curves for bending test simulation done for all shapes for back part .....	58
Figure 4.11 Force-angle curves for bending test simulation done for all shapes for back to sholder connector part.....	59
Figure 4.12 A zoom into the results shown in figure 4.11 .....	59
Figure 5.1 Generic upper-body exoskeleton with the best selected cross-section geomtries for the pipes of the frame .....	64
Figure 5.2 block diagram of the methdology of cross-section selection .....	64

Figure 8.1: Tensile test stress-strain curve with yield line for validation of RISROS for shoulder part .....	75
Figure 8.2: Tensile test stress-strain curve with yield line for validation of EISEOS for shoulder part .....	75
Figure 8.3: Tensile test stress-strain curve with yield line for validation of EISCOS for shoulder part .....	76
Figure 8.4: Tensile test stress-strain curve with yield line for validation of CISEOS for shoulder part .....	76
Figure 8.5: Tensile test stress-strain curve with yield line for validation of CISROS for shoulder part .....	77
Figure 8.6: Tensile test stress-strain curve with yield line for validation of EISROS for shoulder part .....	77
Figure 8.7 Shoulder part with CISCOS cross-section geometry meshed at rest .....	78
Figure 8.8 Shoulder part with CISCOS cross-section geometry meshed and subjected to tension .....	78
Figure 8.9 Shoulder part with CISCOS cross-section geometry meshed and subjected to bending .....	78
Figure 8.10 Shoulder part with RISROS cross-section geometry meshed at rest .....	79
Figure 8.11 Shoulder part with RISROS cross-section geometry meshed and subjected to tension .....	79
Figure 8.12 Shoulder part with RISROS cross-section geometry meshed and subjected to bending about X-axis .....	79
Figure 8.13 Shoulder part with RISROS cross-section geometry meshed and subjected to bending about Y-axis.....	80
Figure 8.14 Shoulder part with EISEOS cross-section geometry meshed at rest.....	80
Figure 8.15 Shoulder part with EISEOS cross-section geometry meshed and subjected to tension .....	80
Figure 8.16 Shoulder part with EISEOS cross-section geometry meshed and subjected to bending about X-axis .....	80
Figure 8.17 Shoulder part with EISEOS cross-section geometry meshed and subjected to bending about Y-axis.....	81
Figure 8.18 Shoulder part with EISCOS cross-section geometry meshed at rest.....	81
Figure 8.19 Shoulder part with EISCOS cross-section geometry meshed and subjected to tension .....	81
Figure 8.20 Shoulder part with EISCOS cross-section geometry meshed and subjected to bending about X-axis .....	82
Figure 8.21 Shoulder part with EISCOS cross-section geometry meshed and subjected to bending about Y-axis.....	82

Figure 8.22 Shoulder part with CISEOS cross-section geometry meshed at rest.....	82
Figure 8.23 Shoulder part with CISEOS cross-section geometry meshed and subjected to tension .....	83
Figure 8.24 Shoulder part with CISEOS cross-section geometry meshed and subjected to bending about X-axis .....	83
Figure 8.25 Shoulder part with CISEOS cross-section geometry meshed and subjected to bending about Y-axis.....	83
Figure 8.26 Shoulder part with CISROS cross-section geometry meshed at rest .....	84
Figure 8.27 Shoulder part with CISROS cross-section geometry meshed and subjected to tension .....	84
Figure 8.28 Shoulder part with EISROS cross-section geometry meshed at rest.....	85
Figure 8.29 Shoulder part with EISROS cross-section geometry meshed and subjected to tension .....	85
Figure 8.30 Shoulder part with EISROS cross-section geometry meshed and subjected to bending about Y-axis.....	85
Figure 8.31 Forearm part with CISCOS cross-section geometry meshed at rest .....	86
Figure 8.32 Forearm part with CISCOS cross-section geometry meshed and subjected to tension .....	86
Figure 8.33 Forearm part with CISCOS cross-section geometry meshed and subjected to bending .....	86
Figure 8.34 Forearm part with RISROS cross-section geometry meshed at rest .....	87
Figure 8.35 Forearm part with RISROS cross-section geometry meshed and subjected to tension .....	87
Figure 8.36 Forearm part with RISROS cross-section geometry meshed and subjected to bending about X-axis .....	87
Figure 8.37 Forearm part with RISROS cross-section geometry meshed and subjected to bending about Y-axis.....	88
Figure 8.38 Forearm part with EISEOS cross-section geometry meshed at rest .....	88
Figure 8.39 Forearm part with EISEOS cross-section geometry meshed and subjected to tension .....	88
Figure 8.40 Forearm part with EISEOS cross-section geometry meshed and subjected to bending about X-axis .....	89
Figure 8.41 Forearm part with EISEOS cross-section geometry meshed and subjected to bending about Y-axis.....	89
Figure 8.42 Forearm part with EISCOS cross-section geometry meshed at rest .....	89
Figure 8.43 Forearm part with EISCOS cross-section geometry meshed and subjected to tension .....	90

Figure 8.44 Forearm part with EISCOS cross-section geometry meshed and subjected to bending about X-axis .....	90
Figure 8.45 Forearm part with EISCOS cross-section geometry meshed and subjected to bending about Y-axis.....	90
Figure 8.46 Forearm part with CISEOS cross-section geometry meshed at rest .....	91
Figure 8.47 Forearm part with CISEOS cross-section geometry meshed and subjected to tension .....	91
Figure 8.48 Forearm part with CISEOS cross-section geometry meshed and subjected to bending about X-axis .....	91
Figure 8.49 Forearm part with CISEOS cross-section geometry meshed and subjected to bending about Y-axis.....	92
Figure 8.50 Forearm part with CISROS cross-section geometry meshed at rest .....	92
Figure 8.51 Forearm part with CISROS cross-section geometry meshed and subjected to tension .....	92
Figure 8.52 Forearm part with CISROS cross-section geometry meshed and subjected to bending about X-axis .....	93
Figure 8.53 Forearm part with CISROS cross-section geometry meshed and subjected to bending about Y-axis.....	93
Figure 8.54 Forearm part with EISROS cross-section geometry meshed at rest .....	93
Figure 8.55 Forearm part with EISROS cross-section geometry meshed and subjected to tension .....	94
Figure 8.56 Forearm part with EISROS cross-section geometry meshed and subjected to bending about X-axis .....	94
Figure 8.57 Forearm part with EISROS cross-section geometry meshed and subjected to bending about Y-axis.....	94
Figure 8.58 Back to shoulder connector part with CISCOS cross-section geometry meshed at rest.....	95
Figure 8.59 Back to shoulder part with CISCOS cross-section geometry meshed and subjected to bending.....	95
Figure 8.60 Back to shoulder connector part with RISROS cross-section geometry meshed at rest.....	96
Figure 8.61 Back to shoulder part with RISROS cross-section geometry meshed and subjected to bending about X-axis .....	96
Figure 8.62 Back to shoulder part with RISROS cross-section geometry meshed and subjected to bending about Y-axis .....	96
Figure 8.63 Back to shoulder connector part with EISEOS cross-section geometry meshed at rest.....	97

Figure 8.64 Back to shoulder part with EISEOS cross-section geometry meshed and subjected to bending about X-axis .....	97
Figure 8.65 Back to shoulder part with EISEOS cross-section geometry meshed and subjected to bending about Y-axis .....	97
Figure 8.66 Back to shoulder connector part with EISCOS cross-section geometry meshed at rest.....	98
Figure 8.67 Back to shoulder part with EISCOS cross-section geometry meshed and subjected to bending about X-axis .....	98
Figure 8.68 Back to shoulder part with EISCOS cross-section geometry meshed and subjected to bending about Y-axis .....	98
Figure 8.69 Back to shoulder connector part with EISCOS cross-section geometry meshed at rest.....	99
Figure 8.70 Back to shoulder part with EISCOS cross-section geometry meshed and subjected to bending about X-axis .....	99
Figure 8.71 Back to shoulder part with EISCOS cross-section geometry meshed and subjected to bending about Y-axis .....	99
Figure 8.72 Back to shoulder connector part with EISCOS cross-section geometry meshed at rest.....	100
Figure 8.73 Back to shoulder part with EISCOS cross-section geometry meshed and subjected to bending about X-axis .....	100
Figure 8.74 Back to shoulder part with EISCOS cross-section geometry meshed and subjected to bending about Y-axis .....	100
Figure 8.75 Back to shoulder connector part with EISROS cross-section geometry meshed at rest.....	101
Figure 8.76 Back to shoulder part with EISROS cross-section geometry meshed and subjected to bending about X-axis .....	101
Figure 8.77 Back to shoulder part with EISROS cross-section geometry meshed and subjected to bending about Y-axis .....	101
Figure 8.78 Back part with CISCOS cross-section geometry meshed at rest .....	102
Figure 8.79 Back part with CISCOS cross-section geometry meshed and subjected to compression .....	102
Figure 8.80 Back part with CISCOS cross-section geometry meshed and subjected to torsion .....	102
Figure 8.81 Back part with CISCOS cross-section geometry meshed and subjected to bending.....	103
Figure 8.82 Back part with RISROS cross-section geometry meshed at rest .....	103
Figure 8.83 Back part with RISROS cross-section geometry meshed and subjected to compression .....	103

Figure 8.84 Back part with RISROS cross-section geometry meshed and subjected to torsion .....	104
Figure 8.85 Back part with RISROS cross-section geometry meshed and subjected to bending about X-axis .....	104
Figure 8.86 Back part with RISROS cross-section geometry meshed and subjected to bending about Y-axis .....	104
Figure 8.87 Back part with EISEOS cross-section geometry meshed at rest.....	105
Figure 8.88 Back part with EISEOS cross-section geometry meshed and subjected to compression .....	105
Figure 8.89 Back part with EISEOS cross-section geometry meshed and subjected to torsion .....	105
Figure 8.90 Back part with EISEOS cross-section geometry meshed and subjected to bending about X-axis .....	106
Figure 8.91 Back part with EISEOS cross-section geometry meshed and subjected to bending about Y-axis .....	106
Figure 8.92 Back part with EISCOS cross-section geometry meshed at rest .....	106
Figure 8.93 Back part with EISCOS cross-section geometry meshed and subjected to compression .....	107
Figure 8.94 Back part with EISCOS cross-section geometry meshed and subjected to torsion .....	107
Figure 8.95 Back part with EISCOS cross-section geometry meshed and subjected to bending about X-axis .....	107
Figure 8.96 Back part with EISCOS cross-section geometry meshed and subjected to bending about Y-axis .....	108
Figure 8.97 Back part with CISEOS cross-section geometry meshed at rest .....	108
Figure 8.98 Back part with CISEOS cross-section geometry meshed and subjected to compression .....	108
Figure 8.99 Back part with CISEOS cross-section geometry meshed and subjected to torsion .....	109
Figure 8.100 Back part with CISEOS cross-section geometry meshed and subjected to bending about X-axis .....	109
Figure 8.101 Back part with CISEOS cross-section geometry meshed and subjected to bending about Y-axis .....	109
Figure 8.102 Back part with EISROS cross-section geometry meshed at rest.....	110
Figure 8.103 Back part with EISROS cross-section geometry meshed and subjected to compression .....	110
Figure 8.104 Back part with EISROS cross-section geometry meshed and subjected to torsion .....	110

Figure 8.105 Back part with EISROS cross-section geometry meshed and subjected to bending about X-axis .....	111
Figure 8.106 Back part with EISROS cross-section geometry meshed and subjected to bending about Y-axis .....	111

## **LIST OF TABLES**

Table 3.1 Areas of the shapes for all the parts except the back part.....	36
Table 3.2 Areas of the shapes for the back part.....	37
Table 3.3 Length and Bending Moments to be applied on each part.....	40
Table 3.4 Time ratio and Amplitude of Loading .....	44
Table 3.5 Metrics of exoskeleton design ranking .....	48

## LIST OF ABBREVIATIONS AND SYMBOLS

A	Surface Area
CISCOS	Circular Inner Shape and Circular Outer Shape
CISEOS	Circular Inner Shape and Elliptical Outer Shape
CISROS	Circular Inner Shape and Rectangular Outer Shape
DARPA	Defense Advanced Research Projects Agency
DOF	Degrees of Freedom
EISEOS	Elliptical Inner Shape and Elliptical Outer Shape
EISCOS	Elliptical Inner Shape and Circular Outer Shape
EISROS	Elliptical Inner Shape and Rectangular Outer Shape
EMG	Electromyography
F	Force
FEA	Finite Elements Analysis
g	Acceleration due to gravity
ID	Inner Diameter
L	Length
M	Mass
Mo	Moment
OD	Outer Diameter
PPA	peak particle acceleration
RISROS	Rectangular Inner Shape and Rectangular Outer Shape
TMo	Torsion moment
TPsm	Torsion Polar section modulus
TS	Torsion Stress

# 1 INTRODUCTION

The known definition for an exoskeleton in general is an artificial external supporting structure [1]. In other words, exoskeletons are wearable machines. Those wearable machines can be operated by using different kinds of power sources such as: electro-mechanical, pneumatic, or hydraulic. Exoskeletons are systems that are considered as human-robotic systems [2]. The optimum target of exoskeleton development is to augment human, or to provide physical improvement [2]. An exoskeleton would assist in the lifting process to improve weightlifting ability or maybe giving the ability of faster moving while carrying a load [3].

From the study of many already existing upper body exoskeletons in the market, it has been concluded that the best frame to have for the exoskeleton would be made out of tubes. That is considering the fact of having ease of manufacturing as priority as well as cost of manufacturing of the frame.

The main target of the presented thesis is to form a methodology that would ease the definition of the best cross-section of the tubes being used as body frame structure for the body of the exoskeleton being manufactured while considering the parameters that would matter while designing and exoskeleton.

The tubes of the body frame that will form the exoskeletons can have many shapes, but to assure the easiness of the manufacturing, it is easier to have symmetric cross-section to avoid the rotation of the part during extrusion process. The symmetric cross-section can be in many shapes. In the thesis, there is a comparison between the different shapes of cross-sections to choose which shapes would be the best in the parameters that are considered while designing an exoskeleton.

As the shapes of cross-section are symmetrical, some of them would have the same shape if subjected to equal compression forces on x-axis against each other in direction but equal in magnitude to the shape if subjected to same forces but on y-axis. However, some other shapes would give different shapes. Therefore, the study is covering some cross-sections being one time subjected to forces on x-axis and y-axis for the aim of comparison of which orientation would the tube be in the frame of the exoskeleton to assure the best durability using the same amount of material. Another aspect of comparison is to fix the area of different shapes being tested as well as the material and forces on the cross-sections.

Methodology of selection of best cross-section for the tubes of the frame is formed.

The software program that has been used for simulation of the cross-sections being subjected to forces is Abaqus. The mathematics has been done on MATLAB.

There is an extensive research about the already existing upper-body exoskeletons have been done to study the exoskeletons that are in the market as well as the exoskeletons that are developed in research labs.

The thesis is focusing on upper-body exoskeletons being used in industry for lifting solutions that would augment the users to lift weights for longer time. So, in short, the exoskeleton would enhance the endurance of the worker who is using the exoskeleton as some examples that are explaining in the industry applications chapter.

## 2 LITERATURE REVIEW

### 2.1 History of exoskeletons

The oldest known exoskeleton by definition was a set of assisted apparatus that are jumping and running, those have been developed in Russia [4]. In USA there were some similar inventions, but they cannot be considered as exoskeletons to the aforementioned definition. General Electric was the first company to develop a real exoskeleton device in the 1960s [5]. It was electrical and hydraulic bodysuit. However, the bodysuit was bulky and heavy [6]. Figure 2.1 has demonstration of the implementation and design of that exoskeleton.

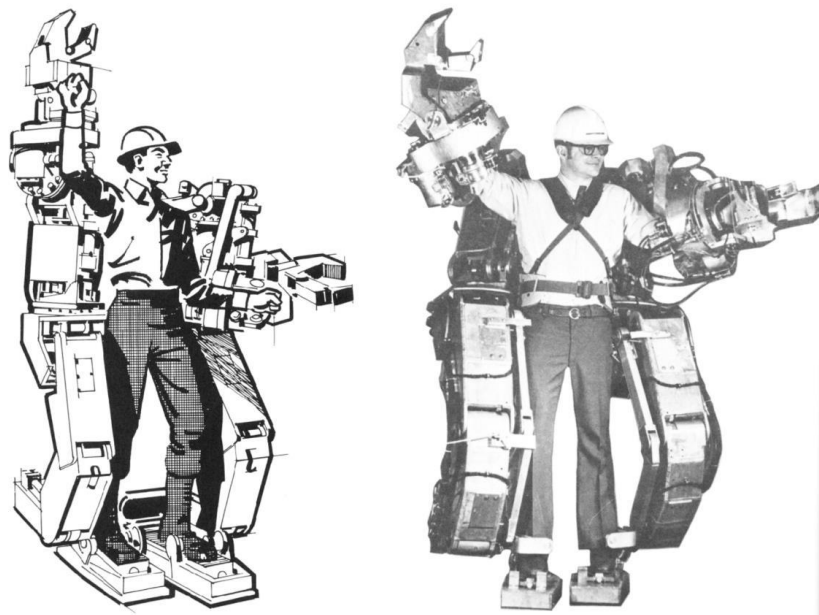


Figure 2.1 GE Hardiman Exoskeleton [6]

Initially between 1969-1972 in Serbia the major projects related to this field were done for medical assistance for disabled people. It is possible to find these works in museums that now are in Russian Federation. Moreover, US army is working on a military oriented exoskeleton that is known by the name of LIFESUIT since 1986. Currently, this project had 17 prototypes and the planned future works extends until 2025 [7]. Nanotechnology started to be implemented by Pentagon to exoskeleton projects starting from 2007. Nowadays, Exoskeletons for Human Performance Augmentation Program of an organization known by the name of DARPA (Defense Advanced Research Projects Agency) is doing mega developments [6].

## 2.2 Exoskeleton types

There are many types of exoskeletons for different applications and purposes. The exoskeletons can be divided in accordance to the power consumption as powered (dynamic or static), passive (weight redistribution, dampening, locking, or energy capture), pseudo-passive, and hybrid-exoskeletons. The exoskeletons can be also differentiated by categories in accordance to their mobility, as they can be fixed, mobile, or supported. There is another way to differentiate the exoskeletons, which is the controlling method, as they can be controlled by joystick, sensors, mind-controlled, not-controlled, control panels, or not-controlled. It is possible as well to distinguish them according to the mechanical properties of the material used for building it, as the material can be rigid or flexible material. Exoskeletons could be from different forms of origin as they can be home built, commercial, research labs, or governments [8]. The most known way to distinguish the exoskeleton and to categorize them is connection to the body parts. Accordingly, it can be three main types, which are full body, lower-body, and upper-body exoskeletons.

One famous example of upper-body exoskeleton companies is ExhauSS, which is a French company that manufacture upper-body exoskeletons for mid-level lifting. ExhauSS is the first company in the world to make industrial exoskeletons to be in the market to be sold. The products can lift up to 25 kg [9]. Figure 2.2 demonstrate examples of exoskeletons from ExhauSS company on work. Another known company for upper-body exoskeletons is known as EksoVest. It is completely mechanical energy dependent as there is no cord, battery, or electricity. It has springs which would store the mechanical energy to make the assistance required. The springs start to work in gradual manner once the person would raise their arms to chest-height or beyond. That exoskeleton can support up to 6,8 kg per arm [10].



Figure 2.2 ExhauSS upper body exoskeletons in work [10]

There is another type of exoskeletons which the lower-body exoskeleton is. As an example, LegX is an exoskeleton which allows worker to squat frequently for longer time because it reduces the force induced on knee joint and quadricep. LegX exoskeleton make the weight go directly to the ground. LegX exoskeleton acts as a chair basically, but it is activated in squatting position. As a result, the user of the exoskeleton will not feel the exoskeleton while standing or walking [11]. There is a second example for lower-body exoskeleton is Hybrid Assistive Limb (HAL) by Cyberdyne. This exoskeleton is used by people who are suffering from disabilities in the lower part of their bodies. In such cases, neural pathways cannot be used by the brain and cannot give the normal order to move the legs. However, HAL makes the person who is wearing it to be able to move according to the will of the person. When a person has a will to make a move, their brain sends various signals from the brain through nerves to muscles. These signals can be detected from the surface of the skin as bio-electric signals. HAL is able to read the signals from the surface of the skin then compensates the power of the muscle of the lower limbs and help the user in performing the normal moves such as standing up, walking, and sitting down [12]. Figure 2.3 demonstrate and show HAL.



Figure 2.3 Lower body exoskeleton HAL of Cyberdyne [12]

The most common form of exoskeletons is the full-body exoskeleton. A proper known example is known as Sacros Robotics' Guardian XO. This exoskeleton assists the user for lifting up to 90 kg. It has contact to ground, so the mass load is directed to the ground, not loaded to the human body. This exoskeleton uses an algorithm known by the name of get-out-of-the-way. There are sensors used in the suit that are responsible for recognizing the moves of the user, which makes the suit mimic the force, direction, and speed of the moves. Accordingly, the exoskeleton has 20 to 1 strength amplification up to the limit of 90 kg, after the limit of 90 kg the assist starts to be reduced [13]. The exoskeleton Guardian XO is shown in figure 2.4 below.



Figure 2.4 Full body exoskeleton Guardian XO of Sarcos Robotics [13]

## 2.3 Human augmentation

Human augmentation as a field is focused on creating physical and cognitive improvements as an integration to the human body [14]. Humans will be able to use more speed, power, and to be more productive when they are supported by any form of human augmentation technologies. The augmentation does not only work to make up for disabilities but also helps healthy human to reach higher physical abilities [15]. Human augmentation does not focus only on exoskeletons. There are various ideas in the market and some still on research level like 3<sup>rd</sup> thumb, which is simply an additional finger to the hand that has functionality which is dynamic and has some purposes to use that 3<sup>rd</sup> thumb [16]. Adding an example, Duoskin tattoo is basically a sticker like device that can be put on skin and able to control electronics devices [17]. Another example is known as airbag helmet which basically acts as the airbags known in cars, but it is for the head protection in helmet that is worn by cyclists [18]. There is another more specific example which is known by the name of Enchroma glasses that are created for people who are suffering from colour blindness as it helps them see their unseen colours through filtering out wavelengths of light [19].

## 2.4 Application fields

Exoskeletons are generally multipurpose devices. It can serve in fields of military, medical field, aerospace, industry, consumer, etc. applications [19].

There are exoskeletons that are commercially available in the market that support manual labour tasks in industry [20]. Exoskeletons in industry are generally used as lifting and moving solution. The exoskeletons are used in a proper way to support workers who lift heavy objects along their day, employees who need to stand up for long period of time, or for supporting a body part while working if that body part need support.

In medical field, the exoskeletons would be helpful for patients who need physiotherapy due to muscle injury. It can help to control to make minimal stress and effort on the muscle and make a gradual controlled progress for muscle rehabilitation. Additionally, the exoskeletons can assist in the process of coalescing of broken bones by applying least stress possible on the bones and apply controlled gradual stress on the bones for healing purposes. However, clinical application is not supported by evidence due to the prohibitive cost [21].

## **2.5 Existing Solutions Analysis Including Industry and academic research**

### **2.5.1 Introduction**

There are many existing solutions and examples of robotic arms and mobile manipulators of industrial companies such as Fetch Robotics, Mobile Automation, Omron, KUKA, and Opiflex.

Many models from companies that made successful exoskeletons were analyzed for the presented thesis such as Nakamura Lab, Atoun Model-Y, Atoun Model-A, ExoVest, Exhaus, SuitX, and Innophys. Some models have been studied in details and a comparison has been made as well as the analysis.

### **2.5.2 Atoun (Model-A)**

This exoskeleton shown down in figure 2.5 has pipe cylindrical main frame of the body that has plastic covers. There would be ease of manufacturing for the structure due to being just pipe structure. The model is as light as 6,7 kg. However, its maximum assist weight is 15 kg [22].

This model as seen in figure 2.5 supports the body through pushing the legs and well as pulling the back from the shoulder point with a motor at the waist level. The model has no arm support. Therefore, the best usage of this exoskeleton would be lifting from ground level to table level and vice versa.

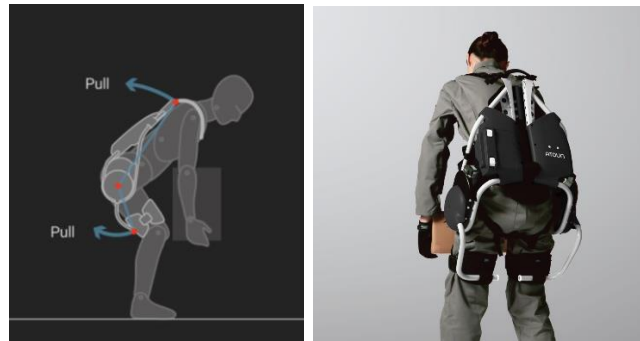


Figure 2.5 Atoun (Model-A) [22]

### 2.5.3 Atoun (Model-Y)

Model-Y is 40% lighter than Model-A, so it is 4,5 kg. On the other hand, its maximum assist ability. The general geometrical shape of the body frame is cylindrical pipe while using many straps as shown in figure 2.6. The ease of manufacturing of this model would be somewhat debatable, but it doesn't have a very complex shape at the end [23]. In this model as seen in figure 2.6, it supports the legs through thigh straps and the back through shoulder straps with the actuator at the waist level and no arm support, which makes it exact to the main features of the Atoun Model-A except for few details. Therefore, it will have the same usage as Model-A which is moving objects from ground to table level and vice versa.



Figure 2.6 Atoun (Model-Y) [23]

### 2.5.4 Innophys (Muscle Upper)

Innophys model as shown in figure 2.7 has strong main support for arm, unlike Atoun models. However, it is not a mobile exoskeleton as Atoun models were. On the other hand, it has very high assist capabilities up to 35 kg. Its frame is formed from mainly also cylindrical pipes geometry. It has heavy body of 8,1kg [24].

This model as shown in figure 2.7 supports arm and back with leg supports this time. Moreover, it has no joint for the elbow movement. It works with compressed air.

Therefore, the best usage of this exoskeleton would be moving items within limited area from table level or shoulder level of vice versa.



Figure 2.7 Innophys (Muscle Upper) [24]

### 2.5.5 Exhauss (Worker)

This exoskeleton is able to assist up to 30 kg in total, it is mobile, somehow heavy mass of 8 kg. The frame has simple components, so manufacturing it would be relatively easy. The exoskeleton has arm and back support without legs supports but has degree of freedom for elbow [9].

The model as shown in figure 2.8 the frame has cylindrical pipes and metal sheets, which shows the ease of manufacturing of this exoskeleton. Moreover, as it has supports for arm and back, it would also be concluded that this robot is best used for lifting objects from table level to shoulder level and vice versa.



Figure 2.8 Exhauss (Worker) [9]

### 2.5.6 Ekso bionics – Ekso Vest

The presented exoskeleton in figure 2.9 is very lightweight exoskeleton, but it is a passive exoskeleton. Passive exoskeleton means that it has no actuator for the support, but just a mechanism that gives some support due to its physical design. It has very light weight body of 4,3 kg, but it supports 6,8 kg per arm. There is ease in

manufacturing the parts of the frame as well as they are cylindrical pipes along with sheets [10].

This exoskeleton does not support the legs but supports the arms and back while being attached to the waist. Due to being passive exoskeleton, its best usage would be about keeping the arm in some position for long time, so workers can do some work conditions that require them to keep their arm in same position for so long.



Figure 2.9 Exo bionics – Ekso Vest [10]

## **2.5.7 Analysis of recent research in the field**

### **2.5.7.1 Recent research for Exoskeleton**

There has been some research around the same general area, either from the aspect of tubes being subjected to mechanical loads, or exoskeleton design.

In reference [25] the mechanical behaviour of casing-infill composite tubes was studied for lightweight structures while taking into consideration the structural stiffness and capacity of the composite. The torsion and bending of the tubes were studied as well by using suitable computational models that are based on finite elements methods. In the study, the analytical approach for the axial behaviour was studied on empty tube with circular cross section as well as the composite tubes, in order to compare the results and verify. The result showed development in structural stiffness due to filling a relatively rigid casing that is tubular by a moderate soft one. This assures the significance of forming more auxetic materials without compromising about the stiffness.

In reference [26] a whole-arm exoskeleton was designed, but for rehabilitation method. It is a 6-DOF (Degrees of freedom) robot which helps in training of the shoulder for rehabilitation purposes. FEA analysis was done to secure that the structure will not fail. The forward kinematics has been done to calculate and simulate the motion of the robot. The simulation was done to assure that the components will be safe for usage after applying maximum expected stress. This exoskeleton has joint movement for the whole arm including fingers, that would help the user to train the shoulder through the joint movement of the whole upper body and would be possible to do the normal daily activities.

To cover also shoulder focused exoskeletons in reference [27] a serial-joint exoskeleton shoulder is designed. It is a 3 DOF powered exoskeleton that can be fixed on anybody without any misalignment due to taking into consideration variability of positioning. The robot is 3 DOF to act just like a normal shoulder ball joint in the human with same axes. The whole designed prototype mass was 4 kg. Force sensor was used for control purposes, but at the end the designed mechanism satisfied the purpose with a problem in torque transmission.

The joint torque estimation along the movements beside safety issues were considered for a single degree of freedom exoskeleton for elbow [28]. Using test-rig mechanism the robot performance was evaluated in kinematical parameters aspect. A proposed one degree of freedom for elbow design was proposed while recording kinematic parameters of elbow with various signals. The design of this exoskeleton can be used publicly, but signals showed that that exoskeleton decreased the muscle activity of the user.

Another 3 DOF exoskeleton was designed for the arm with different DOFs. This was also designed for the purpose of rehabilitation. So, the focus was mainly on human and robot interaction. The length of the links changing relative to the patient was taken care of. The main target is to measure the force between robot and human body through strain gauge sensors. There are 2 DOFs for the shoulder and one for the elbow. The design of this robot has been done and tested, and it is concluded that caring about the motor selection and sensors is critical for the upper limb exoskeletons. However, the structure failure was not one of the considerations while implementing this robot [29].

Another wearable upper limb exoskeleton has been designed while considering anatomic structure of the upper body. A 6 DOFs exoskeleton has been designed. The 6 DOFs are divided into two groups with three DOFs focus on elbow joint, which means basically a joint at the shoulder, one at the elbow, and one at the hand level. Kinematic calculations were done, but structure analysis was not considered. The main focus was on control of the exoskeleton and the kinematics [30].

An exoskeleton was designed using mechanisms that are not serial. The target of this designed exoskeleton is to make the exoskeleton as compact as possible as well as taking care of the aspect of being easy to wear. The shoulder exoskeleton has two spherical mechanisms along with two slider crank mechanisms. The actuators positioning can be changed to achieve better inertia. The design took care of dimensions very much as well as kinematics and statics, but not the stress analysis of the structure. The result was a lightweight exoskeleton due to ability to change the position of the actuators according to the user [31].

There is an upper body exoskeleton that had the design and modelling of it done. The exoskeleton was designed while taking into considerations many factors with aim of designing an exoskeleton for rehabilitation. Kinematics has been taken care of as well

as mechanical design and even stress analysis. Stress analysis was done by applying maximum expected load on the end of the arm of the exoskeleton while using a factor of safety to add which is 1,75 without mentioning why that factor of safety was used. The exoskeleton was meant to be built to make similar motions of every other exoskeleton while including scapulothoracic motion which is contrary to other designs to include that profile of motion [32].

There is a passive balancing mechanism for upper limbs that would compensate the torques on each joint through a passive method. The designed design has decoupling mechanism to isolate the torsional effect between links and a torsional compliant beam that can give specific torsional stiffness function that would make up the mass of the weight of the arm. The result of the manipulator arm is a reduced torque that would be required through the joint for compensation of gravity using two passive ways. A prototype has been built with easy and experiments are performed to show, verify, and assure the effectiveness of the introduced method. The focus is about rehabilitation, it is a passive exoskeleton, the focus of analysis is the torque required, and no stress analysis has been done [33].

There is an active upper body exoskeleton that has been developed. It has pneumatic air muscle, and this gave more degrees of freedom for the exoskeletons other than the exoskeletons that use rigid source of motion as actuator. Stress analysis has been done in many aspects such as structural analysis, heat transfer, fluid flow, mass transport, and electromagnetic potential studies. All the aforementioned studies have been done using ANSYS. For the structural analysis, axial loading of elastic bar has been done, without taking into consideration the plasticity parameters. The designed exoskeleton frame was done by basic tubes and sheets. It has been designed to lift masses up to 35 kg without feeling it [34].

The fatigue of the muscles during the lifting phase has been studied through using EMG signals from local view. There have been various signals to use for comparison, but at the end the fatigue caused to muscles due to lifting has been documented [35].

### **2.5.7.2 Recent research in piping and structure**

Regarding piping and frame structure, there has been done some stress analyses for circular shaped pipes being subjected to pressure and pipe bending. The analyses have been done considering moderately thick walled and thin walled pipes. The profile cross-sectional of the pipe is basically circular inner and outer profile of the pipe. The stress that was applied to the pipe is not axial stress perpendicular to the cross-section, but inner pressure and pipe bending [36].

The frame of the exoskeleton can be formed using pipes. However, pipes shape may differ. One of the shapes that the pipe can be is rectangular. The behaviour of pipes was

considered in order to improve the quality of the product, specifically pipes with rectangular cross-sections under toll-bending. In order to reduce the shrinking load, double stage forming method has been used and showed significant result of reduction of axial wrinkles. Throughout the process it has been noticed that the behaviour of the pipe change when the cross-section of the pipe changes its shape due to external factors of forces [37].

The stress intensity factor which is an important parameter of the singular stress field near the tip of the crack and fracture mechanics has been calculated through new mathematical methods with examples to assure feasibility of the proposed calculations. The example given was oval shape that has flat sides. After using 3 types of cracks to be studied on the structure and calculating the stress intensity factor, the simulation assured the correctness of the theories used for calculations. Therefore, the coverage here is for oval shape with flat sides that has cracks with oval similar shape inside the tube itself that is subjected to the loads [38].

In some other study, a normal steel circular hollow pipe has been subjected to external load while having a dent, then its general behaviour has been studied. More than one type of dent has been applied to study the failure mechanism of the pipe. Moreover, the effect of the diameter-thickness ratio has been studied. The result demonstrated that plastic deformation took place and continued to increase along the unloading process and was concentrated much on the place where the dent is. The depth ratio of the dent after the process of loading and unloading is directly proportional with the diameter-thickness ratio, and inversely proportional with the displacement of the indenter. Moreover, the sides of the dents were more subjected to plastic deformation than the dent itself [39].

The effect of the profile cross-section on dynamic response of tunnels when the tunnels are subjected to train induced vibrations has been studied. The study might seem a bit drifted from the general focus of the presented thesis due to the scale difference, but it has a focus of the effect of changing the cross-section. The shapes that has been studied are the circular, rectangular, and horseshoe shapes. The study showed that cross-sectional shape has important effect on the dynamic behaviour of the tunnel. The rectangular profile had larger response than that of circular and horseshoe profiles. The peak particle acceleration (PPA) of the rectangular profile was 178% of the circular cross-section and 133% of the horseshoe profile. To summarize, the cross-sections showed different behaviour in different situations, which clearly proves that cross-section of the pipe would affect its behaviour [40].

An analytical solution for the axisymmetric elasticity problem for an inhomogeneous solid cylinder that has been subjected to external force loads that would vary in magnitude along the axial coordinate. The geometry that has been used was circular

pipe. The loads that has been subjected to the pipe are radial, circumferential, axial, and shearing stresses with a step profile of loading but with a gradual increase [41].

In medical applications, some tubes known as Chitosan tubes. It is a natural polymer widely studied tube that is considered usually as suitable as biomaterial for the construction of channels of nerve guidance for the injuries of peripheral nerves. There are five different kind of cross-sections that have been taken into consideration in the study. The cross-sections are all circular on the outside, three of them have also circular inner shape, but there are different thicknesses. Two of the five shapes had 4 extra edges or 8 extra edges on the inside surface of the cross section, so the inner profile is not circular. The result showed that the load is distributed along a larger cross-section area, depending on the cross-section that is being subjected to the load, the distribution differs in result [42].

The reliability of metals with corrosion defects have been assessed under axial tension loading using the analysis of damage tolerance. A tube of circular cross-section that is made of cast-iron has been used for simulation. The result showed that the parameter of corrosion has no important effect on the probability of failure. The result of that analysis would be useful for assessing the reliability of structures that are corroded [43]. An analysis for stress applied on a model for embedded bar-wrapped cylinder concrete pressure pipe that is subjected to internal load. The pipe was having a circular outer and inner cross-section. A uniform internal pressure was assumed with uniform distribution. Elasticity has been taken into consideration. The whole study and experiment approve the correlation of thickness and deformation that deformation increase by decreasing the thickness of the cross-section [44].

## **2.6 Conclusion of literature review, industry and academic research**

Exoskeleton has a generally defined definition since the early beginning of exoskeleton development. The exoskeleton development started for human augmentation purposes. The human augmentation applications are very wide, and exoskeletons are one side of the human augmentation. There are various application fields that exoskeletons are being used for, such as military, medicine, industry, aerospace, and other applications. The exoskeletons can be generally divided among 3 general types of exoskeleton which are full-body, upper-body, and lower-body exoskeleton.

There are various types of exoskeletons, but the main types would be full-body, lower-body, and upper-body exoskeletons. There are exoskeletons that are mobile and some others that are not mobile, the focus in the presented thesis is about mobile exoskeletons. The exoskeletons can be passive or active exoskeletons, in the presented

thesis the focus is about the active exoskeletons. The active exoskeletons have wide range of ability of lifting or assisting the user, the presented thesis focus on exoskeletons that are able to provide assistance up to 20 kg. The exoskeletons in the market comes in many shapes and sizes, the difference in shapes and sizes would be a factor about the ability of the exoskeleton of giving assistance for the user. The exoskeletons that exist already in the market with the same focus generally have simple-made items that are manufactured to form the exoskeleton body frame, most probably it is a complex shape of many pipe-shaped complex structure.

The pipe that form the exoskeleton structure in the market is usually a simple circular shaped cross-section pipe. However, in the presented thesis, the other forms of pipes are simulated and discussed such as circular, rectangular, elliptical, and the mix of their shapes between outer and inner profile of the pipe being formed.

After extensive research about what has been done in the field of exoskeletons for stress analysis for the body and for the pipes' shapes, there is a gap of research to have stress analysis for all the aforementioned shapes of pipes cross-section as well as stress analysis for the exoskeleton body having pipe shaped structure of different cross-sections.

Moreover, the methodology of cross-section selection for the exoskeleton is a research gap to be filled, as the target of this thesis is to find a methodology for cross-section selection for exoskeletons, then that is another research gap to be filled through the presented thesis.

There are various groups of research in many countries around the world working on the exoskeleton development. In Denmark there is University of Aalborg working on simulation of mechanical systems with human body, which is very useful for exoskeleton simulation. In China there are various groups that work on exoskeleton topic as well such as National Research Center for Rehabilitation Technical Aids. There is also research in Iran in University of Tehran about exoskeletons as there are numerous scientific contributions about exoskeletons from them. Moreover, there is IEEE International Conference on Rehabilitation Robotics, which has many studies about exoskeletons in general.

For pipes structure analysis, there is a whole conference known as ASME Pressure Vessels and Piping, and that has the strongest impact in the field of pipes FEM analysis in mechanical and structural static aspect. In Sweden there is Lulea university of Technology with division of steel structures that works on that. In China there is a lab known as State Key Laboratory for Strength and Vibration of Mechanical Structures, which has a major focus on structure mechanical analysis as well as pipes. There is also a very well reputable journal focusing on pipes mechanical analyses known as International Journal of Pressure Vessels and Piping.

## **3 METHODOLOGY**

### **3.1 Introduction of methodology**

In the presented thesis, the methodology followed to get the conclusion of the best cross-section geometry for each part of the exoskeleton is through many steps. Some quantitative data have been collected after comprehensive literature review about existing exoskeletons in industry and research. After collection of the data, the data were analysed to come up with a conclusion of using pipes for a generic model modelling in the simulation. A generic model of upper limb exoskeleton is created using pipes and developed after passing through the process of cross-section selection. The presented research is dependent on descriptive research supported by simulation and validated from open source information. After validation of the results of the simulation, the data derived from the simulation is analysed and compared to other simulations, to decide upon the best mechanically behaving cross-section by descriptive analysis of the data after replying on selection prioritization list. The simulations that were done are FEA (Finite Elements Analysis) for the parts of the upper-limb exoskeleton. Moreover, calculation and definition of the loads magnitude and vector that will be used in the simulation of the testing of each part of the exoskeleton have been done.

### **3.2 Geometry**

The exoskeleton is analysed as 4 main parts which are: the forearm, shoulder, back to shoulder connector, and back. In the presented thesis, each part is studied separately with FEA as the analysis is optimally used as simulation for standard tests that are done to specimen such as tension test, bending test, torsion test, and compression test, those tests will give more focused results on the solid part as structure more than the entire structure as a body. Since the aim for the thesis is to find a way to evaluate the best cross-section to be used for exoskeleton frame, so many cross-sections have been considered to be studied. The process started by searching for a regular standard pipe that is having cross-section geometry of hollow round shape as shown in figure 3.2. that is extruded, then use different geometrical shapes that can be extruded.

Extrusion process include pushing through a die that has the required cross-section. There are several ways to do the extrusion process including the direct and indirect extrusion. Both ways can be used to manufacture seamless pipes, but that is explained further in the subsection of manufacturing process [45].

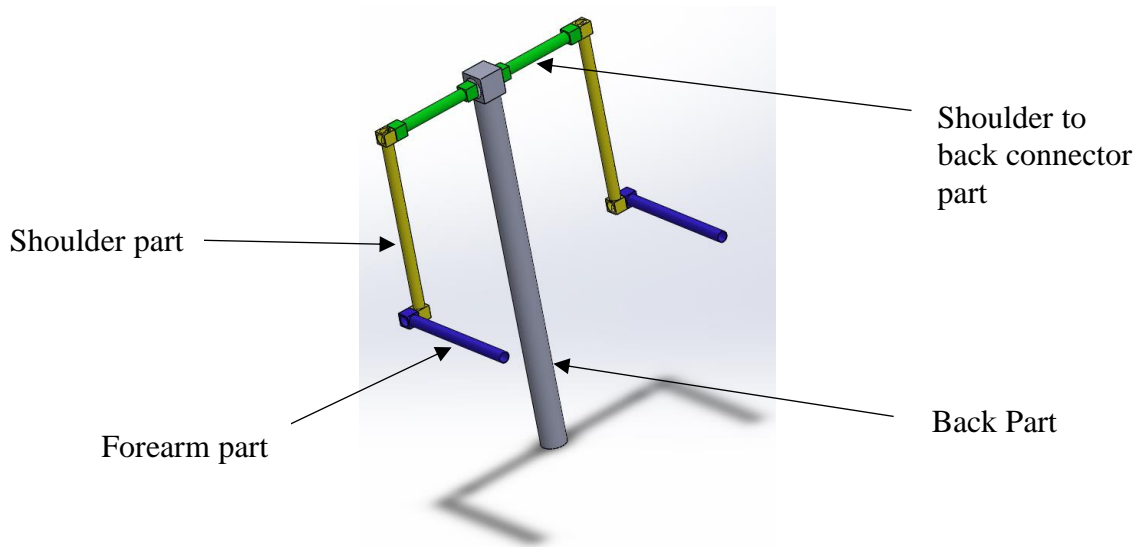


Figure 3.1 Draft model of the exoskeleton using standard pipes

In the presented thesis, the geometries of the cross-sections that are selected are basically switching between the circular, rectangular, and elliptical shape for the internal and external profile of cross-section shape.

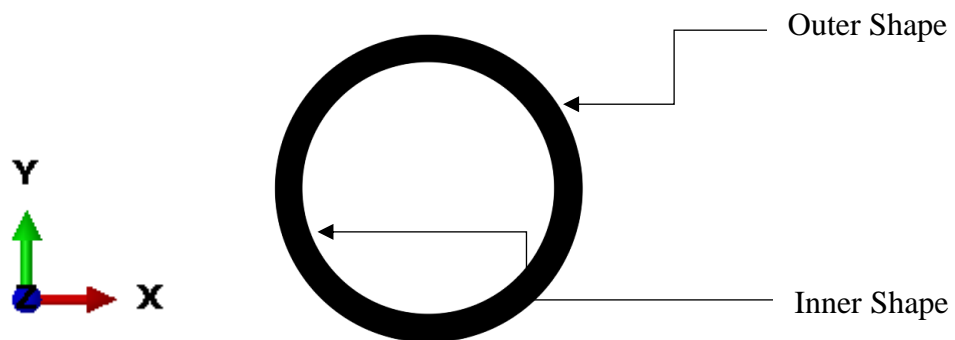


Figure 3.2 Cross-section for pipe with circular outer and circular inner shape

The chosen circular shaped pipe for the simulation and comparison to other possible cross-section shapes is a pipe that has Outer Diameter (OD) of 21,3 mm with nominal wall thickness of 1,6 mm. This specific size is chosen because it is the closest average to the overall diameter of the shoulder bone as known as humeral bone that has overall diameter of  $19,3 \pm 2,3$  mm. This same pipe was used for the other parts of the modelled exoskeleton except the back part [46] [47]. The back part is using the ISO standard dimensions of another pipe dimensions, so the OD is 48,3 mm and thickness of 1,6 mm [46]. These pipe dimensions were chosen for the back part due to comparison to the

dimensions of the width of the vertebral column of average human, as these dimensions were the closest to the vertebral column dimensions [46] [48].

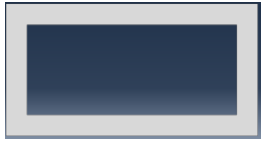
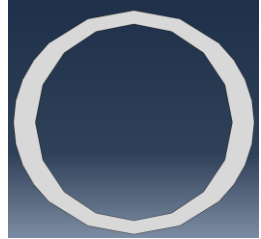
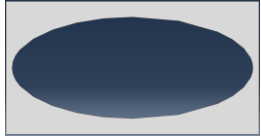
When changing between the geometrical shapes of circle, rectangle, and ellipse for the outer and inner shape normally there shall be 9 shapes of: Circular Inner Shape and Circular Outer Shape (CISCOS), Rectangular Inner Shape and Rectangular Outer Shape (RISROS), Elliptical Inner Shape and Elliptical Outer Shape (EISEOS), Elliptical Inner Shape and Circular Outer Shape (EISCOS), Rectangular Inner Shape and Circular Outer Shape, Circular Inner Shape and Elliptical Outer Shape (CISEOS), Rectangular Inner Shape and Elliptical Outer Shape, Circular Inner Shape and Rectangular Outer Shape (CISROS), and Elliptical Inner Shape and Rectangular Outer Shape (EISROS). However, to keep the same area as the standard circular pipe, so the material usage amount would be equalized, there are two shapes that cannot be doable to maintain the same area, the shapes are Rectangular Inner Shape and Circular Outer Shape, and Rectangular Inner Shape and Elliptical Outer Shape. Moreover, for the back part, adding to the list of the two shapes that are not doable another shape which is the shape that is CISROS, In order to have the aforementioned shapes with the same area of the ISO standard pipes, the inner shape will be cutting through the outer shape. The area of the ISO standard pipe that is used for all shapes except the back part is calculated as following:

$$A_1 = \pi \left(\frac{21,3}{2}\right)^2 - \pi \left(\frac{18,1}{2}\right)^2 = 99.023 \text{ mm}^2 [49] \quad (3.1)$$

Table 3.1 Areas of the shapes for all the parts except the back part [49]

Shape	Description	Area calculated
	Circular Inner Shape and Circular Outer Shape (CISCOS)	$A_1 = \pi\left(\frac{21,3}{2}\right)^2 - \pi\left(\frac{18,1}{2}\right)^2 = 99,023 \text{ mm}^2$
		OD (Outer Diameter): 21,3 mm ID (Inner Diameter): 18,1 mm Thickness: 1,6 mm
	Rectangular Inner Shape & Rectangular Outer Shape (RISROS)	$A_2 = (11 \times 21) - (7,5 \times 17,5) = 99,75 \text{ mm}^2$
		Outer Shape dimensions: 11 mm x 21 mm Inner Shape dimensions: 7,5 mm x 17,5 mm
	Elliptical Inner Shape & Elliptical Outer Shape (EISEOS)	$A_3 = \pi(6,5 \times 10,5) - \pi(4,1 \times 9) = 98,488 \text{ mm}^2$
		Outer Shape dimensions: 6,5 mm x 10,5 mm Inner Shape dimensions: 4,1 mm x 9 mm
	Elliptical Inner Shape & Circular Outer Shape (EISCOS)	$A_4 = \pi(11)^2 - \pi(8,5 \times 10,5) = 99,745 \text{ mm}^2$
		Outer Diameter: 22 mm – Outer Radius: 11 mm Inner Shape dimensions: 8,5 mm x 10,5 mm
	Circular Inner Shape and Elliptical Outer Shape (CISEOS)	$A_5 = \pi(10,25 \times 11) - \pi(9)^2 = 99,745 \text{ mm}^2$
		Outer Shape dimensions: 10,25 mm x 11 mm Inner Diameter: 18 mm – Inner Radius: 9 mm
	Circular Inner Shape and Rectangular Outer Shape (CISROS)	$A_6 = (19,5 \times 20) - \pi(9,62)^2 = 99,26 \text{ mm}^2$
		Outer Shape dimensions: 19,5 mm x 20 mm Inner Diameter: 19,24 mm – Inner Radius: 9,62 mm
	Elliptical Inner Shape and Rectangular Outer Shape (EISROS)	$A_7 = (11 * 21) - \pi(4,2 \times 10) = 99,053 \text{ mm}^2$
		Outer Shape dimensions: 11 mm x 21 mm Inner Shape dimensions: 4,2 mm x 10 mm

Table 3.2 Areas of the shapes for the back part [49]

Shape	Description	Area calculated
	Circular Inner Shape and Circular Outer Shape (CISCOS)	$A_8 = \pi\left(\frac{48,3}{2}\right)^2 - \pi\left(\frac{45,1}{2}\right)^2 = 234,7 \text{ mm}^2 = 0,0002347 \text{ m}^2$
		OD (Outer Diameter): 48,3 mm ID (Inner Diameter): 45,1 mm Thickness: 1,6 mm
	Rectangular Inner Shape & Rectangular Outer Shape (RISROS)	$A_9 = (25,5 \times 46) - (23,5 \times 40) = 233,0 \text{ mm}^2 = 0,000233 \text{ m}^2$
		Outer Shape dimensions: 25,5 mm x 46 mm Inner Shape dimensions: 23,5 mm x 40 mm
	Elliptical Inner Shape & Elliptical Outer Shape (EISEOS)	$A_{10} = \pi(12,5 \times 19) - \pi(9,5 \times 17,1) = 235,776 \text{ mm}^2 = 0,000235776 \text{ m}^2$
		Outer Shape dimensions: 12,5 mm x 19 mm Inner Shape dimensions: 9,5 mm x 17,1 mm
	Elliptical Inner Shape & Circular Outer Shape (EISCOS)	$A_{11} = \pi(21)^2 - \pi(18,3 \times 20) = 235,619 \text{ mm}^2 = 0,000235619 \text{ m}^2$
		Outer Diameter: 42 mm – Outer Radius: 21 mm Inner Shape dimensions: 18,3 mm x 20 mm
	Circular Inner Shape and Elliptical Outer Shape (CISEOS)	$A_{12} = \pi(20 \times 21,75) - \pi(19)^2 = 232,477 \text{ mm}^2 = 0,000232477 \text{ m}^2$
		Outer Shape dimensions: 20 mm x 21,75 mm Inner Diameter: 38 mm – Inner Radius: 19 mm
	Elliptical Inner Shape and Rectangular Outer Shape (EISROS)	$A_{14} = (22 * 42) - \pi(10,7 \times 20,5) = 234,891 \text{ mm}^2 = 0,000234891 \text{ m}^2$
		Outer Shape dimensions: 22 mm x 42 mm Inner Shape dimensions: 10,7 mm x 20,5 mm

### 3.3 Manufacturing Process

The manufacturing method that is suggested to be used to manufacture the parts that are used in forming the frame of the exoskeleton is extrusion.

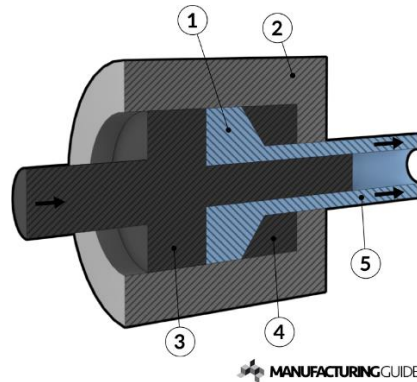


Figure 3.3 Schematic for extrusion [50]

Extrusion for metals is defined as a process in which it involve pushing a block of material (5) that can be cylindrical, oval, rectangular, or polygon through a die that is fixed (2), so the cross-section area will be reduced to give output of a shape that is functional. The shape of the die that is forced through the material is forming the inner shape of the pipe that is being formed by the extrusion. In other words, the plunger (3) pushes the preheated material (1) through a die (4) to form the pipe at the end (5) as shown in figure 3.3. [50] [51] [52] [53] [54].

The extrusion has benefits such as allowing the manufacturing and forming of products that has complex and large cross-sections, as well as the benefit of producing many products from a single billet (the undeformed material) in a manner that would make the production economical and having high-production rate [51].

The die shape can also be cylindrical, oval, rectangular, or polygon, as well as it can be non-axi-symmetric or axi-symmetric. However, being non-axi-symmetric will make the extrusion process more complex, and that is also out of the scope of the presented thesis, as the pipes in the presented thesis are suggested to be produced by axi-symmetric shapes already [51].

In order to have the ability of extrusion of geometrical shapes in cross-sections to form pipes The starting billet may have a hollow cross-section, The hole can also be machined/gun-drilled before loading into the press, or using the process known as piercing where a broach is pressed through the billet that is preheated and that would result in a hole to be left [51].

In order to keep the hollow cross-section maintained without collapsing during forming, a tool is used known as mandrel which is a solid rod that enters the hole [51].

In the presented research, the manufacturing process is used for material pipes, so there is a different approach. That method includes using special porthole die. The material is pushed into separate material streams over a bridge in the die. Afterwards, the material is pushed back together into the chamber of welding portion of the die where it will bond together by diffusion using the high temperature and pressure that are caused by the weld chamber geometry. The weld that is resulted by this process is known by the name of longitudinal weld that runs along the length of the extrudate. Aluminium alloys are usually produced by using this method as it gives high quality of flow properties and extrudability [51].

Just as the study case is using aluminium, the suggested method would be the second one; however, after a material selection process that can be done in the future for the upper-body exoskeleton, other extrusion processes can be used as well.

### **3.4 Loads and Calculations**

As has been studied during the literature review as well as studying a review paper about upper-body exoskeletons for industrial solutions, the upper-body exoskeletons that are used in industrial applications are famously using pipe shapes for the frame, and that is the reason why the thesis is studying the best cross-section for each part of the upper-body exoskeletons in industrial applications [55].

As has been studied as well from the existing exoskeletons in the market, the mass that can be lifted is ranging from 10 to 25 kg [55]. Therefore, in the presented thesis the chosen mass to be simulated is 20 kg, while taking a factor of safety of 1,5, the simulation mass is 30 kg. Factor of safety is taken as 1,5 because the simulation is for a ductile material, and according to Mechanical and Metal Trades Handbook for the static load of ductile material the factor of safety shall range from 1,2 to 1,8, so the chosen factor of safety is 1,5 [49]. The case is defined as static load as the frequency of the loading is not considered as dynamic loading. Dynamic loading usually includes calculation frequency in Hz, which would refer to the loading and unloading process happen more than once in a second, but that is not the case that is being studied in the presented thesis. The acceleration due to gravity is assumed to be  $10 \text{ m/sec}^2$ . The material used in this simulation is not the main focus, as the main focus about knowing the best cross-section for the exoskeleton frame; however, Aluminium alloy 6262 was selected as the material for the simulation but this material that is selected is better in the aspects of manufacturability, mechanical properties, cost, deformability, and availability [55] [56] [57].

Using the known laws of:

$$M_o = F * L \text{ [49]} \quad (3.2)$$

Where  $M_o$  – Moment, N.m

$F$  – Force, N

$L$  – Length, m

$$F = M * g \text{ [49]} \quad (3.3)$$

Where  $F$  – Force, N

$M$  – Mass, kg

$g$  – Acceleration due to gravity, m/sec<sup>2</sup>

$$F = (20 \text{ kg} * 1,5) * 10 \text{ m/sec}^2 = 300 \text{ N} \quad (3.4)$$

Table 3.3 Length and Bending Moments to be applied on each part [49] [58] [59] [60] [61]

<b>Part name</b>	<b>Length (mm)</b>	<b>Bending Moment to be applied</b>
Shoulder	334	$M_1 = 300 * 0,334 = 100,2 \text{ N.m}$
Forearm	254	$M_2 = 300 * 0,254 = 76,2 \text{ N.m}$
Shoulder to back connector	143.8	$M_3 = 300 * 0,1438 = 43,14 \text{ N.m}$
Back	710	$M_4 = 300 * 0,710 = 213 \text{ N.m}$

$$TS = F / A \text{ [49]} \quad (3.5)$$

Where  $TS$  – Torsion Stress, N/m<sup>2</sup>

$F$  – Force, N

$A$  – Surface area, m<sup>2</sup>

$$TS = TMo / TPsm \text{ [49]} \quad (3.6)$$

Where  $TS$  – Torsion Stress, N/m<sup>2</sup>

$TMo$  – Torsion moment, N.m

$TPsm$  – Torsion Polar section modulus, m<sup>3</sup>

$$TPsm \text{ for CISCOS} = \frac{\pi x (OD^4 - ID^4)}{16 x OD} \text{ [49]} \quad (3.7)$$

Where  $TP_{sm}$  for CISCOS – Torsion Polar section modulus for CISCOS,  $m^3$   
 OD – Outer Diameter, m  
 ID – Inner Diameter, m

$$TP_{sm \text{ for CISCOS}} = \frac{\pi \times (0,0483^4 - 0,0451^4)}{16 \times 0,0483} = 0,0000053 \text{ m}^3 \quad (3.8)$$

Where  $TP_{sm}$  for CISCOS – Torsion Polar section modulus for CISCOS,  $m^3$

$$T_{Mo} = \frac{300}{0,0002347} \times 0,0000053 \cong 6,8 \text{ N.m} \quad (3.9)$$

Where  $T_{Mo}$  – Torsion moment, N.m

Aluminium alloy 6262 has high strength-to-weight ratio also known as specific strength of 115 kN.m/kg relative to other materials such as titanium, brass, and stainless steel as they have specific strength of 76 kN.m/kg, 67,8 kN.m/kg, 63,1 kN.m/kg respectively [62] [63]. The aluminium alloy 6262 also has a proper capacity of shape forming, plasticity, and ease of joining while being corrosion resistant, and used for some army and airspace applications. Aluminium 6262 is known to be used for precision design [64]. Aluminium alloy 6262 has density of 2,72  $g/cm^3$ , Young's modulus of 69 GPa, Poisson's ratio of 0,33, and Yield stress 270 MPa while plastic deformation is assumed to be zero, as plasticity is a property that it is not desired in the material for this application [56] [57]. Some other materials are used to manufacture the frame of exoskeletons, but when the used materials are compared in aspect of cost, deformability, availability, ease of manufacturability, and mechanical properties, the aluminium turns to be better option [55] [56] [57].

### 3.5 Kinematics of the draft model upper-body exoskeleton

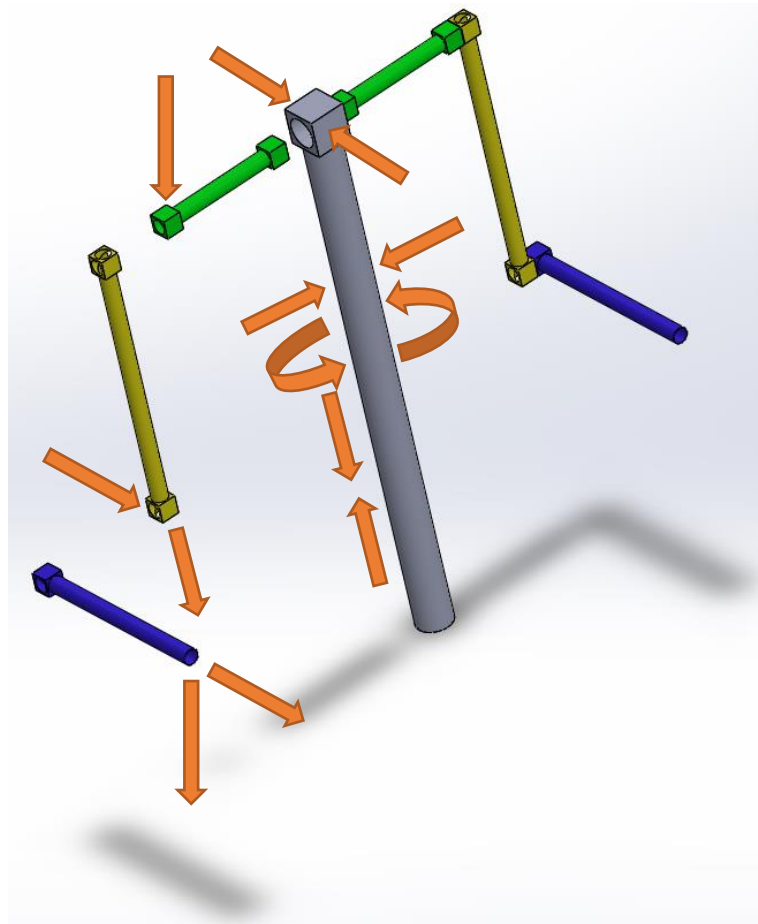


Figure 3.4 Scheme of loading kinematically to the exoskeleton in exploded view

In figure 3.4 it is visualized that the shoulder part has been simulated for tension and bending. The forearm part has been simulated for tension and bending as well. The back part has been simulated for compression, torsion, and bending. The back to shoulder connector part has been simulated for bending.

The process that will be frequent for the exoskeleton is lifting. So, focusing on forearm part, mainly the bending will be the major effect; however, when the forearm part is pointed down there will be tension force. The shoulder part during lifting process will be heavily affected by tension, but if the lifting goes to some angle where the shoulder part starts to move from being vertical and parallel to the body, then bending effect will take place. The back to shoulder connector is mainly subjected to bending as during lifting, it can be moved down by the force of the load while being connected to shoulder part. Last but not least, the back part will be subjected to torsion due to rotation of the body while moving, which might make torsion impact as well as bending action that can

happen due to the bend of the body sometimes towards any direction, and as the weight acts from the point that is the top of the back part, so there will be also compression force that will be implied due to the weight of the object being lifted.

### **3.6 Simulation setting**

In the simulation, each part of the model exoskeleton as shown in figure 3.1 is subject to different kind of loading, as the nature of lifting application, it will cause different kind of stresses on each part as shown in figure 3.4 and explained in kinematics subsection. The FEA simulations has been done on a software program known as ABAQUS, which is a famous tool for solid mechanics and FEA analysis.

The simulation of tension for the part is done by fixing one end of the pipe and pulling the other end using concentrated force on a reference point which exists in the middle of the profile and kinematically coupled with the whole surface of the loading end.

The simulation of bending is done by applying the same strategy of the tension, but instead of having the vector of the force in the same axis of the pipe length the axis that is perpendicular to the axis of the pipe length is used. The moment force is applied on the reference point that is kinematically coupled to the surface of the non-fixed end. The compression simulation is similar to that of tension, just with opposite direction that the vector of the force of the tension simulation.

The torsion simulation is exactly like the bending simulation, but the bending axis is different, just that the moment will be on the axis of the length of the pipe and not perpendicular to it.

All the loads were applied using a step function, but there are different behaviours in each loading case. For tension, bending, and torsion, they have the same type of step function which is a static step function, which is used when the inertia effects can be neglected [65]. For compression, the dynamic explicit step function type was used as it takes into consideration the dynamic response, and it is more effective in analysing large models that have relative short dynamic response time such as the case of compression of the back part [66]. The nonlinearity was considered in all cases and all step functions. There is a formed way of loading, in a way to be as ratio between time and loading capacity. There was a 10% increase in the loading for every 10% increase in the time value. Therefore, the table will be looking as shown in table 3.4.

Table 3.4 Time ratio and Amplitude of Loading

<b>Time/ Frequency</b>	<b>Amplitude</b>
0	0
0.1	0.1
0.2	0.2
0.3	0.3
0.4	0.4
0.5	0.5
0.6	0.6
0.7	0.7
0.8	0.8
0.9	0.9
1	1

Meshing to square elements has been done in order to keep the regularity of the meshing shapes as much as possible, and as the square meshing is known for better depth analysis [67] [68]. The mesh was kept in a form that makes less irregularity with proper calculation time. All meshed shapes are shown in the appendix subsections 8.2, 8.3, 8.4, and 8.5. The mesh that was done was done to the assembly, so the assembly mesh was independent from the part mesh. This was done in order to take into consideration the reference point as it is the point that will have all the loads, and the reference point is appointed at the assembly level and not the part level.

The boundary conditions in all loading cases are having a fixed end, and the force act on a reference point on the other end of the pipe, either compression, tension, bending, or torsion. Just in case of tension and compression, as the axis of the acting force is in the same axis as the pipe length, there is an additional boundary condition to cease moving of the reference point in the other two axes of the cartesian 3D coordinates.

To clarify, as seen in figure 3.5, the tension and compression loads would be along Z-axis acting on reference point which is referred in figure 3.5 as RF-1, but with opposite vector directions. Therefore, a boundary condition is applied to cease the reference point from moving in X or Y axes.

The bending simulation that took place are done by applying moment on the reference point around X and Y axes separately. For the case of regular circular shaped standard pipe, the bending about X or Y axes does not make a difference at all. However, for other shapes, a bending moment about X-axis would be significantly different than about Y-axis; therefore, separate simulations for acting on Y-axis and X-axis have been done as well as results were acquired, so it would be known even the best direction of forces acting and orientation of the best selected pipe for the exoskeleton frame.

The torsion simulation is done by applying moment on the reference point that acts on Z-axis itself, so torsion would take place.

The definition and usage of reference point in the simulation is basically the mid-point of a circular or elliptical shape at the loading end, so it is used as the mid-point to act on the entire face which is coupled to it kinematically.

The material alloy is assumed to be uniform along the pipe, so the behaviour of loading would not be different due to different material distribution. This assumption is made to make the calculation and simulation of the pipe easier and takes reasonable time.

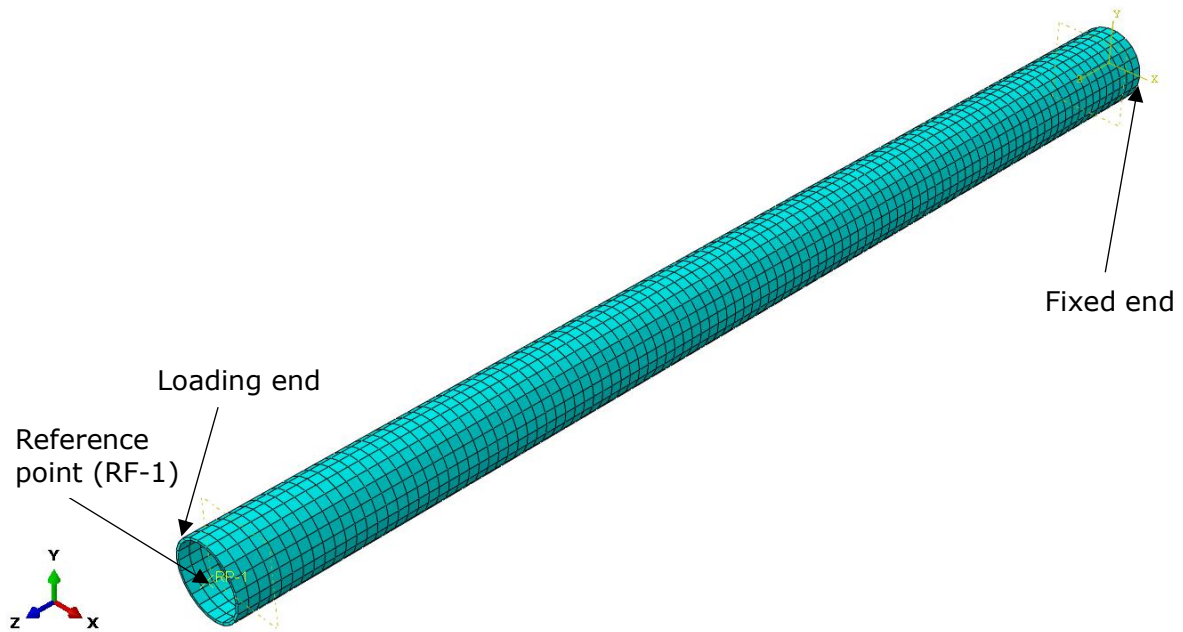


Figure 3.5 Normal standard meshed unloaded pipe for back part

### 3.7 Results deriving

To compare between cross-section shapes, stress-strain curves are produced for each simulation of forces that are applied on the pipes. For validation purposes, the yield point is derived from some curves to assure that the yield point is comparable to that of the material properties. The method that is used is the 0,2% of the stain straight line, as when that straight line touches the stress-strain curve of the test, the touching point is the yield point [69]. The stress-strain curves that are produced are engineering stress-engineering strain curves, as from engineering stress-engineering strain curves the 0,2% method could be used. The true stress-strain data are derived from the software program then mathematical conversion was done using MS Excel. The conversion equations were:

$$\text{True stress} = \text{Engineering stress} * (1 + \text{Engineering strain}) \quad [70] \quad (3.10)$$

$$\text{True strain} = \ln (1 + \text{Engineering strain}) \quad [70] \quad (3.11)$$

The true stress and true strain data were derived from the integration point of the most heavily stressed element in the mesh of the pipe, so it derives the absolute maximum principle stress and absolute maximum principle strain for the curves of the tension. Additionally, the compression representation curves are represented as engineering stress and engineering strain, using the integration point of the most heavily stressed element in the mesh of the pipe, but it derives the Von Mises stress and maximum principle strain for the true strain and true stress data.

Integration point is used to derive the stress or strain, especially when deriving the principle stress and principle strain for tension or compression tests [71].

For the representation of the bending and torsion, a different approach was used. In order to represent the torsion and bending effects and compare different behaviour, the comparison would matter mainly about the deflection. Therefore, the force-deflection curves were used for the representation of the torsion and bending effects as it is a valid method for bending validation as the less deflection happen the better, as deflection is not a desired behaviour in that loading case [72].

In case of bending, the data that are derived from the software tool are moment and angle, but the angle derived in radian. A normal calculation is done by multiplying the moment data by the length of the pipe, so the force that is applied will be resulted.

In case of compression, it will be exactly the same case of bending, except for calculation, as the moment will not be multiplied by the length of the pipe, but by the area of the standard pipe, as the torsion calculations are different than the bending ones as shown in the subsection of the loads and calculations.

In order to validate the results that are driven, the method of 0,2% of the strain was used as aforementioned to show the yield point is similar to that of the known properties of the material. In the material source the yield stress is 270 MPa, which means that the 0,2% line will meet the stress-strain curve at a point of 270 MPa, and at that point the plasticity starts to take effect in the material, and the structure is not perfectly elastic afterwards [57].

In the following figure, tensile test for the standard pipe that is used for all the frame parts except for the back one has been done and using the method of 0,2% of the strain is used to assure the validity of the results that are shown.

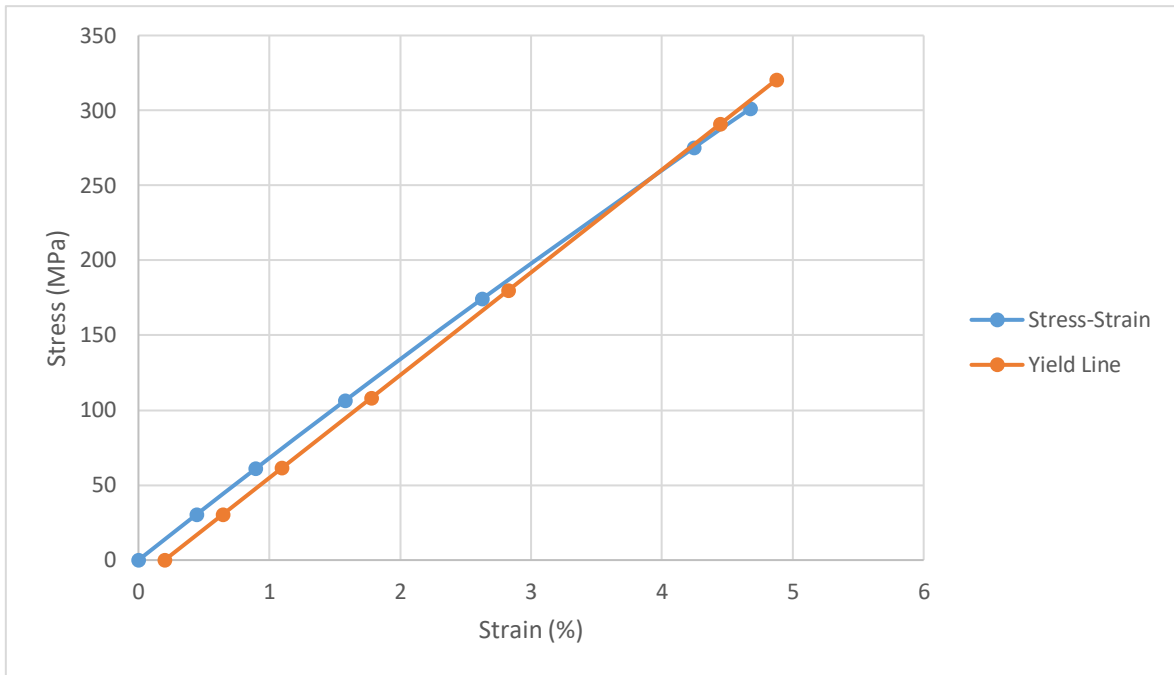


Figure 3.6 Stress-strain of tensile test for the standard pipe with yield line

As observable in figure 3.6, the yield line and stress-strain curve intersect at a point that is roughly having the value of 270 MPa. This validation methodology has been done for all the parts in tensile tests, and the rest of the figures are shown in the appendix subsection 8.1.

For all simulations that are done, some of the results were having negative magnitude for direction or angle, all the negative values were taken as absolute magnitude to make the comparison between different shapes and simulations viable.

### 3.8 Selection criteria

In table 3.1 and table 3.2 it is shown that the same part to be used is having a maintained area in all shapes, so it would assure that all forces applied through tension will be the same as well as total cost of the raw materials. Since the area and length are the same, so the total volume of material to be used, which refers to the consistency of the raw material amount used is the same. However, it differs from table 3.1 area than table 3.2 area, but all maintained within the same table. This aspect mainly is to fix the cost of the raw materials, so comparison between them would be impacted in this way.

After having the simulation is done for all the possible shapes graphs that represents the stress-strain or load-deflection have been generated. The method of their generation is aforementioned in the results deriving subsection. The curves themselves can be seen in results section. Nonetheless, there has to be a method to identify which curve would

be better than the other. The main focus here is about the same curve for the same part comparison. In essence, for the stress-strain curve, the less strain and less stress the better. Less stress and less strain mean that there will be less plasticity in the part while being subjected to the load. For the force-angle curves, the force that is subjected to the part is already constant as it comes from the input. However, the impact of this force differs by having different angle, the less deflection the better in this case, as deflection is not a desired behaviour in this case of designing exoskeleton frame.

After a strong survey about exoskeletons metrics to focus on, the results and discussion of the survey are represented in a full dissertation that was submitted in Iowa State University with a title of "A top-down human centred approach to exoskeleton design" [73]. The survey shows that there are various metrics to consider while designing an exoskeleton, and after the survey about the metrics, the experts in the field have ranked the importance, and the results shows the following ranking of importance of exoskeleton designing aspects:

Table 3.5 Metrics of exoskeleton design ranking [73]

<b>Metric</b>	<b>Ranking</b>
Cost	1
Ease of manufacturing	2
Range of Motion/ Flexibility	3
How the exoskeleton attaches to the body	4
Anthropometry	5
Replaceable parts	6
Formability to the body	7

The list extends to be a very lengthy one up to 55 aspects to consider. However, the focus of the methodology of the presented research is focused on the top ones as shown in table 3.5. Starting from cost, the cost of the raw material is taken into consideration to be constant by having approximately equal area of the same part shapes. Moreover, to consider the ease of manufacturing along with the cost, the manufacturing method that was considered for choosing the aforementioned geometries is extrusion, which does not have high cost along with being a commonly known method of manufacturing. The rest of the ranking shown in table 3.5 is showing case specific aspects, which is not the focus of the presented thesis. However, going through the entire table in the dissertation that was formed that has total of 55 aspects, all aspects divide to either been taken into consideration in this presented thesis, or case specific [73]. It is not easily doable to work on a specific case of an exoskeleton as explained in limitations section.

As the criteria that are mentioned in that dissertation are considered to be constant in all shapes of the parts of the upper-body exoskeleton frame; therefore, the comparison

between shapes will depend on the mechanical behaviour, with slight consideration of the ranking shown in table 3.5.

### **3.9 Limitations**

In every experiment or simulation there are some limitation for sure that are preferably mentioned for future development of the simulation or experiment.

First, it is difficult to have a full simulation, as cases and shapes of exoskeletons differ when the dimensions of anything differ or the producing company. It can differ in what the exoskeleton is used for, how it operates, topology, and conditions. Therefore, the focus of the presented thesis is the theory of selection of the best cross-section for a generalized model that has main parts that would be included in each upper-body exoskeleton for industrial applications.

The mechanical behaviours of each possible cross-section that has same area as the standard pipe are studied and analysed, as that is the focus and main contribution of the presented thesis. By using some metrics and comparisons, it would be known which is the best cross-section for each part to be used.

A full detailed case of a specific upper-body exoskeleton to be studied would be difficult, as this would require a lot of data and information from the manufacturing company, and such data would be surely classified, and there has been no cooperation with any specific exoskeleton makers in the market for this thesis, but there has been a contact about earlier stages of the research in total for some trainings for software tools. Moreover, working fully with a company that produce exoskeleton would require a classified thesis, so this information would not be easily accessible for public for further research, and this is still an ongoing topic that has long way to go, and it would be better for user safety that all companies would have access to this research of the mechanical behaviour of different cross-sections, so a development can be done for existing exoskeletons. Such development for exoskeletons would result is having better performing workers and more durable exoskeletons with cost fixed in aspect of raw material used in manufacturing.

Plastic strain was not considered in this research as the plastic deformity is not an acceptable behaviour as have been aforementioned.

The selected cross-sections to be done for each case shall be basically a mix of circular, elliptical, and rectangular shape. There could be more shapes possible to consider. Moreover, in order to keep an approximate area for each cross-section to have same area as the standard circular pipe, some shapes had to be not done, as in order to keep same area as the ISO standard pipe, the inner shaper will cross the borders of the outer shape, which will make the shape not complete part, so it was not possible to form all

possible shapes with mixing the elliptical, circular, and rectangular shapes. All shapes that were simulated are presented in table 3.1 and table 3.2.

As mentioned in results deriving subsection, the simulations have been represented in form of curves that are stress-strain curves or force-angle curves. In reality, there would be a mix of forces, for example having tension and bending at the same time. Nevertheless, the bending is represented by force-angle curve and tension is represented by stress-strain curve. Therefore, having a single curve to represent the mix of the forces would be difficult, as the stress-strain components from the software tool that produces the data of the simulation does not take into consideration the shear force that is applied on the single element, and the force-angle curve is not considering the force being subjected on the same axis of the pipe length. As a result, each force type was represented separately as represented in the results section. The integration point of the most stressed element is the point that is considered for the stress-strain curve as explained in results deriving subsection, but the force-angle curve is using the data of the reference point, which is totally different point as explained in results deriving subsection. However, this aspect of forces mixing and representing can be considered for future plans.

The actuator sizing or type selecting process was not done, as the focus of the thesis is different than this aspect. Moreover, it would require more time to be considered, and time was a challenge that was faced during forming the presented thesis. The places of actuators on the exoskeleton also was not taken into consideration as this would be very case specific, and the focus of the presented thesis is generic and cannot be for a specific case of an exoskeleton as aforementioned. Additionally, this aspect can be considered for future plans.

The placement of electronics components also was not taken into consideration for the same reasons as the actuator type, place, and sizing. Similarly, can be considered for future plans.

One of the major limitations for sure for the presented thesis was the time challenge, as the more time was available the more results were driven and more trails of expanding the research were done. This is a part of an ongoing research that has been done through some time, and there are more and more results are getting driven as well as data. The research in total is held in Tallinn University of Technology by various students with the support and supervision of the professors in various departments.

## 4 RESULTS

### 4.1 Shoulder Part Results

#### 4.1.1 Tension Test

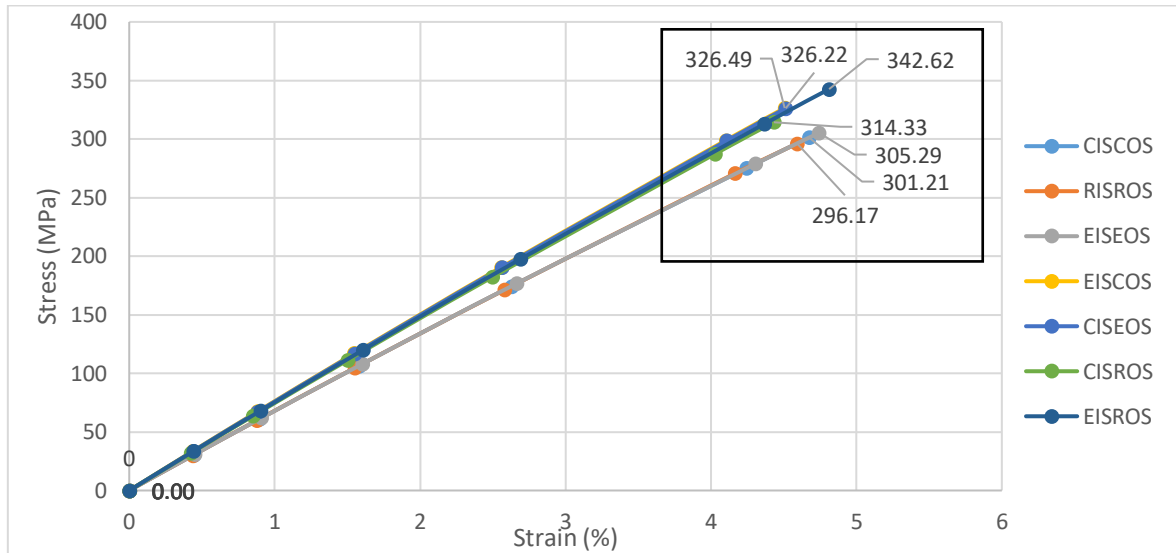


Figure 4.1 Tension test stress-strain curves for all possible shapes for shoulder part

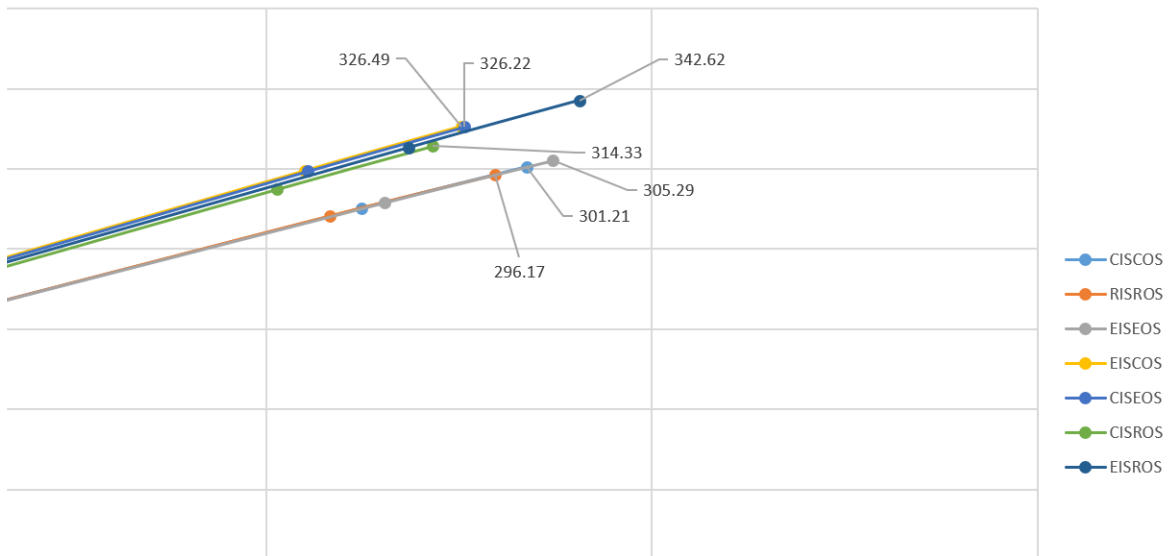


Figure 4.2 A zoom into the results shown in figure 4.1

In figures 4.1 and 4.2, the stress-strain curves are shown for the tensile test for the shoulder part of the upper-body exoskeleton frame. As tensile test is part of the testing for this part as explained in methodology. The force that has been applied, methodology of simulation and force applying, and magnitude of moment, and geometry of each case

are all shown and explained in methodology section. It is observable here that EISROS has the highest stress and highest strain followed by CISEOS and EISCOS. Speaking of the least stress it is remarkably RISROS followed by CISCOS then EISEOS. The least strain is CISROS with a moderate stress relative to other shapes.

### 4.1.2 Bending test

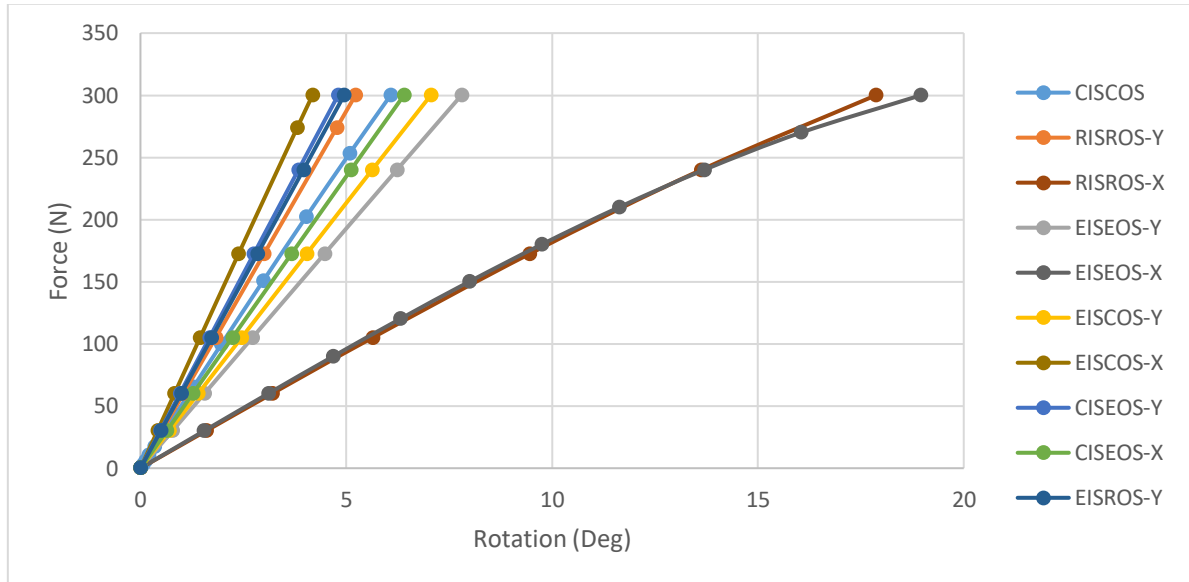


Figure 4.3 Force-Angle curves for bending test done for all shapes for shoulder part

As has been discussed in methodology section, in force-angle curves, it is better to have less deflection, as the same force has been applied to all kinds of shapes already. Moreover, it is important to mention that all shapes would behave differently when the bending is done about different axis except for CISCOS case. Therefore, as shown in figure 4.3, all shapes have Y axis load and X axis load except CISCOS case as it is symmetrical as well as EISROS that does not have X axis loading represented in the graph as it has reached the plastic limit at lower force. It can be clearly observed which case has the least deflection, which is the EISCOS-X, which is basically the pipe that has EISCOS profile when subjected to bending on X axis. The second least deflection is CISEOS-Y case which is basically CISEOS profile subjected to moment about Y-axis, then followed by EISROS-Y case. The most deflected cases are the EISEOS-X, RISROS-X, and EISEOS-Y respectively from most deflected to the least deflected case.

## 4.2 Forearm Part Results

### 4.2.1 Tension Test

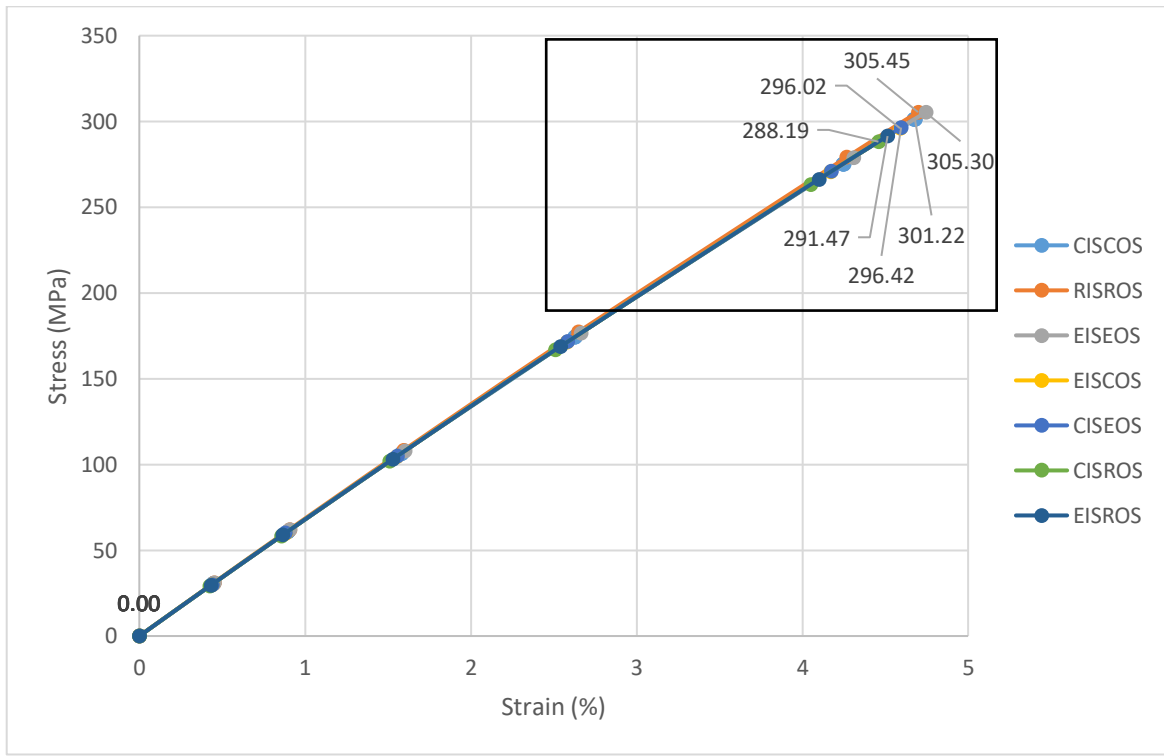


Figure 4.4 Tension test stress-strain curves for all possible shapes for forearm part

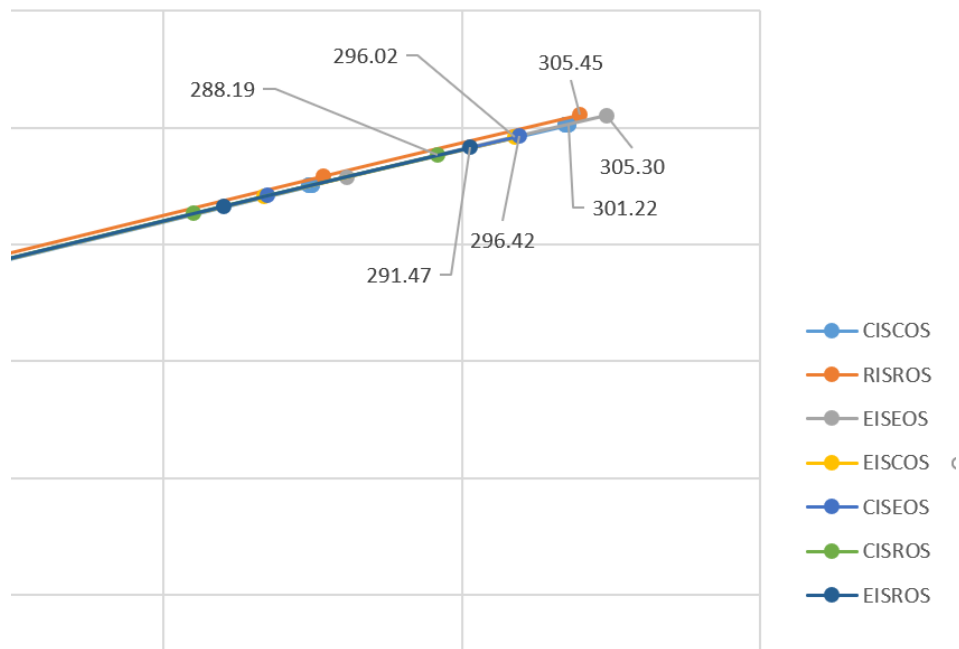


Figure 4.5 A zoom into the results shown in figure 4.4

In figures 17 and 18, the tensile test results are represented. The tensile test simulation that has been done for the forearm part. The results being so close that they are almost equal with a very slight difference, and that can be explained that this represent the stress applied on each part is basically force divided by area. The area is kept being almost equal in all shapes, and force is an input in the simulation, so it is also constant across all simulations that are done for that purpose. Therefore, the stress-strain curves of each case shall be almost identical. There is a slight difference in this case and the shoulder case, as the data derived for tensile test results is driven from the most heavily stressed element in the structure, and that would exist in the middle of the part. When tensile test takes place, the middle of the part gets a little bit thinner than the rest of the structure, which would result in a different area total from one case and another case. Moreover, the stress concentration factor of each shape is taken into consideration of the calculation of the software tool that was used.

### 4.2.2 Bending test

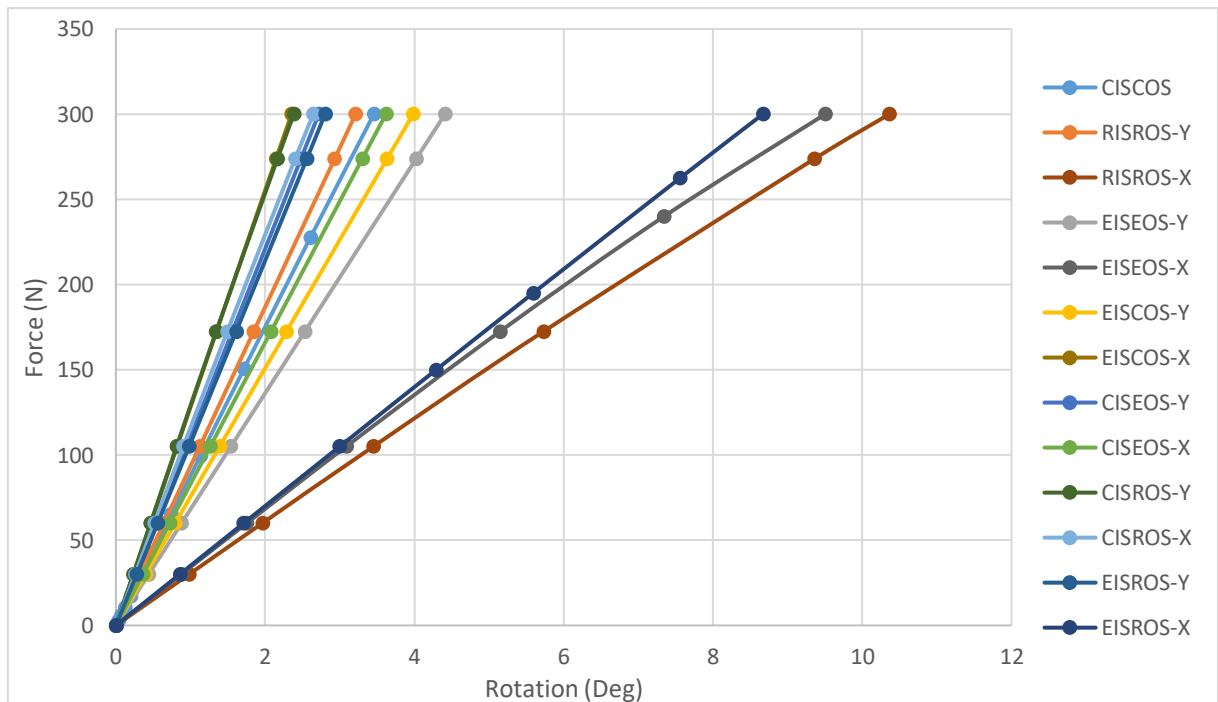


Figure 4.6 Force-Angle curves for bending test done for all shapes for forearm part

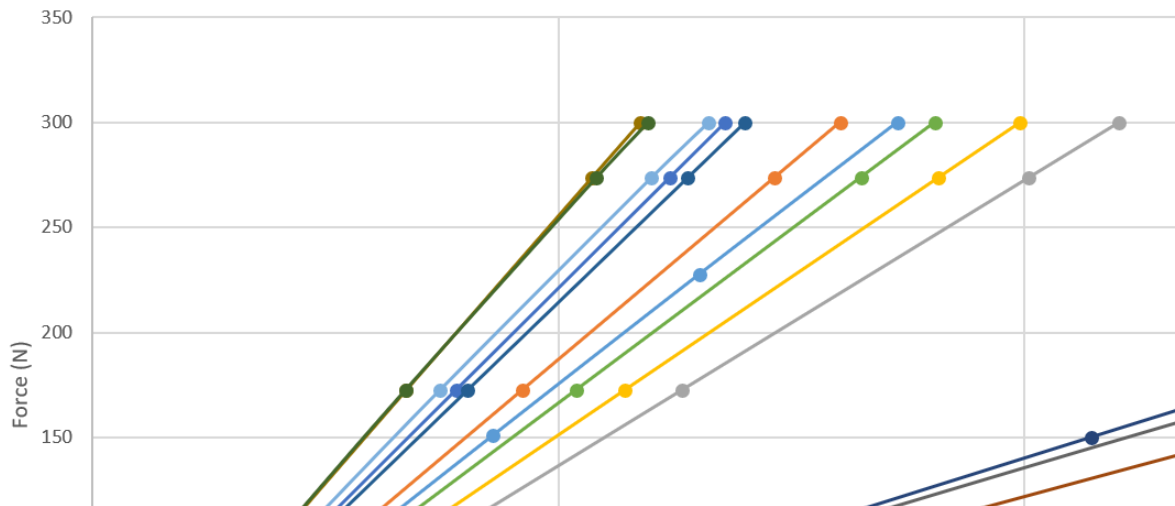


Figure 4.7 A zoom into the results shown in figure 4.6

As discussed formerly, in the force-angle curves, forces will be the same for all cases, but angle would differ, and the less deflection the better.

The least deflection happened as seen in figures 4.6 and 4.7 to the EISCOS-X, which is the part with EISCOS that is subjected to bending about X-axis. Followed by CISROS-Y, then CISROS-X. The most deflected cases are RISROS-X, EISEOS-Y, and EISROS-X respectively from most deflected to less deflected.

## 4.3 Back Part Results

### 4.3.1 Compression test

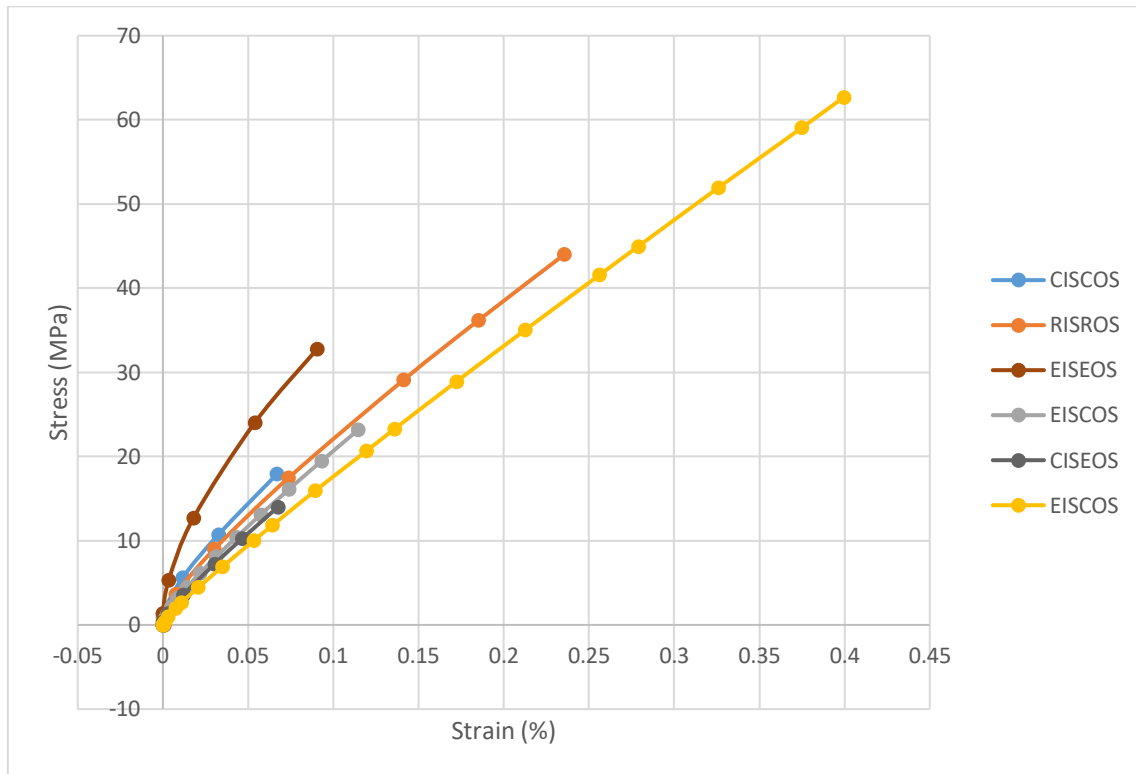


Figure 4.8 Stress-strain curves for compression test simulation done for all shapes for back part

In figure 4.8, there is a significant difference between each case, which would be logical, as the compression acts on a side of the pipe whereas the other side is fixed, so one side is significantly way more stressed than the rest of the body. As one side has all the stress as shown in appendix subsection 8.5, the shape of the area being compressed would make a major difference in results, as results are mainly derived from the most heavily stressed element, and that element is probably having less area than the other parts of the shape, and the area of that element would differ from one shape to another. Therefore, there are major difference in results of each shape. The behaviour of each individual case is very normal by having zero strain for a while, then starts to have strain after certain threshold of the stress. The most stressed and strained shape is EISCOS, followed by the RISROS, then the EISCOS and EISEOS having almost similar strain, but significantly different stress levels. The least stressed is at the same time least strained is the CISEOS followed by CISCOS.

### 4.3.2 Torsion test

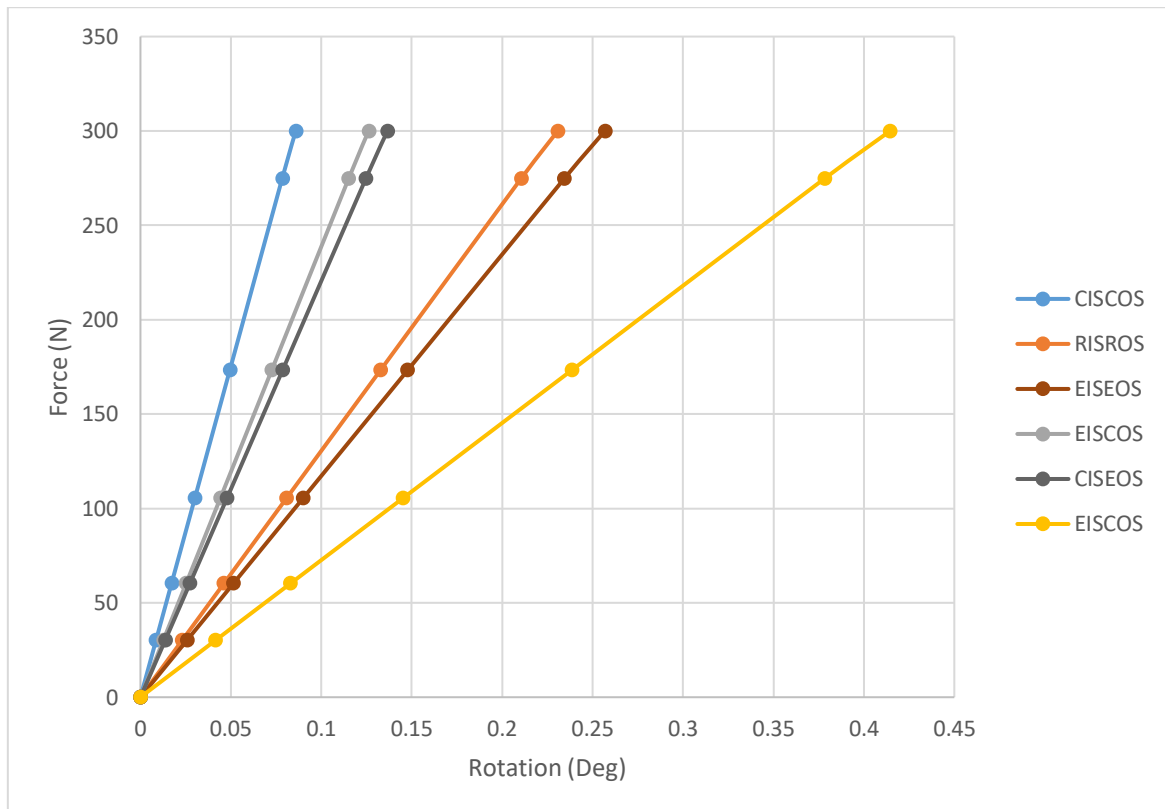


Figure 4.9 Force-angle curves for torsion test simulation done for all shapes for back part

In figure 4.9, the force-angle curves of torsion test simulation that is processed for the back part of the upper-body exoskeleton are presented. The results are clear and easy to notice that the least deflected shape is CISCOS followed by EISEOS then CISEOS. And the most deflected shapes are EISCOS followed by EISEOS then RISROS. However, it is important to note that the most deflected shape is not even deflected by 0,5 deg, which is considerably very low, and shows that all shapes are generally strong enough to withstand the torsion force that is being subjected to each shape in the back part. So, the comparison between them in torsion aspect would not be significant metric to consider, but still important enough to consider it for further safety.

### 4.3.3 Bending test

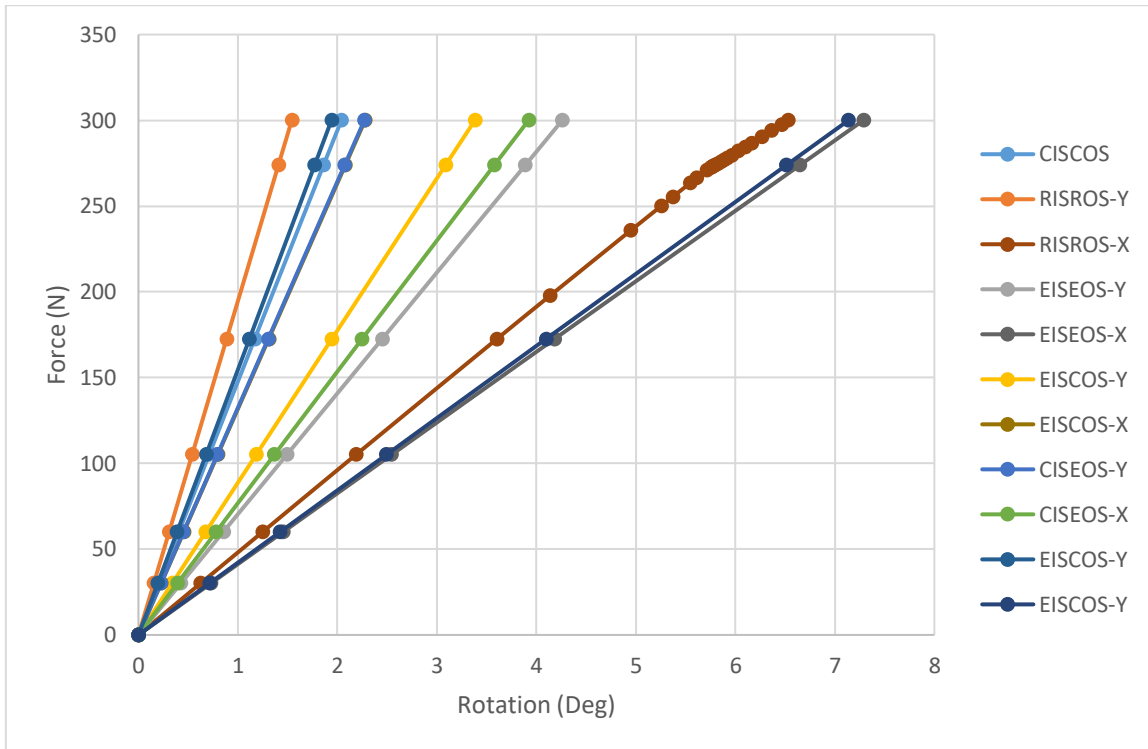


Figure 4.10 Force-angle curves for bending test simulation done for all shapes for back part

In figure 4.10, the force-angle curves of bending test simulation that is processed for the back part of the upper-body exoskeleton are presented. The difference between each case is clear and significant. The difference between the least deflected and the most deflected is important with high magnitude of difference to be considered very important during the comparison. The least deflected is already deflected by an angle between 1 and 2 deg which is RISROS-Y followed by EISCOS-Y then CISCOS as they have values approximately 2 deg. The most deflected shapes are EISEOS-X followed by EISCOS-Y then RISROS-X. The most deflected shape is deflected by angle of more than 7 deg, and that is considerably high. In order to specify a balance between the bending in X and Y axes, CISCOS would be the most balanced one, as whatever shape has less deflection than this shape when being subjected to bending about one axis, when the same shape get subjected to bending on the other axis there is a huge difference between this and that. And for the back part, it would be difficult to predict the direction of the bending to only one axis of both axes.

## 4.4 Back to Shoulder Connector Part Results

### 4.4.1 Bending test

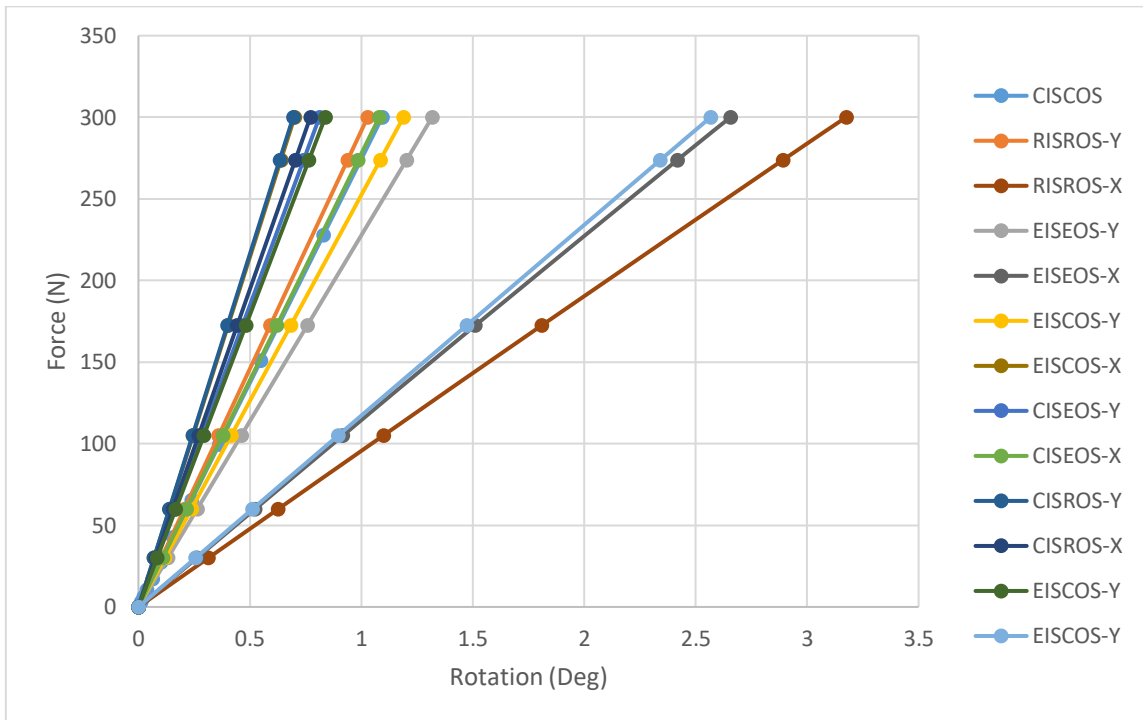


Figure 4.11 Force-angle curves for bending test simulation done for all shapes for back to shoulder connector part

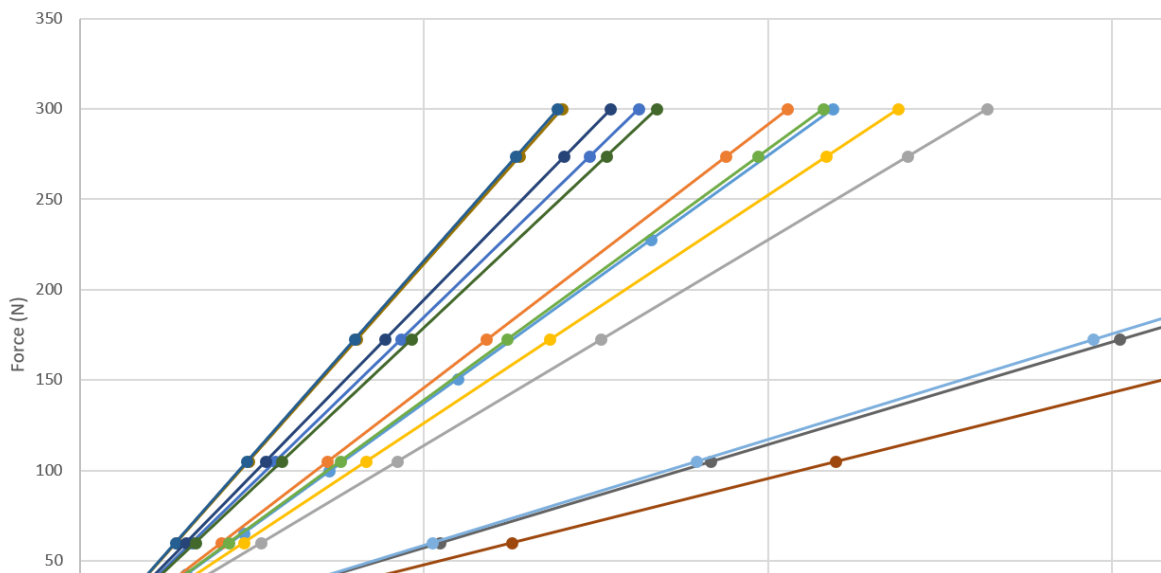


Figure 4.12 A zoom into the results shown in figure 4.11

In figures 4.11 and 4.12, the focus is on the bending test for the back to shoulder connector part as this part would be subjected heavily to bending. The least deflected shapes are having almost identical results with a tad of shift. So, the least deflected

would be the CISROS-Y case followed by the almost identical result of EISCOS-X then the sequence that are having a value of bending less than 1 deg are CISROS-X, CISEOS-Y, and EISCOS-Y respectively. The most deflected ones having deflection angle that ranges from 2,5 to 3,5 deg. The order from the most deflected to less deflected among the 3 most deflected shapes are the RISROS-X, EISEOS-X, then CISCOS. The comparison between the most deflected and the least deflected in that case would be important to consider in the comparison as the difference between the most deflected and the least deflected is about 3 degrees, which is significant value to consider while designing an important part such as the back to shoulder connector. Specially that the bending in this case shall not be in high numbers are already the part is shorter than all other parts while having same area as the shoulder and forearm and also being subjected to same magnitude of force.

## **5 DISCUSSION**

### **5.1 General discussion**

As exoskeletons are having higher demand in industry section, it was important enough to research deep and find the available ones in the market and the known types of exoskeletons. As one of the forms of exoskeleton is the upper-body exoskeleton that is used for light weights that ranges from 10-25 kg, that was the focus of the research as there is already demand for such a product to assist workers in industry who have to lift objects in that range of weight multiple times a day which causes fatigue. The usage of exoskeleton eases the process for the workers and cause less problems to their muscles. As observation by looking at all the available upper-body exoskeletons that are used for industrial solutions, it is noticed that many of them have a frame body that is made out of pipes that are jointed together by different means. However, all the pipes are made of the same cross-section shape which is circular outer shape and circular inner shape. It is just using the normal standard pipes that are extruded, so it would be easy to extrude, weld, and form.

In the presented thesis, the focus is about finding out the best cross-section that can be used as the cross-section of the pipe that is extruded to be used to form the frame of the exoskeleton. The suggested shapes to be simulated are basically a mix of the geometrical shapes of circle, ellipse, and rectangle. There has been a switching of the aforementioned geometrical shapes between the inner and outer shape of the pipe. All the simulated cross-section shapes are presented in tables 3.1 and 3.2.

The areas of the cross-sections are kept being approximately equal to the standard circular pipes in ISO standard of aluminium pipes sizes. Aluminium 6262 alloy is chosen as the simulation material as this alloy is used in pipes forming by extrusion, which is a simple manufacturing method. Since the area and length of the same part of the exoskeleton are the same, so the cost of raw material will be the same. Moreover, the material selection is not the focus in this research, but it focuses on selecting the best cross-section for each part of the generic exoskeleton form that is shown in figure 3.1. Every part of the upper-body exoskeleton has different length and dimensions, so forces and moments in the simulation were adjusted accordingly as shown and explained in the methodology section.

The simulation was done for generic upper-body exoskeleton as using a specific case of a specific exoskeleton would require knowing very deep classified details that would be difficult to have access to due to policies of the companies that have upper-body exoskeletons that exist in the market.

After the validation of the tension tests that the material behaviour is acting as expected, the rest of the simulations were done as explained in the methodology section.

## 5.2 Discussion of the results

For shoulder part, it is found that the pipe of EISROS is having the best behaviour in tension for handling higher stress than all other pipe shapes with a slightly higher than all strain, and that slight difference is not a lot, and followed by CISEOS and EISCOS pipes that have a bit less stress to handle, but also the strain is low; therefore, they are the best 3 forms to be considered along with the other simulations of the shoulder part. When it comes to bending simulation of the shoulder part, the best behaviour pipes are EISCOS on X axis, CISEOS on Y axis, EISROS on Y-axis. As a conclusion EISROS-Y, CISEOS-Y, and EISCOS-X are having the best behaviour in both tension and bending. Therefore, those are the recommended best cross-sections to be used for pipes for the shoulder part, and the cost factor of manufacturing of each part would be the deciding factor about which one of the three to select.

For the forearm part, it is found that the tension values are so close to each other in stress and strain with a very slight difference; therefore, the differentiation between them would not matter much when considering only tension. The difference between the shape that has the highest tension and strain to the lowest one is less than 25 MPa in stress and less than 0,25% in strain. But, considering also mentioning the shapes that has best behaviours are EISEOS followed by RISROS then CISCOS respectively. Then, it would matter to consider the bending test simulation results for the forearm part. It is found that the least deflection is caused by EISCOS-X followed by CISROS-Y, then CISROS-C and the order afterwards goes as CISEOS-Y, EISROS-Y, RISROS-Y. It is very difficult in this case to find the best shape that would fit for both the tension and the bending simulation, but as the tension results are very close, the bending deflection would be the main criteria of selection in this case. As a result, the best recommended shapes are the CISROS-Y, CISROS-X, and EISCOS-X. The decision about which one would be the most cost efficient would matter about the selection, but in general, those are the best behaving shapes in mechanical aspect when subjected to the load.

For the back part, the simulation of the part is subjected to 3 kinds of loads, which are compression, torsion, and bending. In compression simulation, the results in general are insignificant, as the maximum stress is less than 70 MPa and maximum strain is less than 0,45%, which are relatively low numbers. There is a huge difference in the behavior of each shape in compression as the compression on each element of the surface that is subjected to the compression is different, and that makes huge difference in results as shown in figure 4.8. It is very difficult to decide about the best behaving shape in the

compression test, as stress and strain are very directly proportional in this case. When the stress is high, the strain is also high, and it is not possible to find two shapes having a stress or strain values that are close, except deciding about the worst shape which is CISEOS, as it has as much strain as CISCOS with less stress, but the difference in stress level also is insignificant. The torsion test simulation has clear results about which shapes have the least deflection, which is clearly CISCOS, followed by EISCOS, then CISEOS. However, as the most deflected shape is not even deflected by 0.45 deg, so the decision will not heavily be relying on the torsion test. The bending test in this case is the most significant factor to consider. The least deflected is RISROS-Y with a good gap until the following ones that are EISCOS-Y then CISCOS. The difference between the most and least deflected shapes in bending test are significant; therefore, the decision about what shape is the best will depend on it. As a result, the best shapes to consider for the back part is RISROS-Y, EISCOS-Y, and CISCOS. As RISROS-Y and EISCOS-Y are force vector dependent, and for the back part it is difficult to assure the bending stay in one direction, so the best cross section for the back part is CISCOS in mechanical behaviour aspect. Cost factor can also affect the decision.

For the back to shoulder connector part, only bending test simulation was done, as this is the main force that will be subjected to the part. The results are significant enough to consider for comparison between shapes. The best shapes that are making the least deflection are the pipes of CISROS-Y and EISCOS-X followed by CISROS-X, CISEOS-Y, and EISCOS-Y respectively. Those shapes all can be recommended if the vector of the force is known in every happening case, but if not known about the direction of the force, then the best behaving general shape is the CISROS as in X and Y axes it is behaving the best out of all other shapes.

It is noticed that through all the results that have been represented out of mechanical test simulations, the bending test simulation is always the most important test simulation to consider in comparing the shapes that are used for the part. Thus, the bending test simulation is the main criterion in selection in this range of force when the other tests are basically tension, compression, and torsion even when the nonlinearity is considered during all simulations.

Cost consideration would matter so much in the decision of choosing the cross-section, but as also the safety and durability of the product matters, this comparison is important to consider. Moreover, when the durability and ability of the exoskeleton is better, the long term cost of maintenance of the exoskeleton will affect the price, and as the price of the raw material is already fixed by having similar areas, so considering the represented comparison between cross-sections will affect the cost decision on long term aspect.

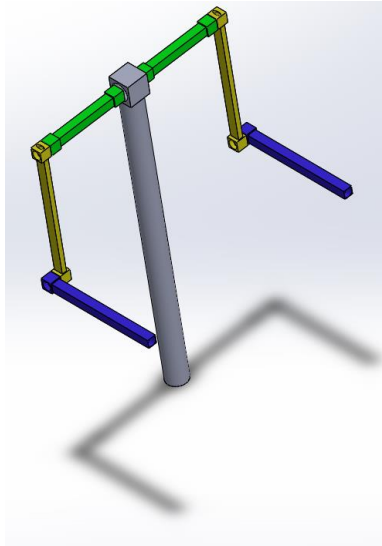


Figure 5.1 Generic upper-body exoskeleton with the best selected cross-section geometries for the pipes of the frame

### 5.3 Methodology to be followed

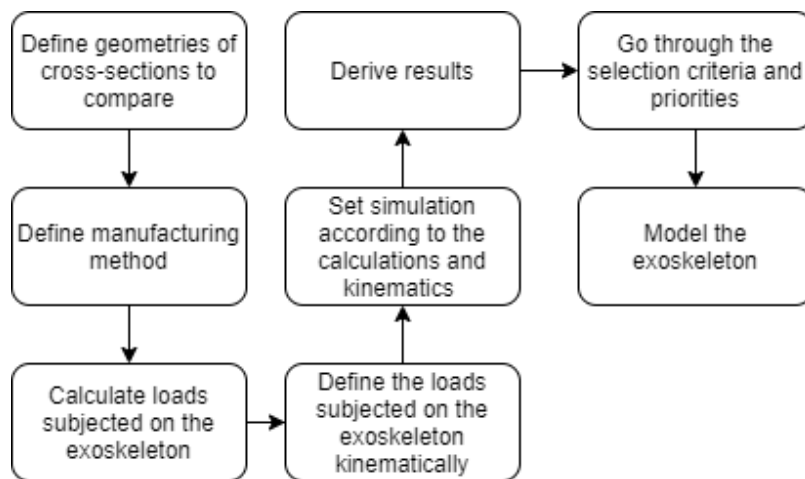


Figure 5.2 block diagram of the methodology of cross-section selection

The methodology that has been followed through this research is as shown in the previous figure. It starts by defining the available for manufacturing geometries and that would be suitable for the design of the exoskeleton while taking into consideration all the circumstances of the exoskeleton that is being designed.

Afterwards, the optimum manufacturing method to be defined according to the cost, availability, and manufacturability of each certain part. As the common design for exoskeleton parts is using pipes then weld them, so the easiest method would be extrusion for the pipes.

Next, to calculate all the loads that will be subjected on each part of the exoskeleton by knowing the exact conditions that the exoskeleton will be dealing with while using it in

its special environment. The factor of safety must be taken into consideration depending on the required standards of the place of usage of the exoskeleton.

The kinematic definition of the loads that will affect each part of the exoskeleton and then simulate each part separately to know the exact impact on the part while having all the previous steps defined and make the simulation similar to the conditions.

After doing the simulation, derive the right results from the simulation as each way of testing of a part would have different results that can be derived from the simulation.

In order to define what is the actual best cross-section geometry for the exoskeleton, there are selection criteria, which might differ from an exoskeleton to the other one, but there are general interests among many exoskeleton experts according to a survey as explained in selection criteria subsection in the methodology section.

Last, to model the exoskeleton for visualization purposes, and to make a final check on the possibility to use such model.

## **5.4 Plans of the future**

As there are some limitations that are mentioned in limitations subsection, so for sure there are some plans that can be done in the future.

One of the plans to be considered for the future is to use an actual existing exoskeleton and use the defined cross-sections for pipes and compare the difference in performance between the already existing one and the one that has the recommended cross-sections.

In addition to, to study the mixing of forces representation for the same part, to get somewhat a close representation to the real situation stress that is subjected to each part of the upper-body exoskeleton.

A full body exoskeleton can be also studied in the same manner for further development in the cross-section selection of the body frame of the exoskeletons in general.

Moreover, a physical model can be developed to be tested for each part and if successful, that would be a prototype of an exoskeleton that can contribute in the development processes of the current exoskeletons.

The design of the exoskeleton can be more detailed and not generic, so there will be more parts to evaluate, but that can be done after narrowing down to a specific case.

The actuators and electronics peripherals placement places can be considered for the future simulation, as well as the selection of each of them.

Additionally, the material selection process for the exoskeleton while taking into consideration all the standards, hazards, and requirements of the exoskeleton design for industrial applications can be done as further development.

## 6 CONCLUSION

Exoskeletons recently are being used in several applications such as military, medical, and industrial applications, and even more. After comprehensive research about the current situation of the upper-limb exoskeletons that are used to help working labour in industry applications existing in research or market level, it is found that there is lack of definite cross-section selection method for the exoskeleton parts. Therefore, a methodology has been created through this thesis and the methodology is used for a case of designing a generic exoskeleton, and the methodology showed success of being useful in the decision about cross-section selection. As the results showed that using the standard hollow circular shaped pipes is not the best in all cases or all parts, but other shapes and geometries are more successful in some parts.

The comparison between different cross-section geometries was heavily relying on mechanical behaviour, as the area of the different cross-section geometries are kept being approximately the same. The mechanical behaviour comparison means to compare which cross-section geometry will be least deformed while being subjected to the same loads that is subjected also to all cross-section geometries of the same part. The less deflection the better. The geometrical shapes that are used to create the cross-section geometries are circle, rectangle, and ellipse. Mixing the aforementioned shapes between inner and outer profile of the cross-section geometry would result in many geometries, and those geometries are the ones that are compared together while keeping almost constant area as the standard hollow circular shaped pipes dimensions in ISO standard.

The research that is conducted has used simulation and validation. Each part of the exoskeleton is simulated separate, then the loads and boundary conditions are set as well as all other simulation settings. The results of tension tests that are done for the parts were validated by comparison of the yield point that is derived from the resulted data and the yield stress data of the used material. The material that is used in the simulation is Aluminium 6262 alloy. This alloy is used for pipes, and usually it is extruded to create pipes.

Extrusion is a common manufacturing method that is used to manufacture pipes. Different cross-section geometries can be extruded. Extrusion is selected to be the suggested method for manufacturing of the pipes due to availability and manufacturability as well as cost aspect.

The simulations were testing parts of the generic exoskeleton parts, as using a specific case of an exoskeleton would be challenging due to hardship of access to classified details of exoskeletons that are existing in the market. However, the methodology can

be used for such exoskeletons and contribute in developing the performance of the exoskeleton in mechanical aspect.

The generic model that is created for the upper body exoskeleton contains of 4 main parts, which are the shoulder, back, forearm, and back to shoulder connector parts.

The simulations that are held are simulating testing of the parts, such as tension, compression, bending, and torsion tests. Each part is subjected to different kind of loading, and the loading type of each part is separate from other parts. The loading analysis and kinematics are done to simulate the lifting process as the exoskeleton is supposedly to be used for lifting in the industry applications. The assumed load was 20 kg for the simulation adding a factor of safety of 1.5, so the simulated mass that makes the load was 30 kg.

After the simulations are held for each part with different cross-sections, it has been concluded that the best cross-section geometry in the generic exoskeleton for shoulder part is EISROS-Y. EISROS-Y means that the best cross-section geometry to be used for the shoulder part is the Ellipse Inner Shape and Rectangular Outer Shape (EISROS) but when subjected to bending on Y-axis, so the longer side of the rectangle will be parallel to the body to take the bending.

For the forearm part, the best mechanically behaving cross-section geometry is CISROS. That means that Circular Inner Shape and Rectangular Outer Shape (CISROS) cross-section geometry is the best to be used for forearm part.

For the back part, the best mechanically behaving cross-section geometry is CISCOS. That means that Circular Inner Shape and Circular Outer Shape (CISCOS) cross-section geometry is the best to be used for the back part, which is basically the ISO standard dimensions pipe without change in the cross-section geometry.

For the back to shoulder connector, the cross-section geometry that makes the best mechanical behaviour is CISROS-Y, so the longer side of the rectangular outer shape will be parallel to the body, so the best bending behaviour will be obtained.

The bending results of each part were the most influential as it makes major effect on the part in each simulation that has been done.

The cost is the main consideration of the selection process, as it is the most important factor to consider while designing an exoskeleton according to the experts that are involved in exoskeleton design and production. Moreover, it is important also to consider other factors that are considered important as well which are safety and durability.

The methodology would help in developing the safety and durability of the exoskeleton, while maintaining the cost of the raw material used for the manufacturing of the exoskeleton. Therefore, that would make the long-term cost reduced.

In the future, there is a room for development of the methodology and further validate its results through experiments.

## 7 SUMMARY

Exoskeletons are having higher demand by more time in many applications. One type of the exoskeletons is the upper-body exoskeleton. The upper-body exoskeletons that exist in the market for industrial applications have a common general feature of having a body that is shaped out of pipes that are welded or assembled. Therefore, the focus of the presented thesis is to find out the best cross-section of a pipe that can be used for each part of the upper-body exoskeleton. Assuming a load of 20 kg and factor of safety of 1,5, the simulation was done for each part of the exoskeleton with all possible geometries that can be manufactured using the extrusion method as easy manufacturing method for pipes. The area and volume of the same part with different cross-section geometries are kept the same, so the cost of the raw materials will be kept constant. The material selected for the simulation was aluminium 6262 alloy.

The upper-body exoskeleton was simulated in generic form as four parts that are back, forearm, shoulder, and back to shoulder connector.

In results, each part had different cross-section geometry that would behave the best in mechanical aspect.

The best cross-sections for the shoulder part are EISROS-Y, CISEOS-Y, and EISCOS-X as those are having the best behaviour in both tension and bending.

The best cross-section for the back part is CISCOS as the back part is difficult to assume only one vector of bending force unto the part.

The best cross-sections for the forearm part are CISROS-Y, CISROS-X, and EISCOS-X.

The best cross-sections for the back to shoulder connector part is CISROS as in X and Y axes it is behaving the best out of all other shapes

The cost factor can play a major role in choosing which cross-section will be the best out of the chosen best, as those are having almost equal results in simulation of mechanical behaviour aspect.

It is also noticed that the best aspect to consider in the simulation and results while comparing different cross-section geometries is the bending test simulation, as this test simulation is the one that makes a huge difference between shapes results and affect the decision of knowing which cross-section geometry is the best.

There is a plenty of room for development also in the field as mentioned in the plans of the future subsection. The developments could be in research aspect and in development of the current exoskeletons in the market.

## 8 KOKKUVÕTE

Mitmes valdkonnas nõudlus välisskelettide järgi on jõudselt kasvanud. Välisskeleti üks tüüpidest on ülajäseme välisskelett (eksoskelett). Turul pakutavate tööstuslikuks kasutamiseks ettenähtud välisskelettide ühiseks jooneks on torukujulistest profiilidest kokku keevitatud või monteeritud kere. Seepärast antud lõputöö eesmärgiks on uurida välja iga ülajäseme välisskeletti komponendi sobilikuma ristlõikega profiili. Ekstrudeerimise teel valmistatavate välisskeletti komponendi kõikide ristlõigete variatsioonide kohta on teostatud simulatsioonid arvestades 20 kg koormusega ja 1,5 kordse ohutusteguriga. Välisskeletti sarnaste komponentide erineva sisemise kujuga profiilide ristlõige pindala ja ruumala on hoitud võrdseks, seega materjali omahind on olnud konstantne. Simulatsioonide tegemiseks profiilide materjaliks on valitud 6262 alumiiniumi sulam.

Välisskeletti ülajäseme simuleerimiseks kasutatud üldkuju koosneb neljast komponendist: selg; käsivars; õlg ning õla ja selja ühenduskoht.

Vastavalt mehaanilisele koormamisele simulatsioonide tulemusena on igal komponendil saadud erinev ristlõige kuju.

Õla komponendi tõmbe- ja painde koormamisel parima tulemusega ristlõige kujud on EISROS-Y, CISEOS-Y ja EISCOS-X.

Selja profiili sobilikuma ristlõikega kujuks on osutunud CISCOS, sest selja komponendile mõjuvad mitte ainult ühesuunalised jõuvektorid.

Käsivarre parema tulemusega profiili ristlõige kujud on CISROS-Y, CISROS-X, and EISCOS-X.

Õla ja selja ühenduskomponendi sobilikuma ristlõige kujuga on CISROS profiil, sest ta käitub kõige paremini nii X kui ka Y teljel avaldatud koormamisel.

Optimaalse ristlõige kuju valimisel pakutud parimate tulemustega ristlõigete seas suure tähtsusega teguriks saab olla maksumuse hinnang, sest erineva kujuga profiilide simuleerimisel saadud mehaanilise käitumise tulemused on peaaegu võrdsed.

Peab olema väljatoodud et erinevate ristlõigete kujude simuleerimise tulemuste parema võrdluse saamiseks tuleb kasutada painde koormamise skeemi simulatsiooni, sest antud simulatsiooni tulemused toovad välja ristlõigete kujude erinevused ja võimaldavad teadlikuma otsuse tegemist ristlõigete kuju valimisel.

Tuleviku plaanide osas on mainitud mitmed potentsiaalsed arenguvaldkonnad. Arendustegevused on võimalik siduda nii teadus- ja arendustegevuse aspektidega kui ka turul olemasolevate välisskelettide arendamisega.

## 9 LIST OF REFERENCES

- [1] "Definition of exoskeleton," [Online]. Available: <https://www.merriam-webster.com/dictionary/exoskeleton?src=search-dict-box>. [Accessed 1 February 2019].
- [2] H. Kazerooni, "Exoskeletons for Human Performance Augmentation," in *Springer Handbook of Robotics*, 2008.
- [3] D. P. Ferris and A. J. Young, "Exoskeleton (Robotics)," in *Encyclopedia of Biomedical Engineering*, Elsevier, 2019.
- [4] H. Herr, "Exoskeletons and orthoses: classification, design challenges and future directions," *Journal of NeuroEngineering and Rehabilitation*, p. 6:21, 2009.
- [5] "1965-71 – G.E. Hardiman I Exoskeleton – Ralph Mosher (American)," General Electric, 4 April 2010. [Online]. Available: <http://cyberneticzoo.com/man-amplifiers/1966-69-g-e-hardiman-i-ralph-mosher-american/>. [Accessed 2 February 2019].
- [6] M. Bellis, "Exoskeleton," 6 April 2017. [Online]. Available: <https://www.thoughtco.com/exoskeleton-for-humans-1991602>. [Accessed 5 January 2019].
- [7] "Timeline," [Online]. Available: <http://www.theyshallwalk.org/about/timeline/>. [Accessed 5 January 2019].
- [8] B. Marinov, "Types And Classifications of Exoskeletons," 19 August 2015. [Online]. Available: <https://exoskeletonreport.com/2015/08/types-and-classifications-of-exoskeletons/>. [Accessed 5 January 2019].
- [9] "Exhauss," Exhauss System, [Online]. Available: <http://www.exhauss.com/index.html>. [Accessed 30 January 2019].
- [10] "EksoVest," EksoBionics, [Online]. Available: <https://eksobionics.com/eksoworks/eksovest/>. [Accessed 5 January 2019].
- [11] "LegX," SuitX, [Online]. Available: <https://www.suitx.com/legx>. [Accessed 5 January 2019].
- [12] "HAL for Medical Use," Cyberdyne, [Online]. Available: [https://www.cyberdyne.jp/english/products/LowerLimb\\_medical.html](https://www.cyberdyne.jp/english/products/LowerLimb_medical.html). [Accessed 30 January 2019].
- [13] "Guardian™ XO," Sarcos, [Online]. Available: <https://www.sarcos.com/products/guardian-xo/>. [Accessed 30 January 2019].
- [14] "Human Augmentation," [Online]. Available: <https://www.gartner.com/it-glossary/human-augmentation>. [Accessed 5 January 2019].
- [15] H. Herr, "Robotics for Human Augmentation," [Online]. Available: <https://www.sciencemag.org/journals/robotics/human-augmentation>. [Accessed 5 January 2019].
- [16] D. Clode, "The Third Thumb," [Online]. Available: <https://www.daniclodedesign.com/thethirdthumb>. [Accessed 5 January 2019].
- [17] C. H.-L. Kao, A. Roseway, C. Holz, P. Johns, A. Calvo and C. Schmandt, "DuoSkin," MIT Media Lab, 2016. [Online]. Available: <https://duoskin.media.mit.edu>. [Accessed 5 January 2019].
- [18] "Airbag For Urban Cyclists," Hovding, [Online]. Available: <https://hovding.com>. [Accessed 2 February 2019].
- [19] S. Forge and C. Blackman, *A Helping Hand for Europe: The Competitive Outlook for the EU Robotics Industry*, Luxembourg: Publications Office of the European Union, 2010.

- [20] D. Kara, "Industrial exoskeletons: new systems, improved technologies, increasing adoption," 6 December 2018. [Online]. Available: <https://www.therobotreport.com/industrial-exoskeletons/>. [Accessed 5 January 2019].
- [21] A. S. Gorgey, "Robotic exoskeletons: The current pros and cons," *World Journal of Orthopedics*, vol. 9, no. 9, pp. 112-119, 18 September 2018.
- [22] "ATOUN MODEL A," ATOUN, [Online]. Available: <http://atoun.co.jp/products/atoun-model-a>. [Accessed 10 November 2019].
- [23] "ATOUN MODEL Y," ATOUN, [Online]. Available: <http://atoun.co.jp/products/atoun-model-a>. [Accessed 10 November 2019].
- [24] "Muscle Upper," Innophys, [Online]. Available: <https://innophys.jp/en/product/upper/>. [Accessed 10 November 2019].
- [25] G.-P. Zehil, "A combined analytical and computational approach to the structural behavior of composite tubes," in *3rd International Conference on Advances in Computational Tools for Engineering Applications (ACTEA)*, 2016.
- [26] G. Ma, M. Lin and Q. Wang, "Mechanical Design of a Whole-arm Exoskeleton Rehabilitation Robot Based on PNF," in *13th International Conference on Ubiquitous Robots and Ambient Intelligence (URAI)*, Xian, 2016.
- [27] H. Seo and S. Lee, "Design and Experiments of an Upper-Limb Exoskeleton Robot," in *14th International Conference on Ubiquitous Robots and Ambient Intelligence (URAI)*, Jeju, 2017.
- [28] B. Beigzadeh, M. Ilami and S. Najafian, "Design and Development of One Degree of Freedom Upper Limb Exoskeleton," in *RSI International Conference on Robotics and Mechatronics*, Tehran, 2015.
- [29] M. Mahdavian, A. Yousefi-Koma and A. G. Toudeshki, "Design and Fabrication of a 3DoF Upper Limb Exoskeleton," in *RSI International Conference on Robotics and Mechatronics*, Tehran, 2015.
- [30] G. C. Wan, F. Z. Zhou, C. Gao and M. S. Tong, "Design of Joint Structure for Upper Limb Exoskeleton Robot System," in *Progress In Electromagnetics Research Symposium*, Singapore, 2017.
- [31] H.-C. Hsieh, L. Chien and C.-C. Lan, "Dimensional Synthesis of a Lightweight Shoulder Exoskeleton," in *IEEE International Conference on Advanced Intelligent Mechatronics (AIM)*, Busan, 2015.
- [32] Y. Rosales, R. Lopez, I. Rosales, S. Salazar and R. Lozano, "Design and Modeling of an Upper Limb Exoskeleton," in *19th International Conference on System Theory, Control and Computing (ICSTCC)*, Cheile Gradistei, 2015.
- [33] Z. Cheng, S. Foong, D. Sun and U.-X. Tan, "Towards a multi-DOF Passive Balancing Mechanism for Upper Limbs," in *IEEE International Conference on Rehabilitation Robotics (ICORR)*, Singapore, 2015.
- [34] M. V. Pawar, S. Ohol and A. Patil, "Modelling and Development of Compressed Air Powered Human Exoskeleton Suit Human Exoskeleton," in *Reliability, Infocom Technologies and Optimization (Trends and Future Directions) (ICRITO)*, Noida, 2018.
- [35] L. Chen, C. Zhang, Z. Liu and T. Zhang, "Evaluation of Muscle Fatigue Based on CRP and RQA for Upper Limb Exoskeleton," in *2018 Chinese Automation Congress (CAC)*, Xian, 2018.
- [36] M. Möller, L. Hallin and M. Veljkovic, "LIMIT ANALYSIS INTERACTION FORMULAE FOR THIN-WALLED & MODERATELY THICK-WALLED PIPES SUBJECTED TO PRESSURE & PIPE BENDING," in *Proceedings of the ASME 2013 Pressure Vessels and Piping Conference*, Paris, 2013.
- [37] D.-S. Shim, K.-P. Kim and K.-Y. Lee, "Double-stage forming using critical pre-bending radius in roll bending of pipe with rectangular cross-section," *Journal of Materials Processing Technology*, no. 236, pp. 189-203, 2016.

- [38] C. Li, L. Xie, Y. Xie, B. Zhao, Z. Hu, H. Zhao and W. Yin, "A computational method of stress intensity factor for flat-oval cross-section thin-walled pipe," *International Journal of Pressure Vessels and Piping*, no. 171, pp. 299-304, 2019.
- [39] C. Han, S. Tan, J. Zhang and C. Zhang, "Simulation investigation of dent behavior of steel pipe under external load," *Engineering Failure Analysis*, no. 90, pp. 341-354, 2018.
- [40] W. Yang, C. Zhang, D. Liu, J. Tu, Q. Yan and Y. Fang, "The effect of cross-sectional shape on the dynamic response of tunnels under train induced vibration loads," *Tunnelling and Underground Space Technology*, no. 90, pp. 231-238, 2019.
- [41] Y. Tokovyy and C.-C. Ma, "Axisymmetric Stresses in an Elastic Radially Inhomogeneous Cylinder Under Length-Varying Loadings," *Journal of Applied Mechanics*, vol. 83, 2016.
- [42] J. Gomes, J. Belinha, L. Dinis and R. N. Jorge, "The structural analysis of chitosan tubes using meshless methods," in *IEEE 5th Portuguese Meeting on Bioengineering (ENBENG)*, Coimbra, 2017.
- [43] K. Mulenga, C.-Q. Li and M. Xie, "Reliability Assessment of Metals with Corrosion Defects under Axial Tension Loading using Damage Tolerance Analysis," in *Annual Reliability and Maintainability Symposium (RAMS)*, Orlando, 2019.
- [44] Y. Sun, S. Hu, Y. Huang and X. Xue, "Analytical stress model for embedded bar-wrapped cylinder concrete pressure pipe under internal load," *Thin-Walled Structures*, 2019.
- [45] H. Al-jabbouli, E. Koç and Y. Akça, "Classification of Main Faults in the Production Process of Extruded Aluminium Profiles," *International Journal of Engineering and Technology (IJET)*, vol. 7, no. 1, pp. 84-90, 2015.
- [46] "Comparison ISO / ANSI Piping System," OSTP, [Online]. Available: [https://www.ostp.biz/sites/313/content/docs/OSTP\\_Comparison\\_ISO\\_ANSI\\_20141014.pdf](https://www.ostp.biz/sites/313/content/docs/OSTP_Comparison_ISO_ANSI_20141014.pdf). [Accessed 10 April 2020].
- [47] M. AH, Mathias KJ and S. FW, "Measurement of the bony anatomy of the humerus using magnetic resonance imaging," in *Proceedings of the Institution of Mechanical Engineers*, 2002.
- [48] I. Busscher, J. J. W. Ploegmakers, G. J. Verkerke and A. G. Veldhuizen, "Comparative anatomical dimensions of the complete human and porcine spine," *European Spine Journal*, vol. 19, pp. 1104-1114, 2010.
- [49] U. Fischer, M. Heinzler, F. Näher, H. Paetzold, R. Gomeringer, R. Kilgus, S. Oesterle and A. Stephan, *Mechanical and Metal Trades Handbook*, Haan-Gruiten: Europa Lehrmittel, 2008.
- [50] M. Guide, "Direct hollow extrusion," [Online]. Available: <https://www.manufacturingguide.com/en/direct-hollow-extrusion>. [Accessed 14 May 2020].
- [51] W. Z. Misiolek and V. K. Sikka, "Physical and Numerical Analysis of Extrusion Process for Production of Bimetallic Tubes," August 2006. [Online]. Available: <https://www.osti.gov/servlets/purl/889030>. [Accessed 06 May 2020].
- [52] W. Xianghong, Z. Guoqun, L. Yiguo and M. Xinwu, "Numerical simulation and die structure optimization of an aluminum rectangular hollow pipe extrusion process," *Materials Science and Engineering: A*, Vols. 435-436, pp. 266-274, 2006.
- [53] M. K. Choi, C.-G. Park, Y. Choi and T.-Y. Won, "Aluminum tube extrusion with the porthole die for deconcentrated welding lines," *Journal of Mechanical Science and Technology*, vol. 32, pp. 2245-2251, 2019.

- [54] E. A. Association, "Products – Automotive tubes," 2002. [Online]. Available: <https://www.european-aluminium.eu/media/1540/aam-products-3-automotive-tubes.pdf>. [Accessed 06 May 2020].
- [55] M. Abdelmomen, F. O. Dengiz, H. Samir and M. Tamre, "Research on Upper-Body Exoskeletons for Performance Augmentation of Production Workers," in *30th DAAAM International Symposium on Intellegent Manufacturing and Automation*, Zadar, 2019.
- [56] E. A. Avallone and T. B. III, *Mark's Standard Handbook For Mechanical Engineers*, New York: McGRAW-HILL, 1916.
- [57] "6262-T651 Aluminum," MakeItFrom, 08 November 2019. [Online]. Available: <https://www.makeitfrom.com/material-properties/6262-T651-Aluminum>. [Accessed 8 April 2020].
- [58] G. Mall, M. Hubig, A. Büttner, J. Kuznik, R. Penning and M. Graw, "Sex determination and estimation of stature from the long bones of the arm," *Forensic Science International Journal*, vol. 117, pp. 23-30, 2001.
- [59] G. Kayalioglu, "The Vertebral Column and Spinal Meninges," in *The Spinal Cord*, Elsevier, 2009, pp. 17-36.
- [60] N. Zarzycka and S. Załuska, "Measurements of the forearm i inhabitants of the Lublin region," *Annals Universitatis Mariae Curie- Skłodowska Medicina Journal*, vol. 44, pp. 85-92, 1989.
- [61] K. Nagarchi, J. P. T, S. H. Saheb, K. Brekeit and M. alharbi, "Morphometry of Clavicle," *Journal of Pharmaceutical Sciences and Research*, vol. 6, no. 2, pp. 112-114, 2014.
- [62] J. M. (. Holt, *Structural alloys handbook*, West Lafayette, Ind., USA: CINDAS/Purdue University, 1996.
- [63] H. E. Boyer and T. L. Gall, *Metals Handbook*, Metals Park, Ohio, USA: American Society for Metals, 1985.
- [64] P. Mukhopadhyay, "Alloy Designation, Processing, and Use of AA6XXX Series Aluminium Alloys," *ISRN Metallurgy*, vol. 2012, 2012.
- [65] "Static stress analysis," [Online]. Available: <https://abaqus-docs.mit.edu/2017/English/SIMACAEANLRefMap/simaanl-c-static.htm>. [Accessed 25 April 2020].
- [66] "Configuring a dynamic, explicit procedure," [Online]. Available: <https://abaqus-docs.mit.edu/2017/English/SIMACAECAERefMap/simacae-t-simconfiguredynamicexplicit.htm>. [Accessed 25 April 2020].
- [67] G. M.V, G. R.B and N. P.D, "Finite Element Analysis of frame with square meshing & radial meshing in Soil Structure Interaction," *International Journal Of Modern Engineering Research (IJMER)*, vol. 5, no. 3, pp. 16-22, 2015.
- [68] D. S. Lo, "Mesh Generation on planar domain," in *Finite Elment Mesh Generation*, New York, CRC Press, 2015, pp. 84-85.
- [69] C. Leser, "Tensile Properties & the Tension Test," [Online]. Available: [https://www.mts.com/university/Tension\\_Test.pdf](https://www.mts.com/university/Tension_Test.pdf). [Accessed 10 April 2020].
- [70] N. Mavrodontis, "Converting Engineering Stress-Strain to True Stress-Strain in Abaqus," 9 October 2017. [Online]. Available: <https://info.simuleon.com/blog/converting-engineering-stress-strain-to-true-stress-strain-in-abaqus>. [Accessed 10 April 2020].
- [71] L. N. Trefethen, "Is Gauss Quadrature Better than Clenshaw–Curtis?," *Society for Industrial and Applied Mathematics*, vol. 50, no. 1, pp. 67-87, 2008.
- [72] H. F. Abdalla, "Load carrying capacities of pressurized 90 degree miter and smooth bends subjected to monotonic in-plane and out-of-plane bending loadings," *International Journal of Pressure Vessels and Piping*, vol. 171, pp. 253-270, 2019.

- [73] T. M. Schnieders, "A top-down human-centered approach to exoskeleton design," 2019. [Online]. Available: <https://lib.dr.iastate.edu/cgi/viewcontent.cgi?article=8103&context=etd>. [Accessed 20 April 2020].

# 10 APPENDIX

## 10.1 Validation of tension test simulation

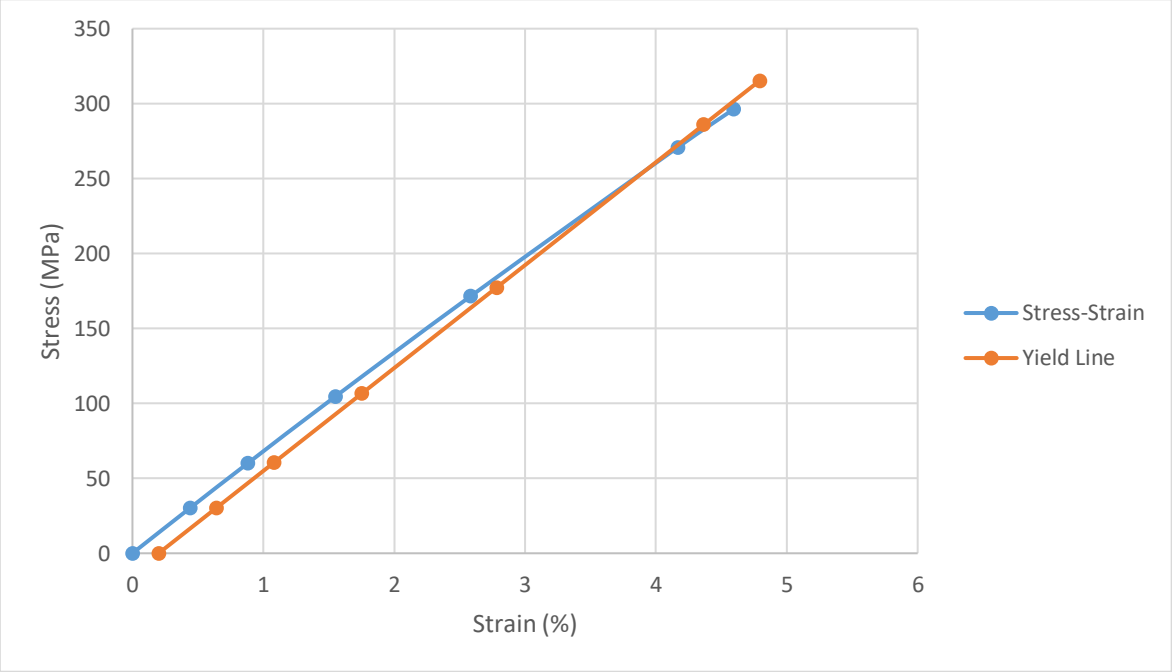


Figure 10.1: Tensile test stress-strain curve with yield line for validation of RISROS for shoulder part

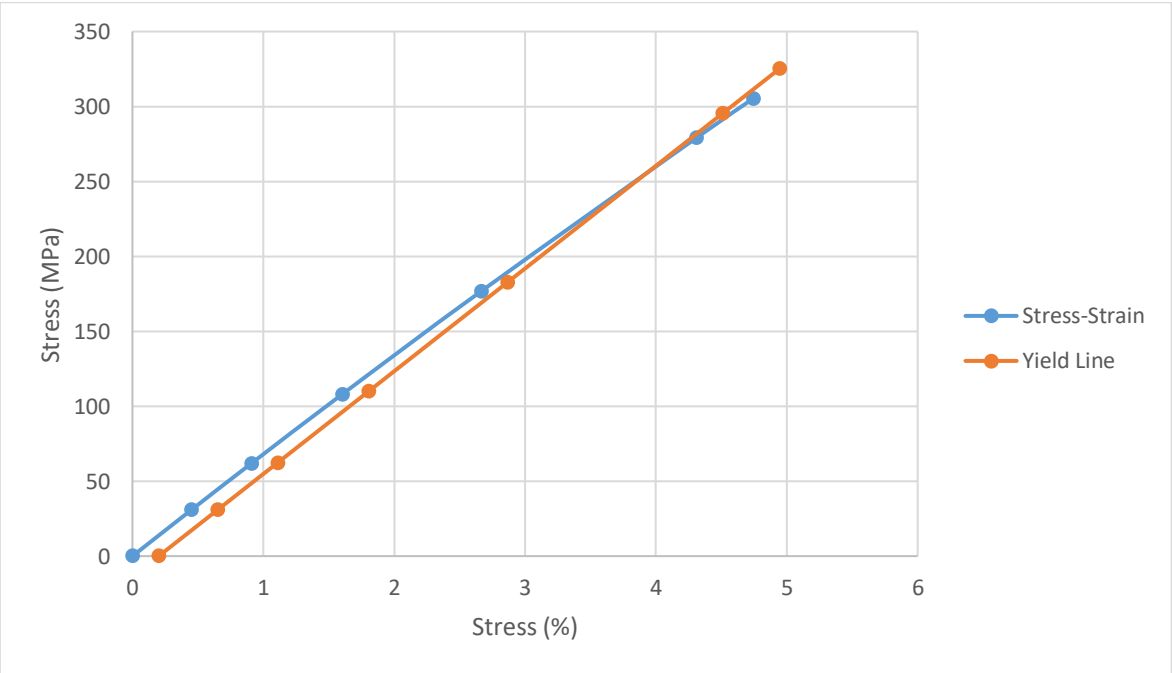


Figure 10.2: Tensile test stress-strain curve with yield line for validation of EISEOS for shoulder part

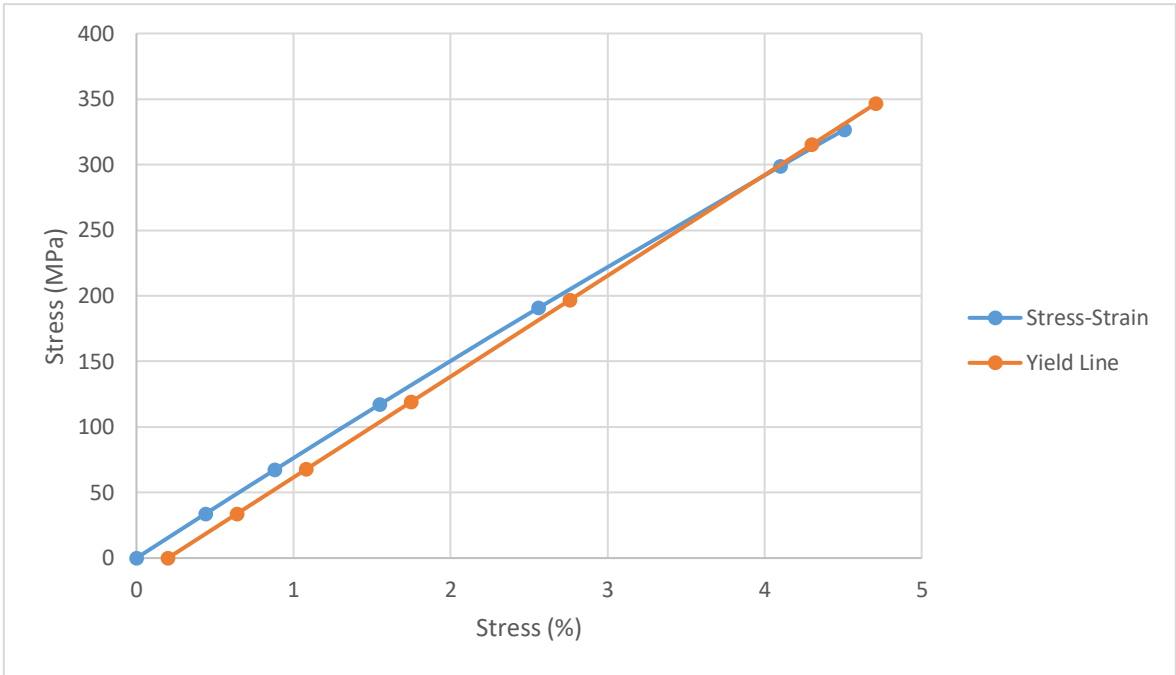


Figure 10.3: Tensile test stress-strain curve with yield line for validation of EISCOS for shoulder part

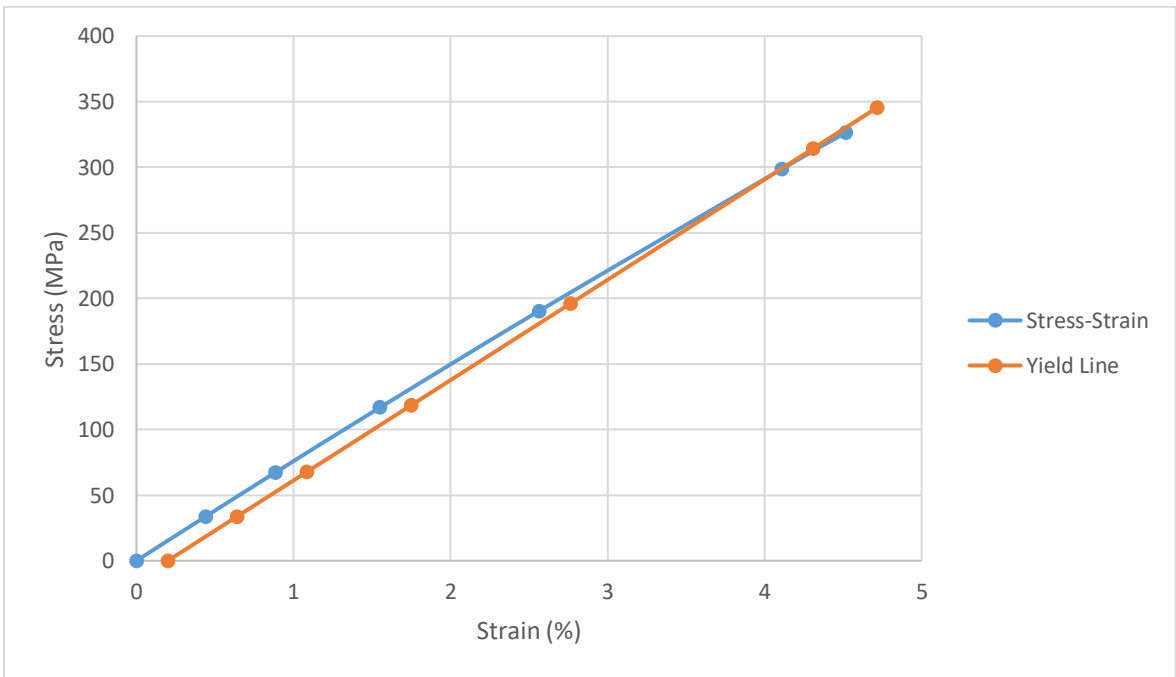


Figure 10.4: Tensile test stress-strain curve with yield line for validation of CISEOS for shoulder part

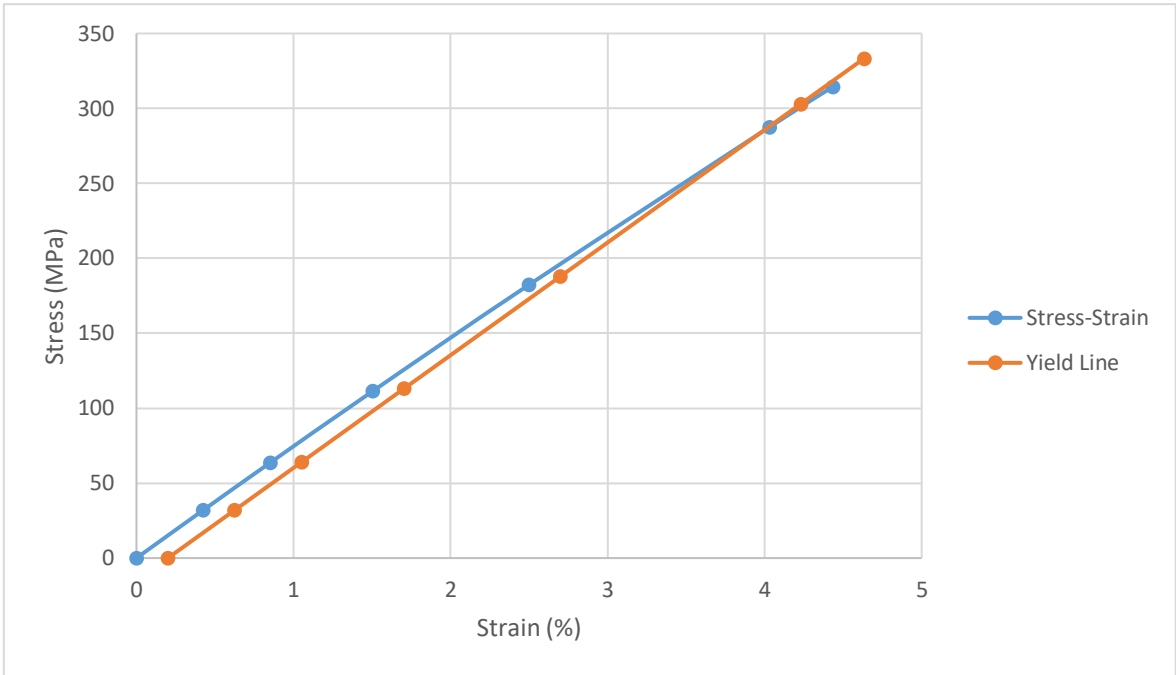


Figure 10.5: Tensile test stress-strain curve with yield line for validation of CISROS for shoulder part

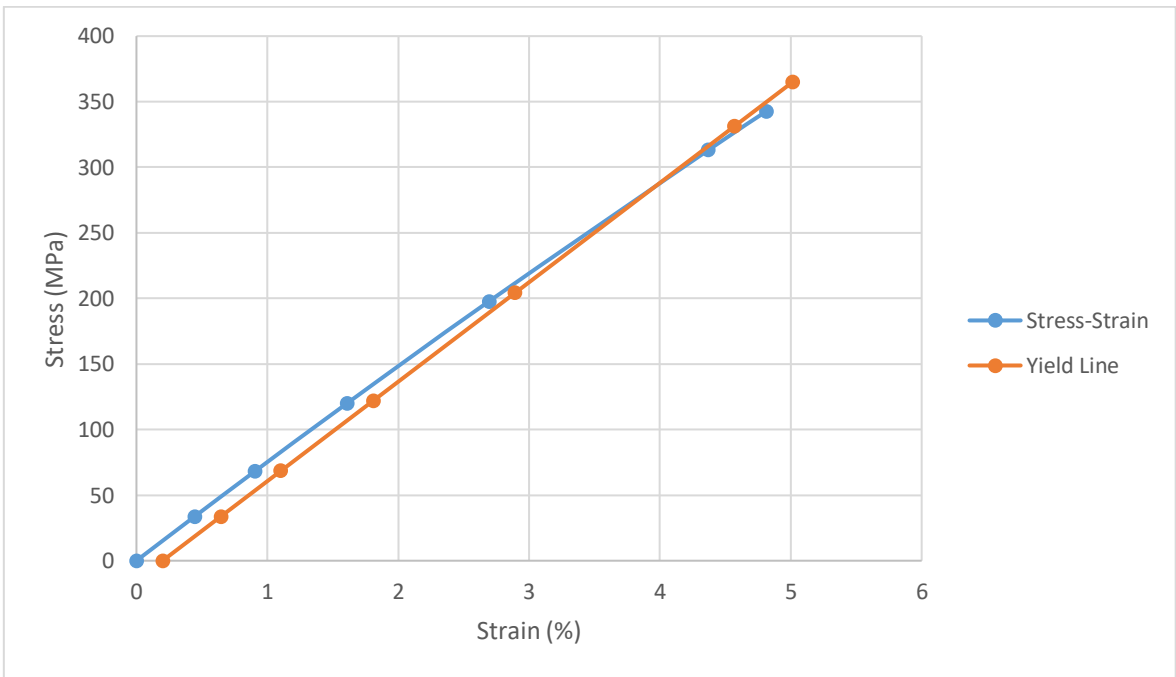


Figure 10.6: Tensile test stress-strain curve with yield line for validation of EISROS for shoulder part

## 10.2 Test simulation for Shoulder part using different cross-section geometries

### 10.2.1 CISCOS cross-section geometry for shoulder part test simulations

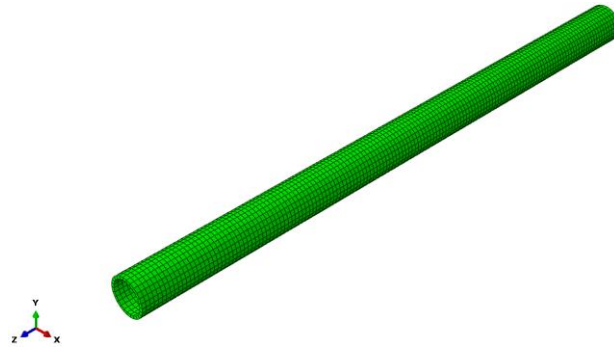


Figure 10.7 Shoulder part with CISCOS cross-section geometry meshed at rest

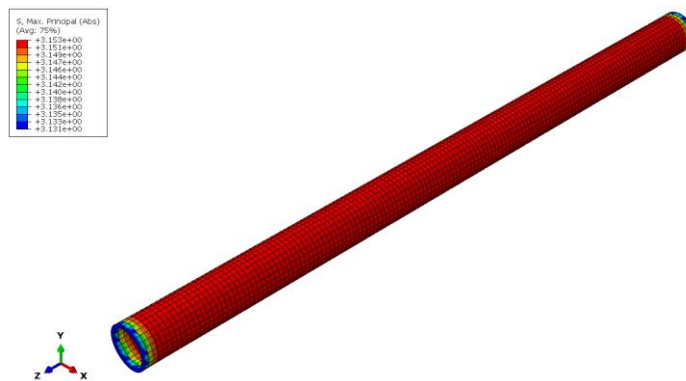


Figure 10.8 Shoulder part with CISCOS cross-section geometry meshed and subjected to tension

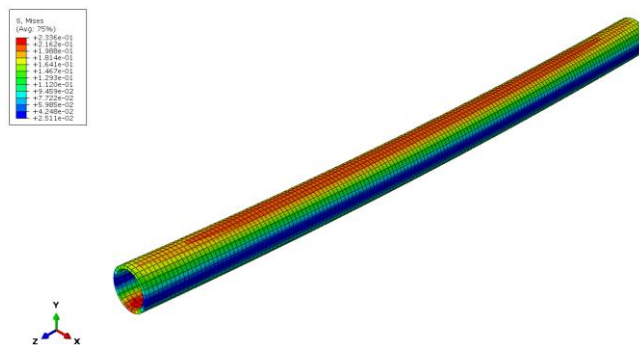


Figure 10.9 Shoulder part with CISCOS cross-section geometry meshed and subjected to bending

## 10.2.2 RISROS cross-section geometry for shoulder part test simulations

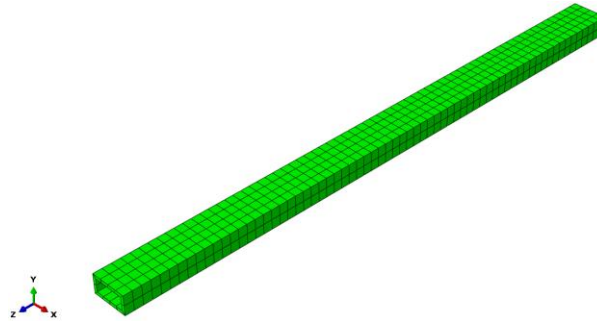


Figure 10.10 Shoulder part with RISROS cross-section geometry meshed at rest

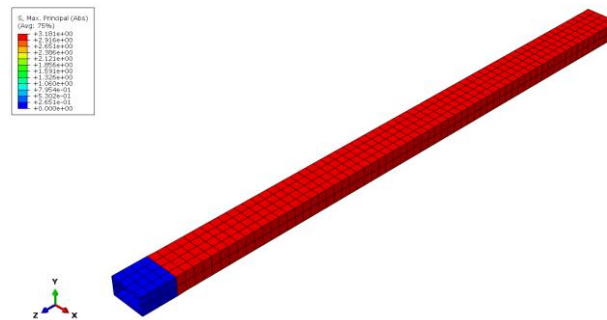


Figure 10.11 Shoulder part with RISROS cross-section geometry meshed and subjected to tension

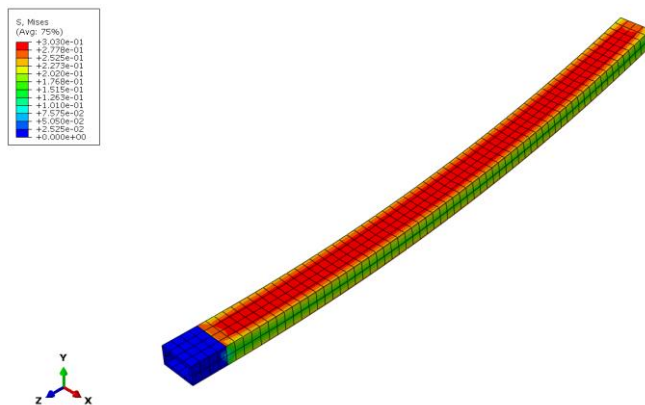


Figure 10.12 Shoulder part with RISROS cross-section geometry meshed and subjected to bending about X-axis

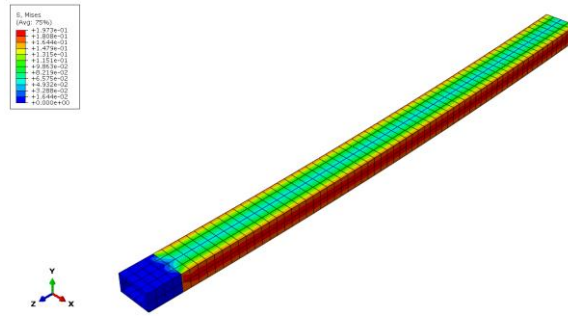


Figure 10.13 Shoulder part with RISROS cross-section geometry meshed and subjected to bending about Y-axis

### 10.2.3 EISEOS cross-section geometry for shoulder part test simulations

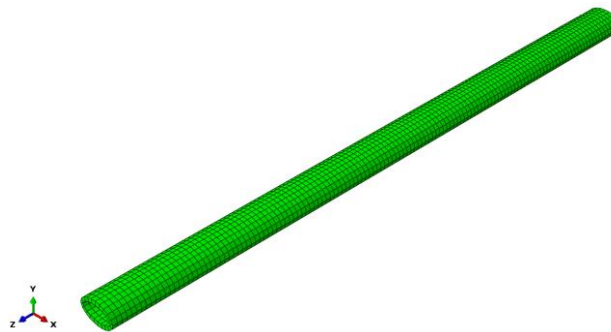


Figure 10.14 Shoulder part with EISEOS cross-section geometry meshed at rest

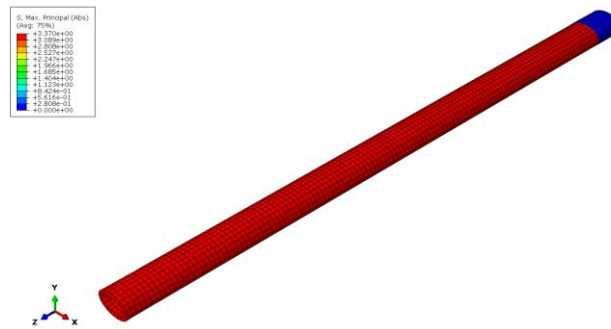


Figure 10.15 Shoulder part with EISEOS cross-section geometry meshed and subjected to tension

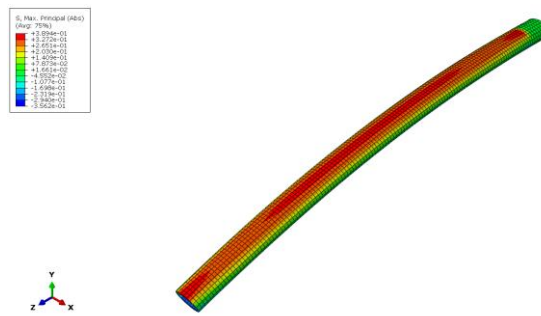


Figure 10.16 Shoulder part with EISEOS cross-section geometry meshed and subjected to bending about X-axis

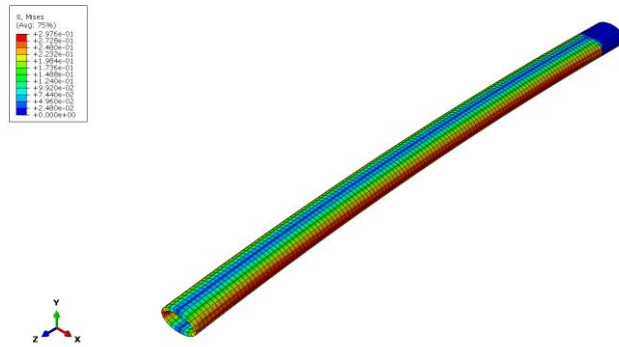


Figure 10.17 Shoulder part with EISEOS cross-section geometry meshed and subjected to bending about Y-axis

### 10.2.4 EISCOS cross-section geometry for shoulder part test simulations

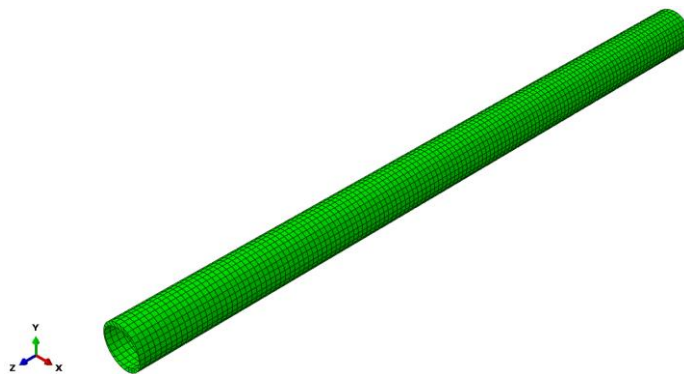


Figure 10.18 Shoulder part with EISCOS cross-section geometry meshed at rest

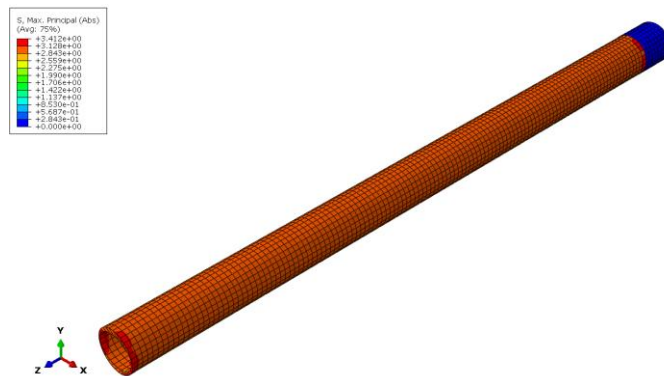


Figure 10.19 Shoulder part with EISCOS cross-section geometry meshed and subjected to tension

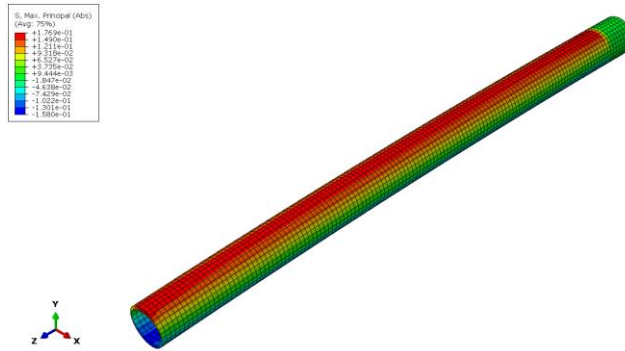


Figure 10.20 Shoulder part with EISCOS cross-section geometry meshed and subjected to bending about X-axis

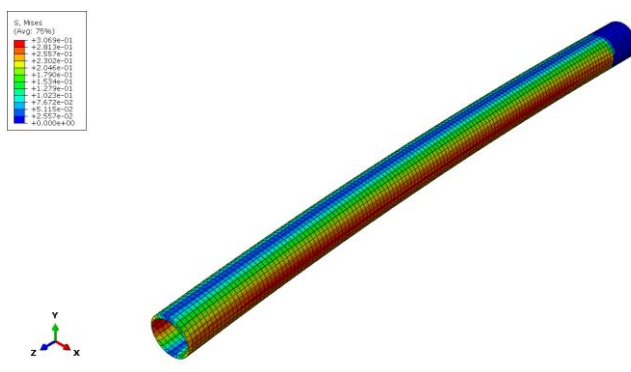


Figure 10.21 Shoulder part with EISCOS cross-section geometry meshed and subjected to bending about Y-axis

### 10.2.5 CISEOS cross-section geometry for shoulder part test simulations

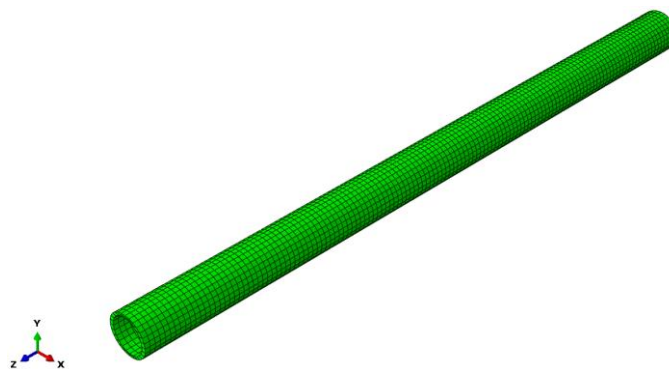


Figure 10.22 Shoulder part with CISEOS cross-section geometry meshed at rest

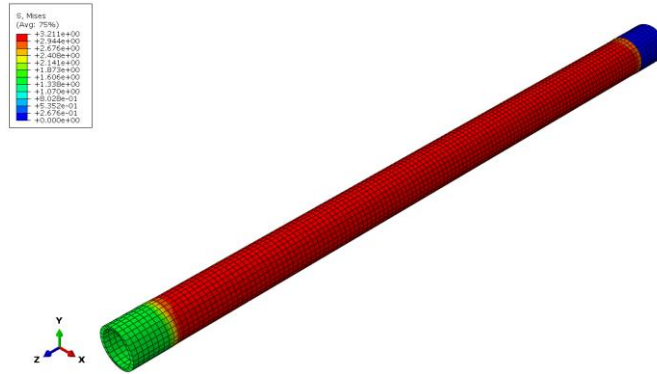


Figure 10.23 Shoulder part with CISEOS cross-section geometry meshed and subjected to tension

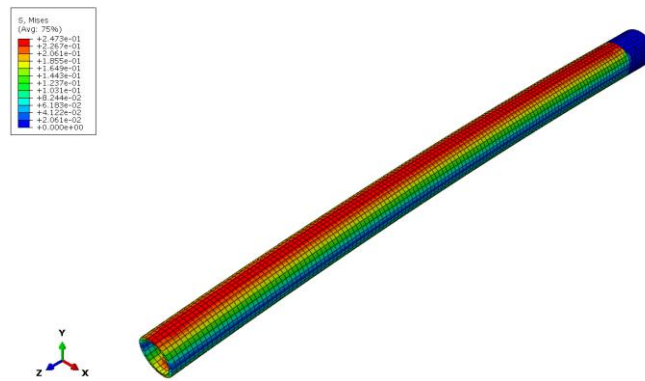


Figure 10.24 Shoulder part with CISEOS cross-section geometry meshed and subjected to bending about X-axis

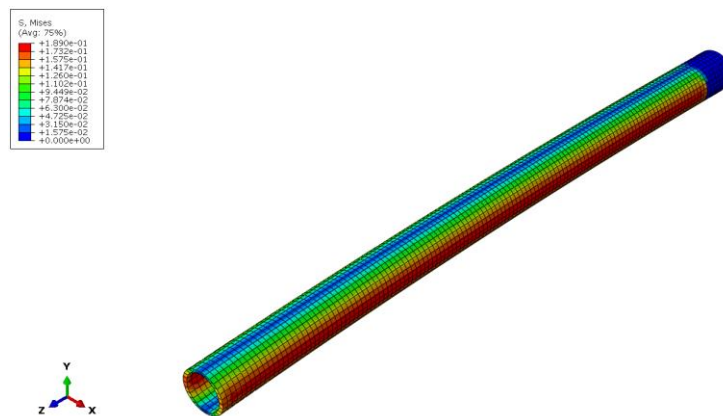


Figure 10.25 Shoulder part with CISEOS cross-section geometry meshed and subjected to bending about Y-axis

## 10.2.6 CISROS cross-section geometry for shoulder part test simulations

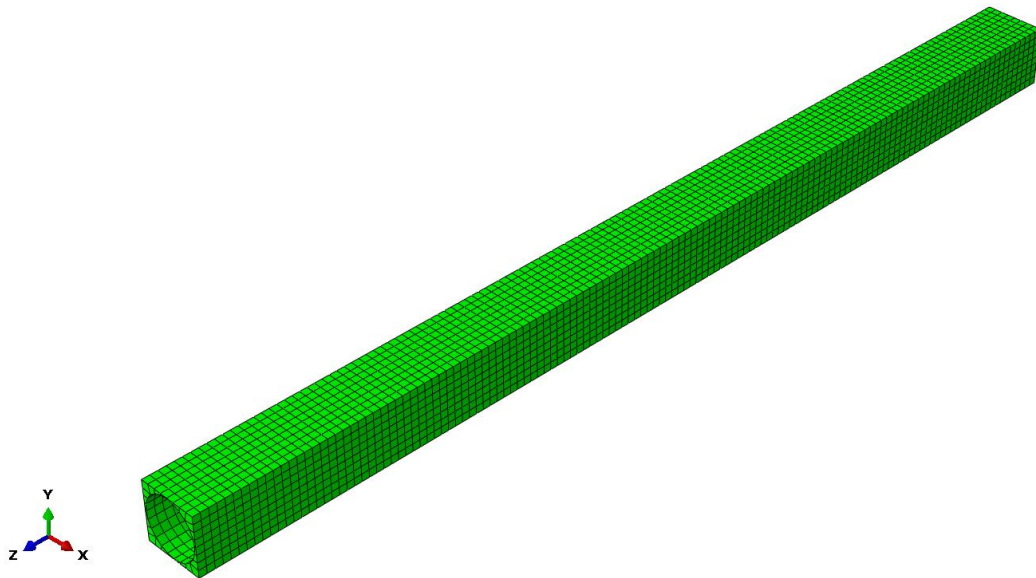


Figure 10.26 Shoulder part with CISROS cross-section geometry meshed at rest

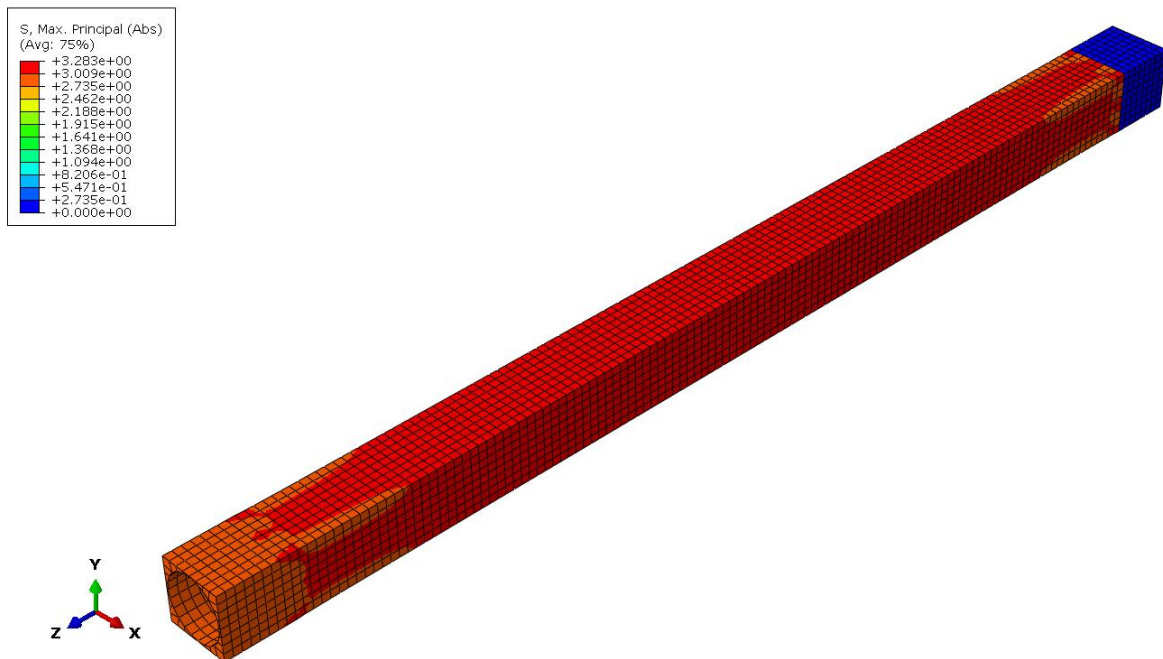


Figure 10.27 Shoulder part with CISROS cross-section geometry meshed and subjected to tension

## 10.2.7 EISROS cross-section geometry for shoulder part test simulations

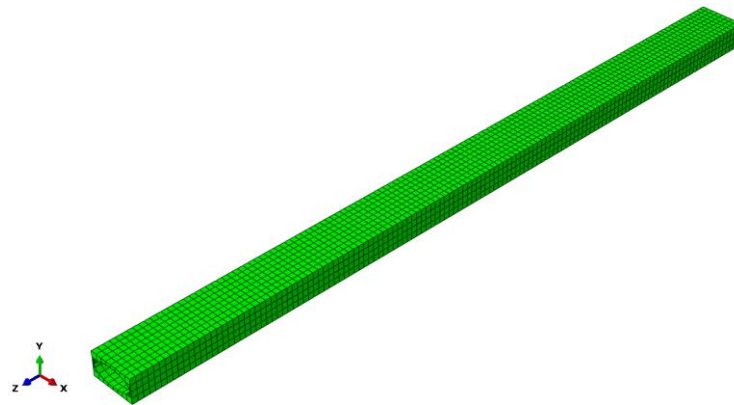


Figure 10.28 Shoulder part with EISROS cross-section geometry meshed at rest

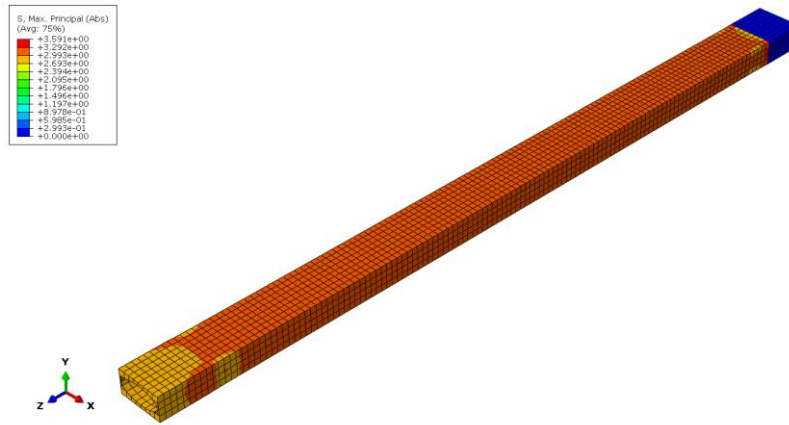


Figure 10.29 Shoulder part with EISROS cross-section geometry meshed and subjected to tension

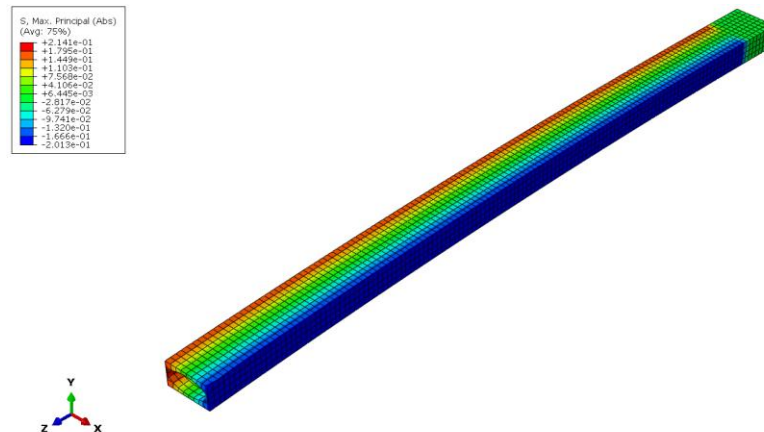


Figure 10.30 Shoulder part with EISROS cross-section geometry meshed and subjected to bending about Y-axis

## 10.3 Test simulation for Forearm part using different cross-section geometries

### 10.3.1 CISCOS cross-section geometry for forearm part test simulations

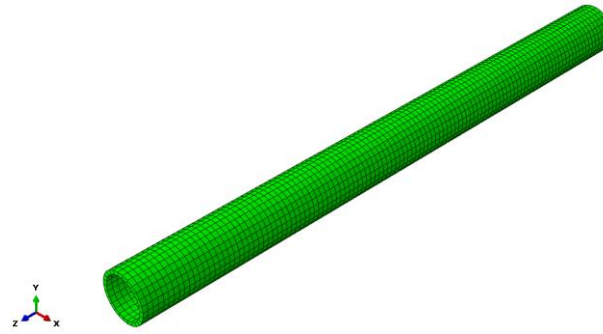


Figure 10.31 Forearm part with CISCOS cross-section geometry meshed at rest

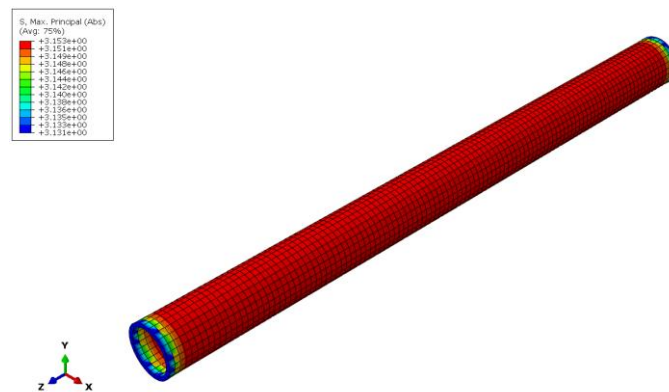


Figure 10.32 Forearm part with CISCOS cross-section geometry meshed and subjected to tension

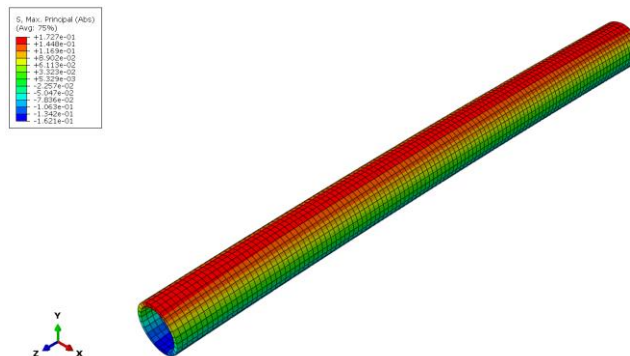


Figure 10.33 Forearm part with CISCOS cross-section geometry meshed and subjected to bending

### 10.3.2 RISROS cross-section geometry for forearm part test simulations

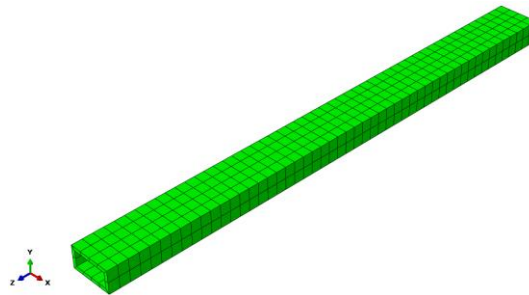


Figure 10.34 Forearm part with RISROS cross-section geometry meshed at rest

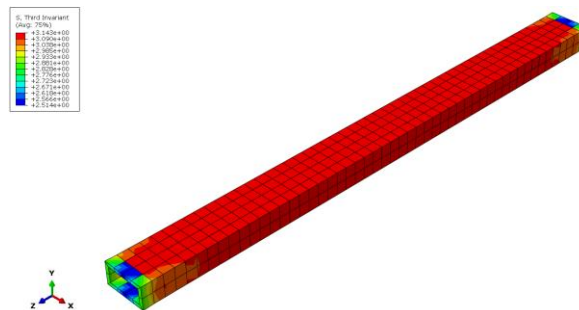


Figure 10.35 Forearm part with RISROS cross-section geometry meshed and subjected to tension

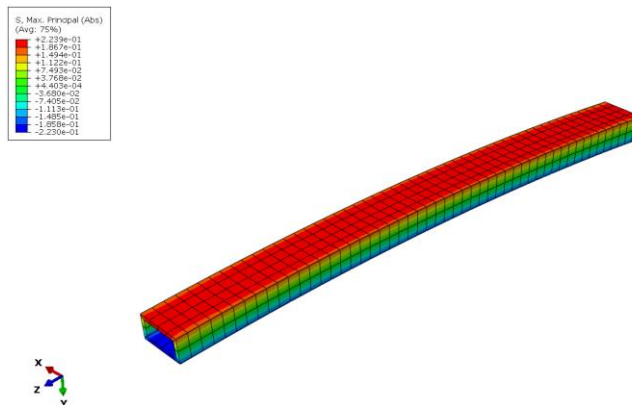


Figure 10.36 Forearm part with RISROS cross-section geometry meshed and subjected to bending about X-axis

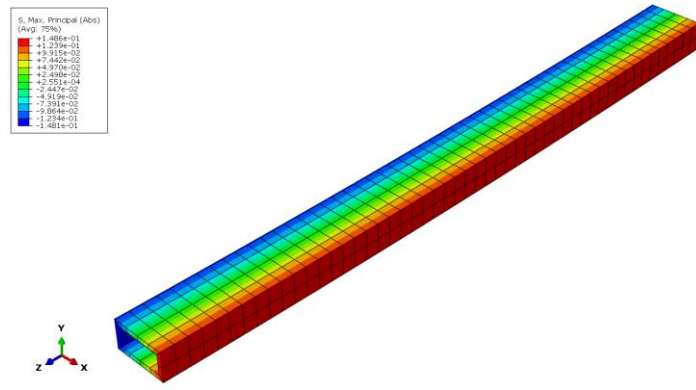


Figure 10.37 Forearm part with RISROS cross-section geometry meshed and subjected to bending about Y-axis

### 10.3.3 EISEOS cross-section geometry for forearm part test simulations

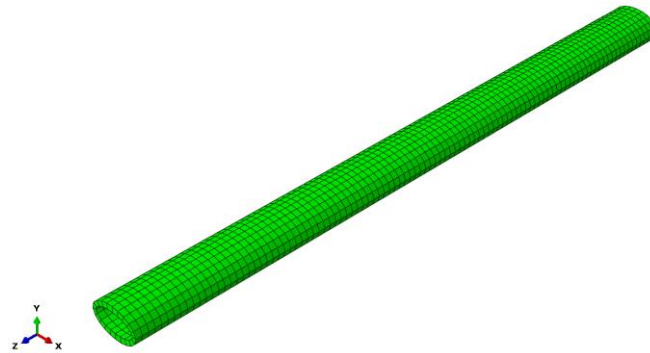


Figure 10.38 Forearm part with EISEOS cross-section geometry meshed at rest



Figure 10.39 Forearm part with EISEOS cross-section geometry meshed and subjected to tension

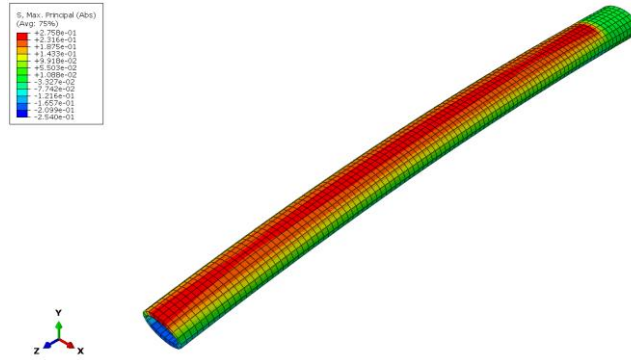


Figure 10.40 Forearm part with EISEOS cross-section geometry meshed and subjected to bending about X-axis

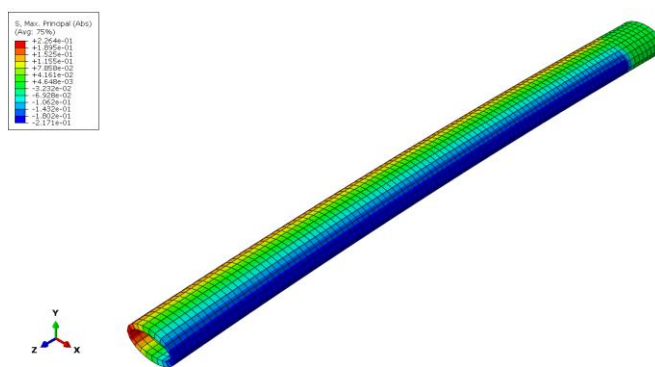


Figure 10.41 Forearm part with EISEOS cross-section geometry meshed and subjected to bending about Y-axis

### 10.3.4 EISCOS cross-section geometry for forearm part test simulations

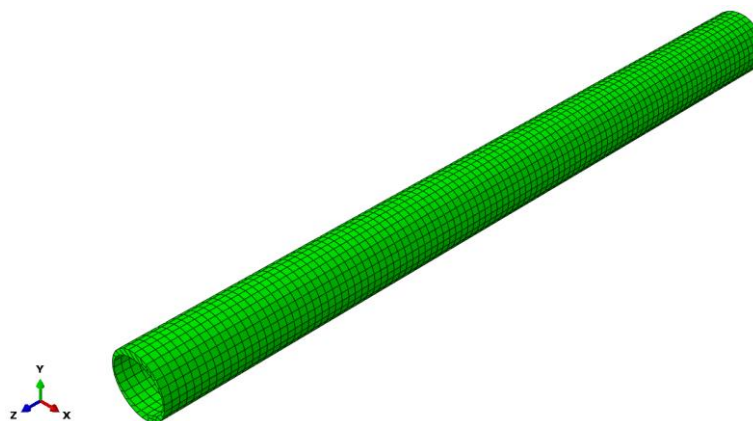


Figure 10.42 Forearm part with EISCOS cross-section geometry meshed at rest

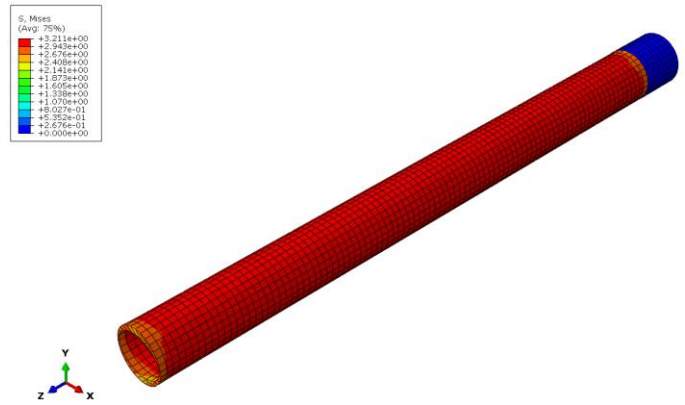


Figure 10.43 Forearm part with EISCOS cross-section geometry meshed and subjected to tension

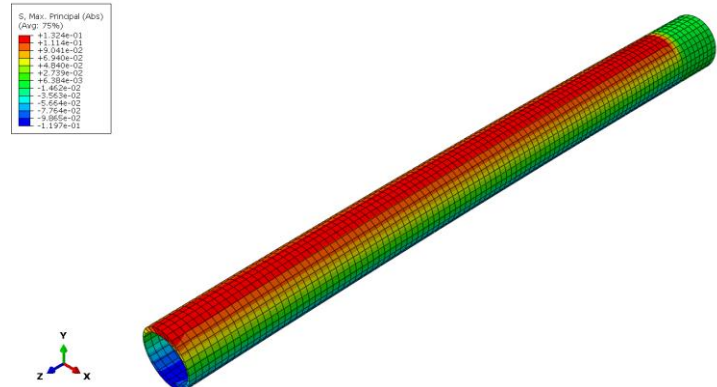
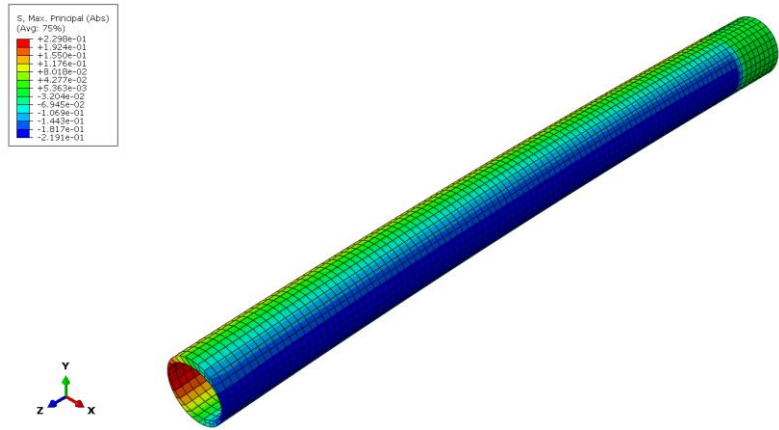


Figure 10.44 Forearm part with EISCOS cross-section geometry meshed and subjected to bending about X-axis



### 10.3.5 CISEOS cross-section geometry for forearm part test simulations

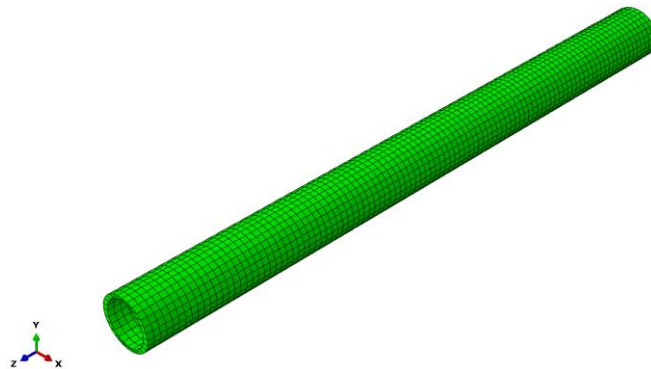


Figure 10.46 Forearm part with CISEOS cross-section geometry meshed at rest

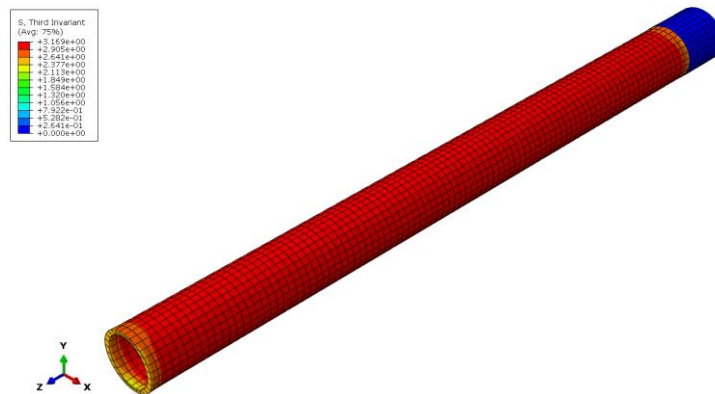


Figure 10.47 Forearm part with CISEOS cross-section geometry meshed and subjected to tension

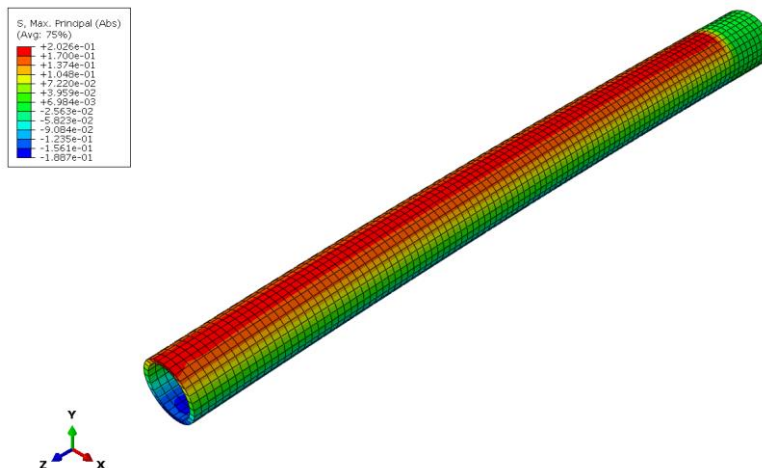


Figure 10.48 Forearm part with CISEOS cross-section geometry meshed and subjected to bending about X-axis

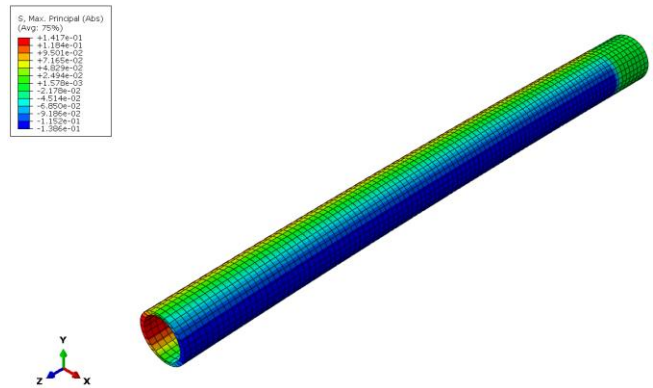


Figure 10.49 Forearm part with CISEOS cross-section geometry meshed and subjected to bending about Y-axis

### 10.3.6 CISROS cross-section geometry for forearm part test simulations

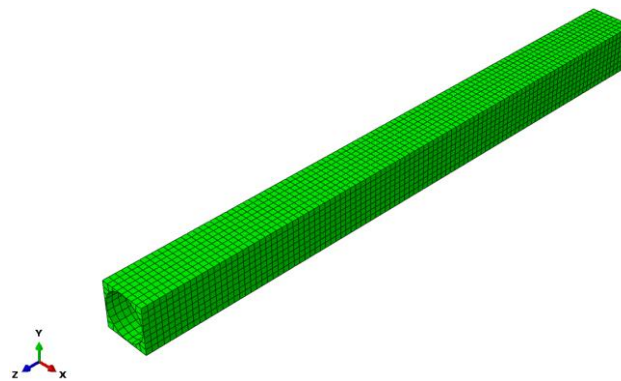


Figure 10.50 Forearm part with CISROS cross-section geometry meshed at rest

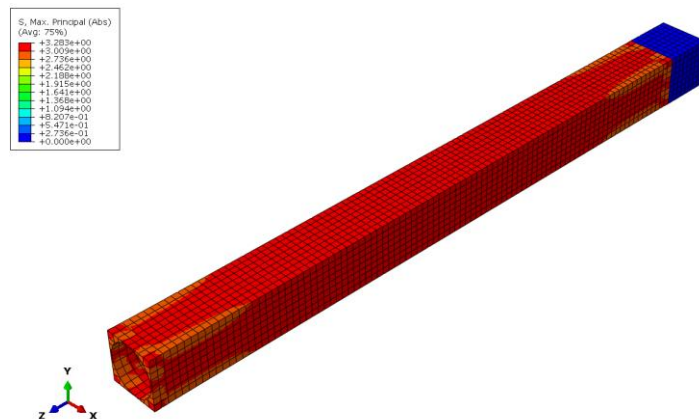


Figure 10.51 Forearm part with CISROS cross-section geometry meshed and subjected to tension

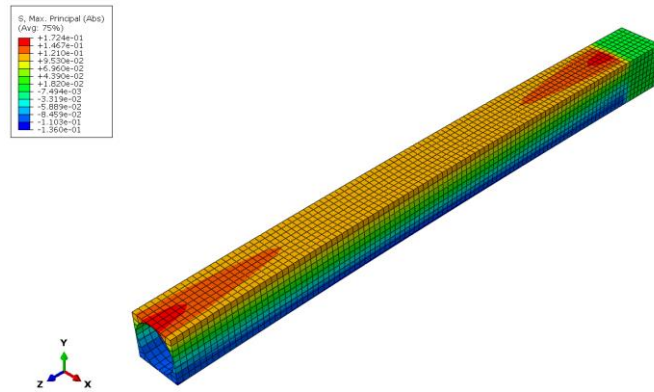


Figure 10.52 Forearm part with CISROS cross-section geometry meshed and subjected to bending about X-axis

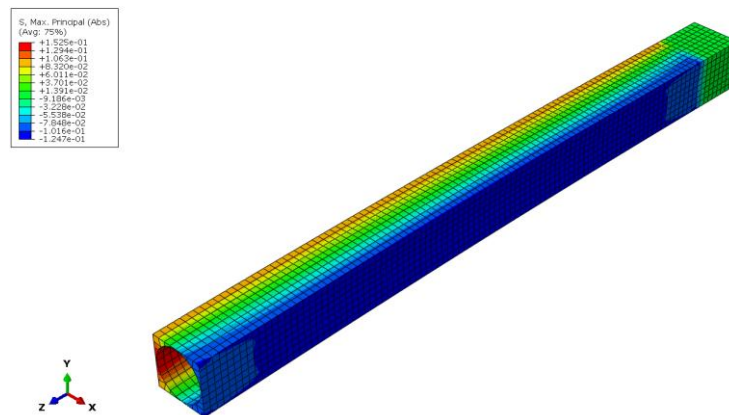


Figure 10.53 Forearm part with CISROS cross-section geometry meshed and subjected to bending about Y-axis

### 10.3.7 EISROS cross-section geometry for forearm part test simulations

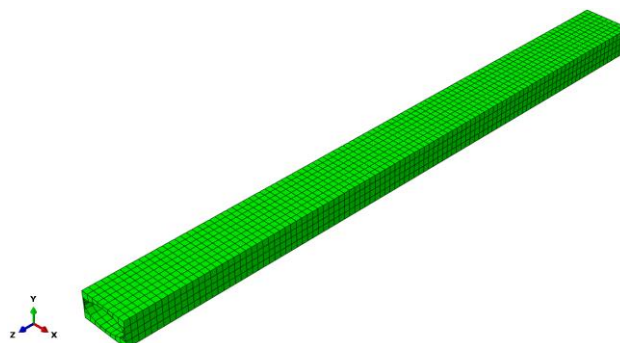


Figure 10.54 Forearm part with EISROS cross-section geometry meshed at rest

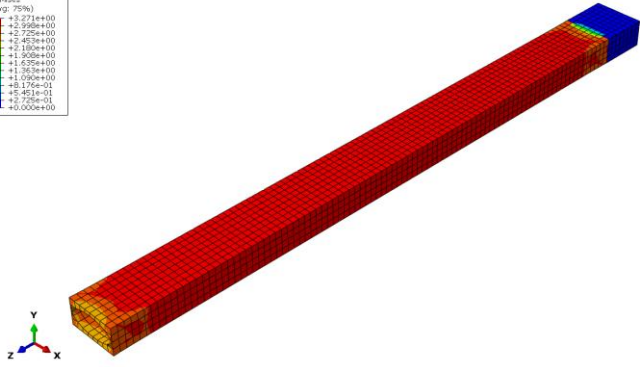
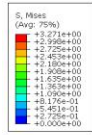


Figure 10.55 Forearm part with EISROS cross-section geometry meshed and subjected to tension

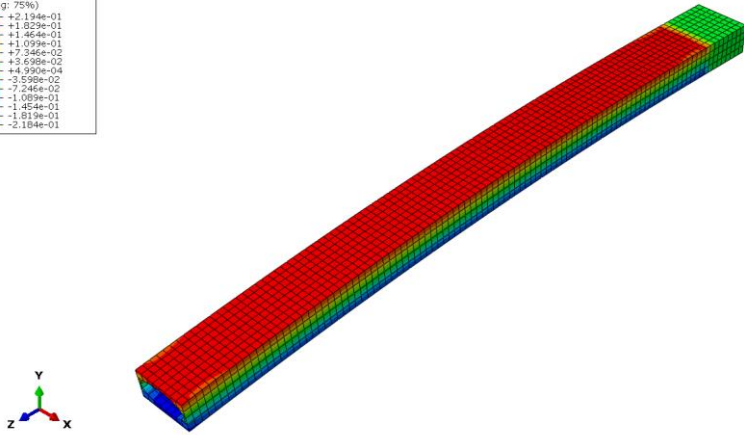
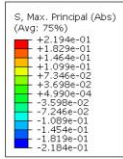


Figure 10.56 Forearm part with EISROS cross-section geometry meshed and subjected to bending about X-axis

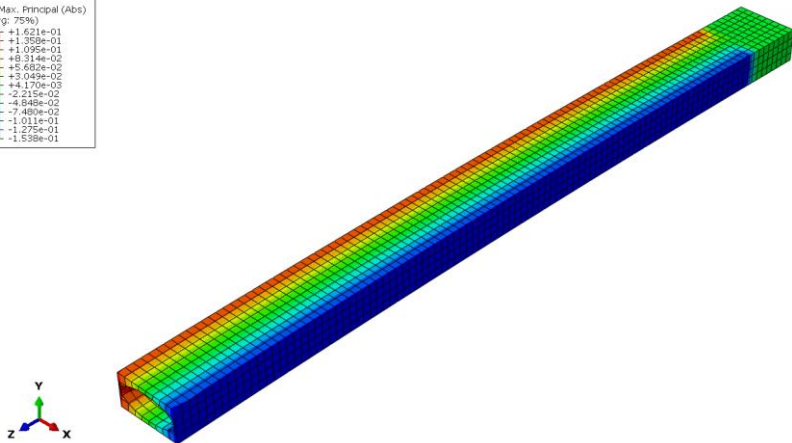
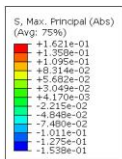


Figure 10.57 Forearm part with EISROS cross-section geometry meshed and subjected to bending about Y-axis

## 10.4 Test simulation for Back to shoulder connector part using different cross-section geometries

### 10.4.1 CISCOS cross-section geometry for Back to shoulder connector part test simulations

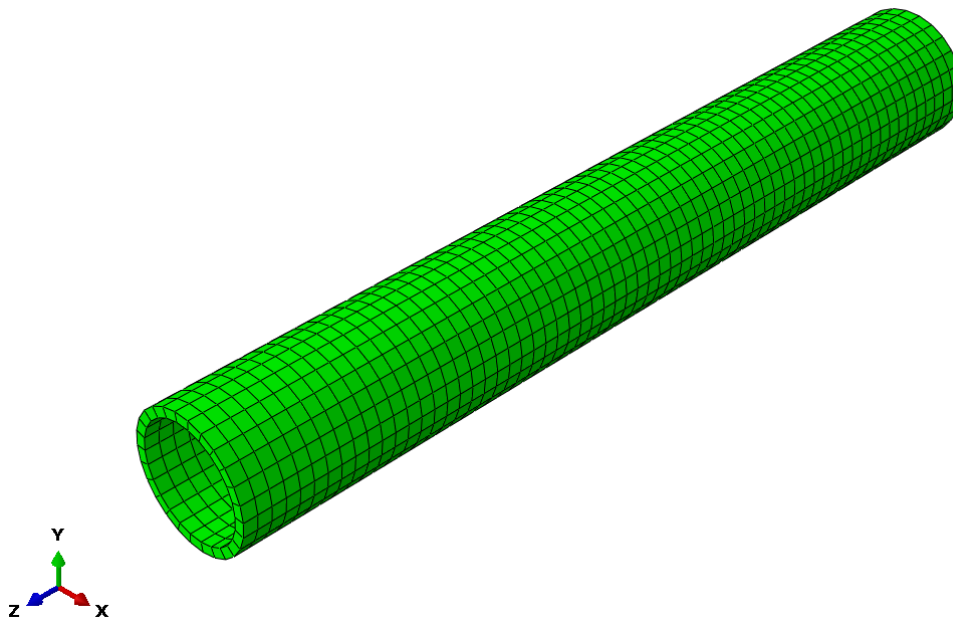


Figure 10.58 Back to shoulder connector part with CISCOS cross-section geometry meshed at rest

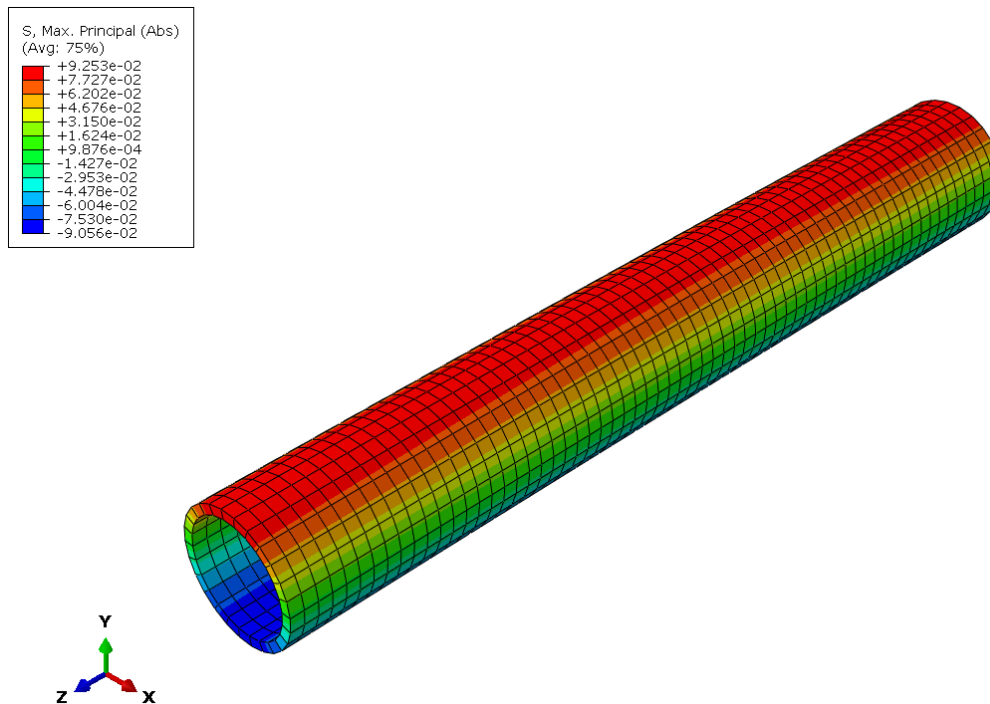


Figure 10.59 Back to shoulder part with CISCOS cross-section geometry meshed and subjected to bending

## 10.4.2 RISROS cross-section geometry for Back to shoulder connector part test simulations

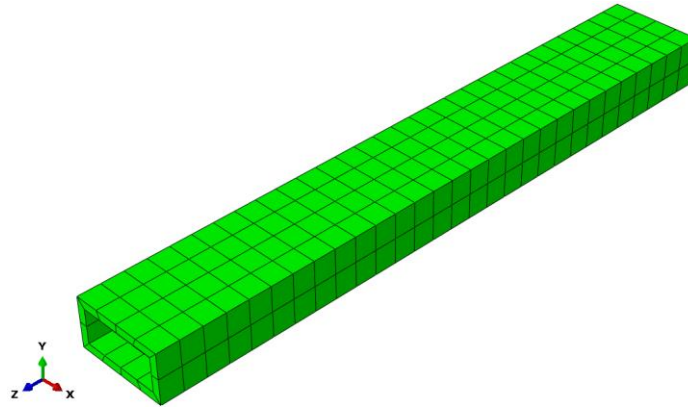


Figure 10.60 Back to shoulder connector part with RISROS cross-section geometry meshed at rest

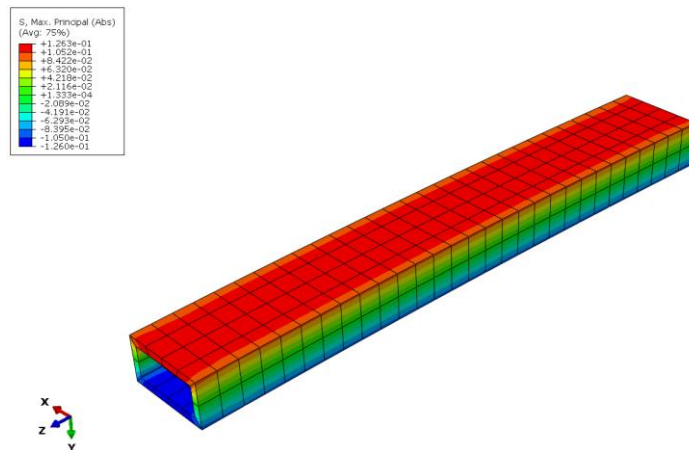


Figure 10.61 Back to shoulder part with RISROS cross-section geometry meshed and subjected to bending about X-axis

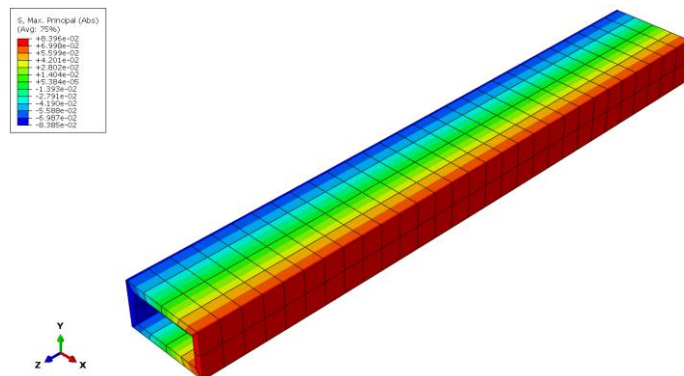


Figure 10.62 Back to shoulder part with RISROS cross-section geometry meshed and subjected to bending about Y-axis

### 10.4.3 EISEOS cross-section geometry for Back to shoulder connector part test simulations

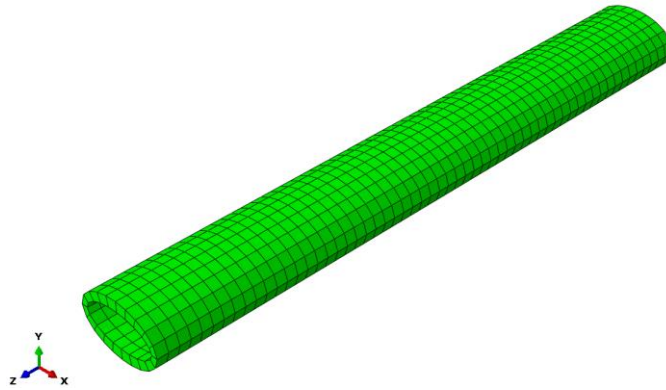


Figure 10.63 Back to shoulder connector part with EISEOS cross-section geometry meshed at rest

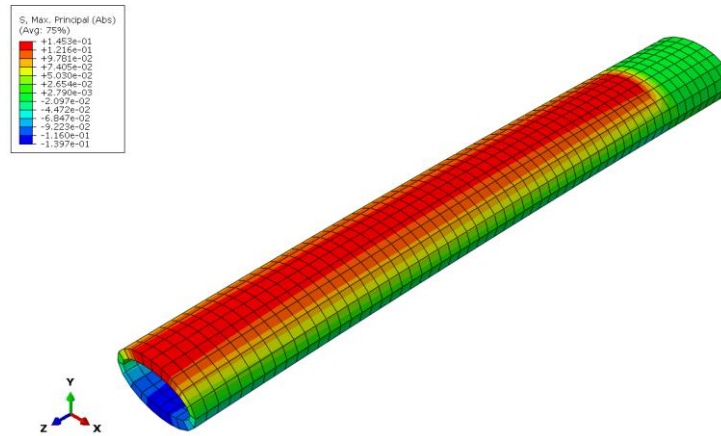


Figure 10.64 Back to shoulder part with EISEOS cross-section geometry meshed and subjected to bending about X-axis

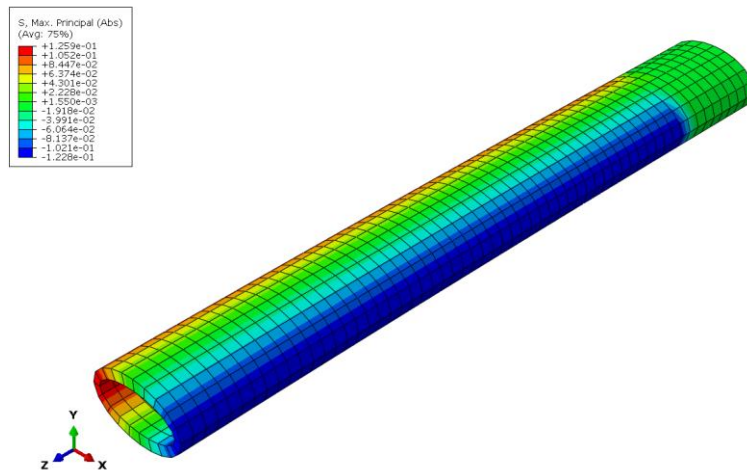


Figure 10.65 Back to shoulder part with EISEOS cross-section geometry meshed and subjected to bending about Y-axis

## 10.4.4 EISCOS cross-section geometry for Back to shoulder connector part test simulations

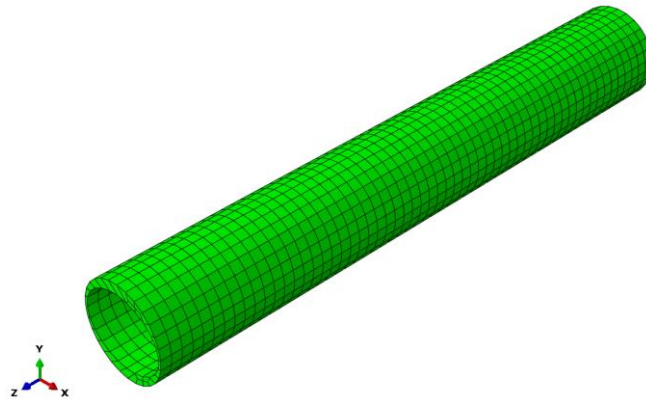


Figure 10.66 Back to shoulder connector part with EISCOS cross-section geometry meshed at rest

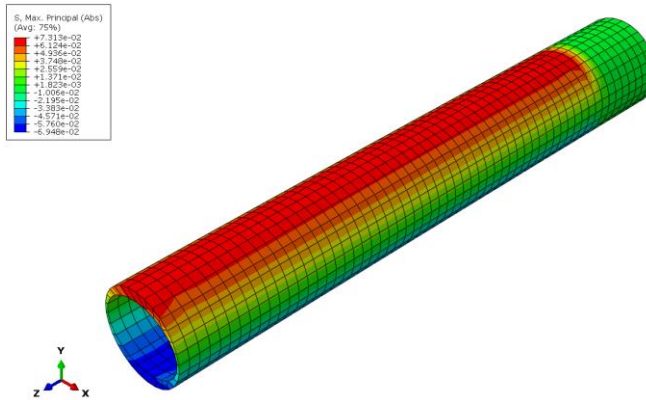


Figure 10.67 Back to shoulder part with EISCOS cross-section geometry meshed and subjected to bending about X-axis

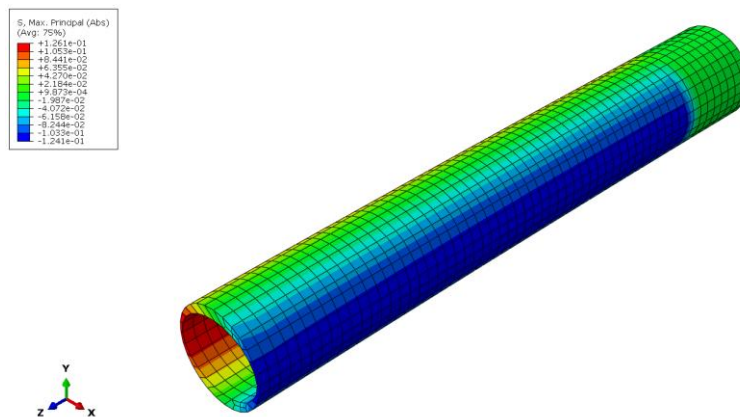


Figure 10.68 Back to shoulder part with EISCOS cross-section geometry meshed and subjected to bending about Y-axis

## 10.4.5 CISEOS cross-section geometry for Back to shoulder connector part test simulations

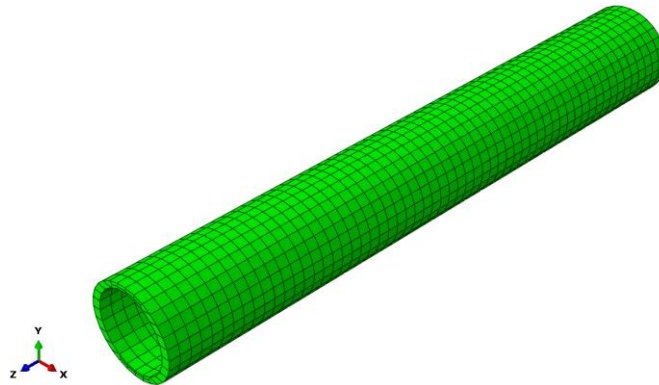


Figure 10.69 Back to shoulder connector part with EISCOS cross-section geometry meshed at rest

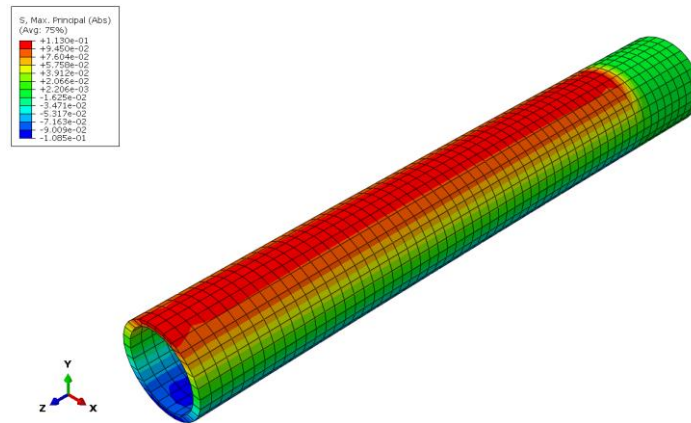


Figure 10.70 Back to shoulder part with EISCOS cross-section geometry meshed and subjected to bending about X-axis

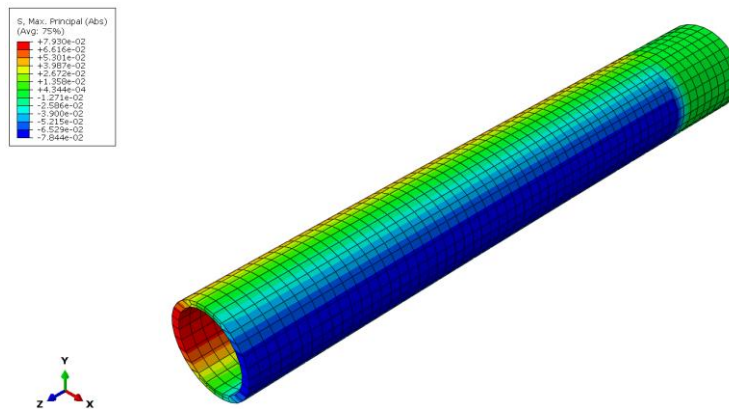


Figure 10.71 Back to shoulder part with EISCOS cross-section geometry meshed and subjected to bending about Y-axis

## 10.4.6 CISROS cross-section geometry for Back to shoulder connector part test simulations

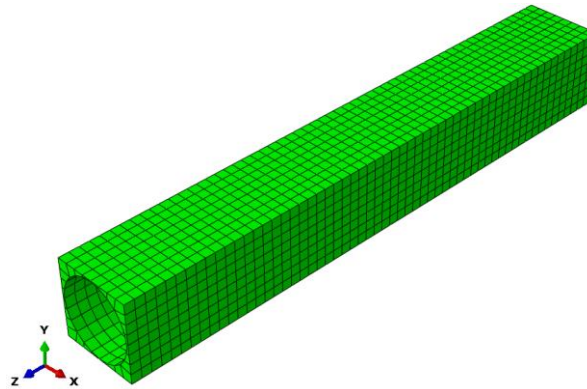


Figure 10.72 Back to shoulder connector part with EISCOS cross-section geometry meshed at rest

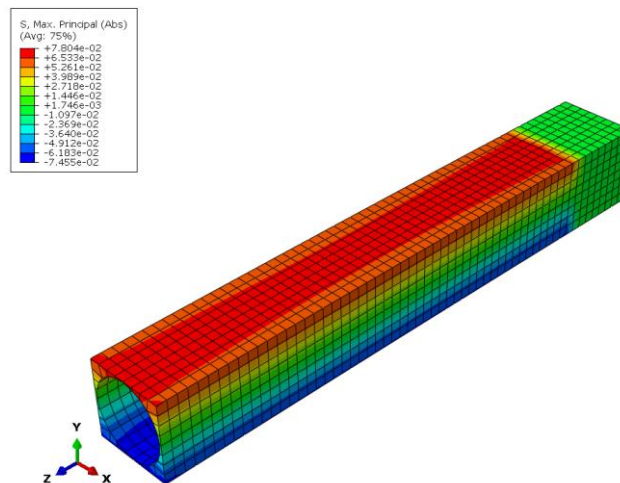


Figure 10.73 Back to shoulder part with EISCOS cross-section geometry meshed and subjected to bending about X-axis

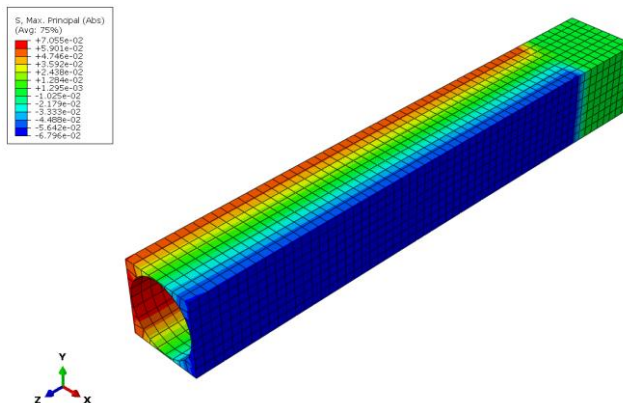


Figure 10.74 Back to shoulder part with EISCOS cross-section geometry meshed and subjected to bending about Y-axis

## 10.4.7 EISROS cross-section geometry for Back to shoulder connector part test simulations

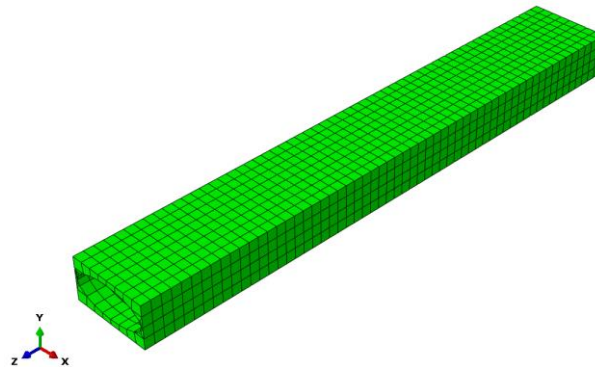


Figure 10.75 Back to shoulder connector part with EISROS cross-section geometry meshed at rest

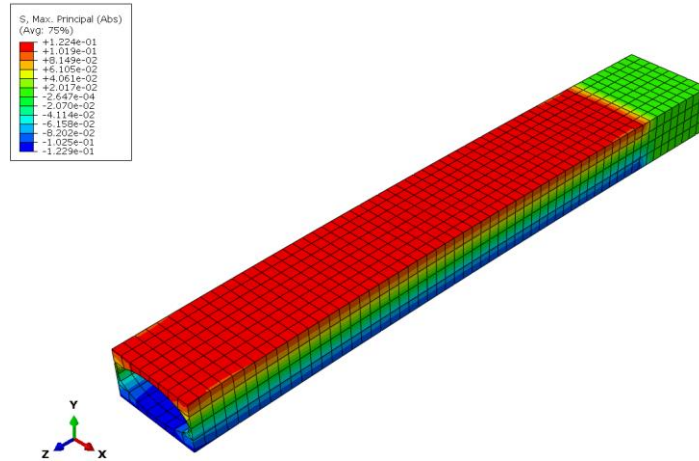


Figure 10.76 Back to shoulder part with EISROS cross-section geometry meshed and subjected to bending about X-axis

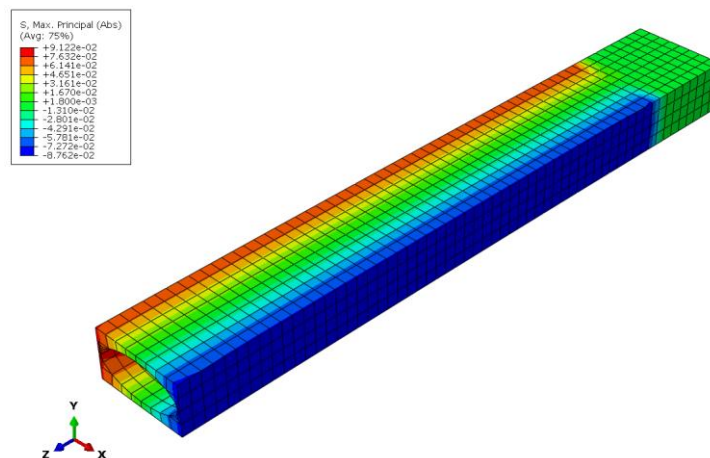


Figure 10.77 Back to shoulder part with EISROS cross-section geometry meshed and subjected to bending about Y-axis

## 10.5 Test simulation for Back part using different cross-section geometries

### 10.5.1 CISCOS cross-section geometry for Back part test simulations

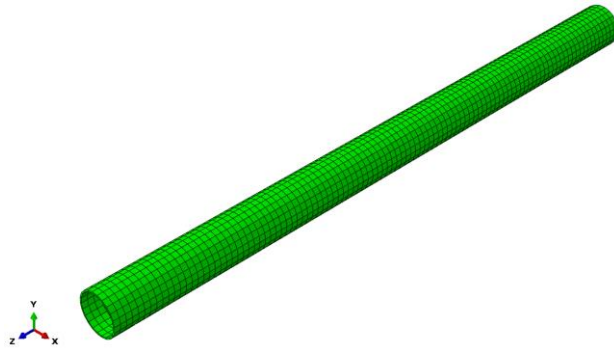


Figure 10.78 Back part with CISCOS cross-section geometry meshed at rest

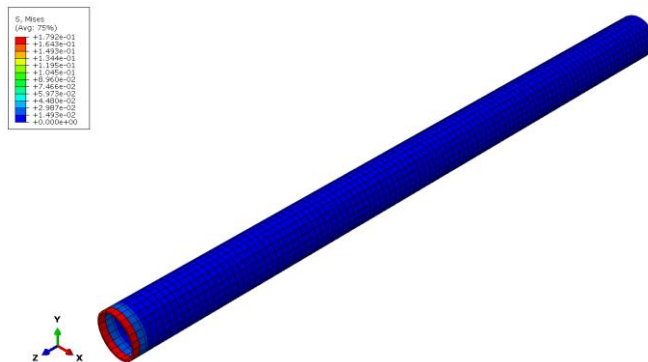


Figure 10.79 Back part with CISCOS cross-section geometry meshed and subjected to compression

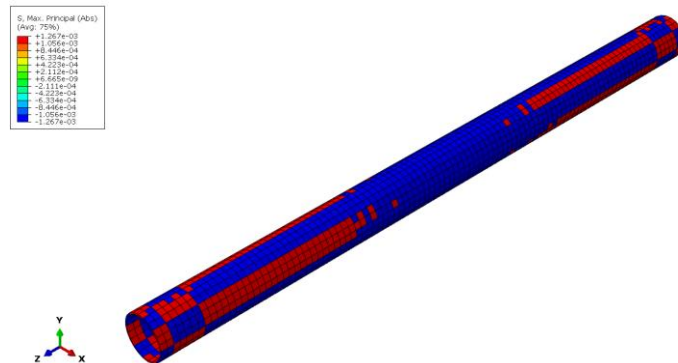


Figure 10.80 Back part with CISCOS cross-section geometry meshed and subjected to torsion

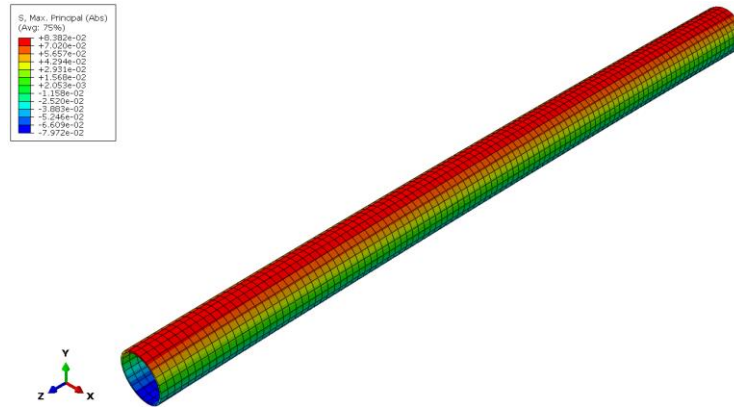


Figure 10.81 Back part with CISCOS cross-section geometry meshed and subjected to bending

## 10.5.2 RISROS cross-section geometry for Back part test simulations

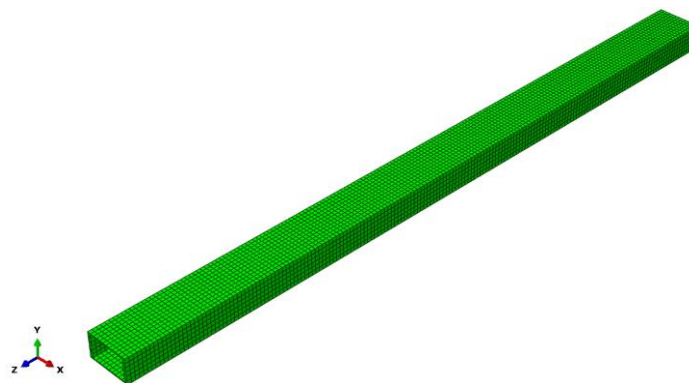


Figure 10.82 Back part with RISROS cross-section geometry meshed at rest

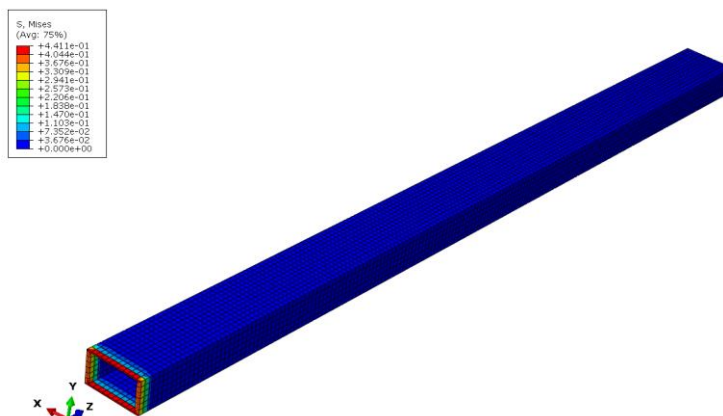


Figure 10.83 Back part with RISROS cross-section geometry meshed and subjected to compression

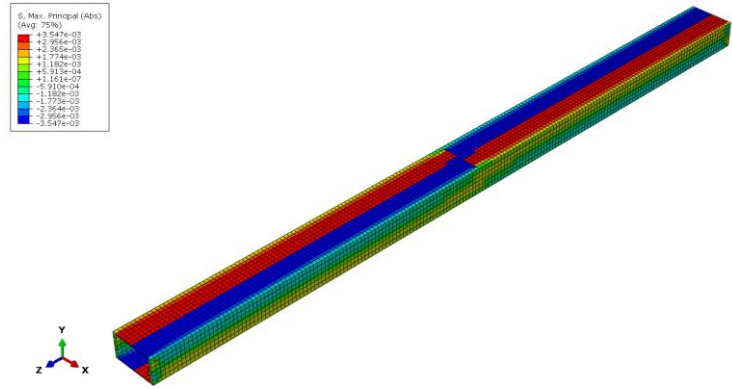


Figure 10.84 Back part with RISROS cross-section geometry meshed and subjected to torsion

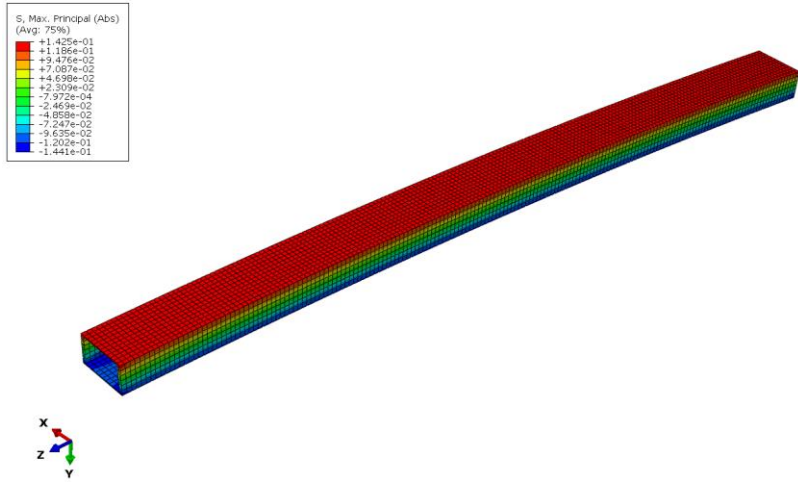


Figure 10.85 Back part with RISROS cross-section geometry meshed and subjected to bending about X-axis

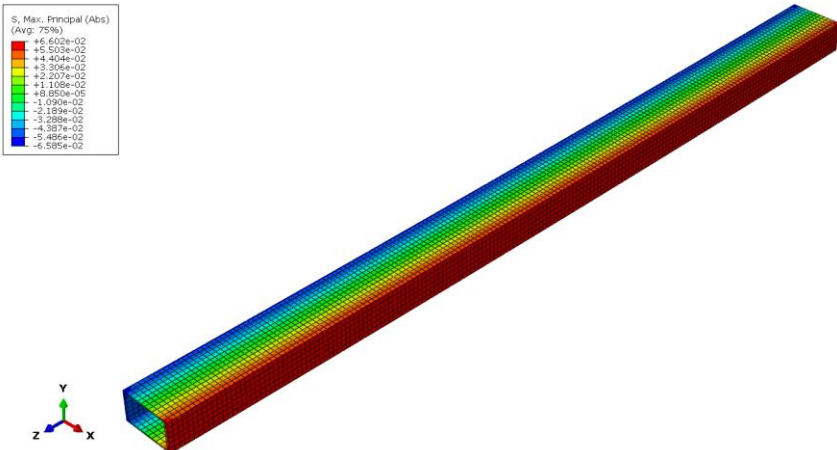


Figure 10.86 Back part with RISROS cross-section geometry meshed and subjected to bending about Y-axis

### 10.5.3 EISEOS cross-section geometry for Back part test simulations

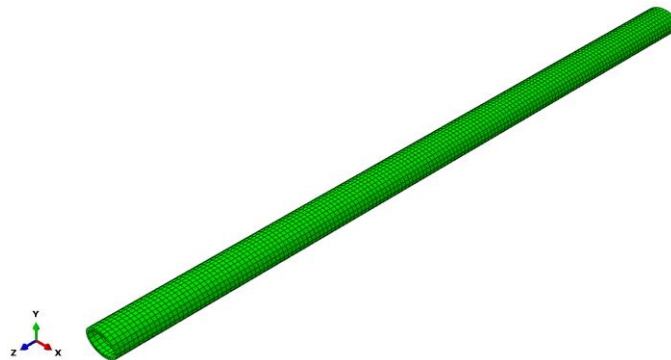


Figure 10.87 Back part with EISEOS cross-section geometry meshed at rest

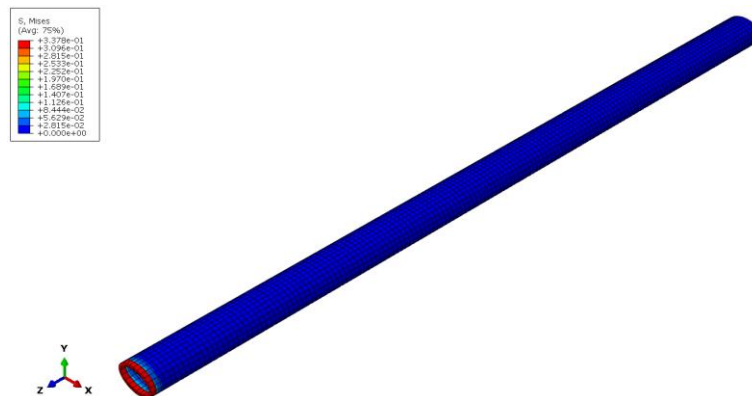


Figure 10.88 Back part with EISEOS cross-section geometry meshed and subjected to compression

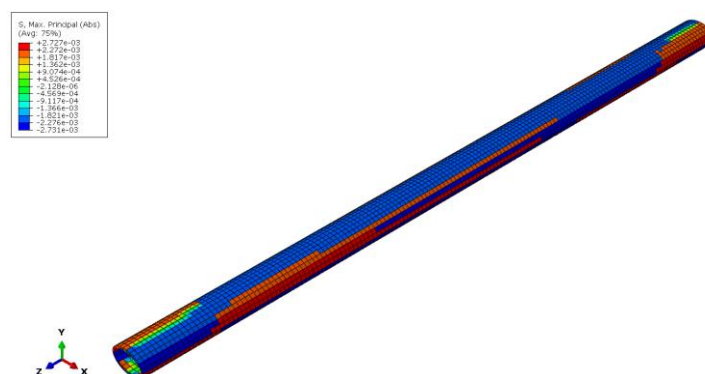


Figure 10.89 Back part with EISEOS cross-section geometry meshed and subjected to torsion

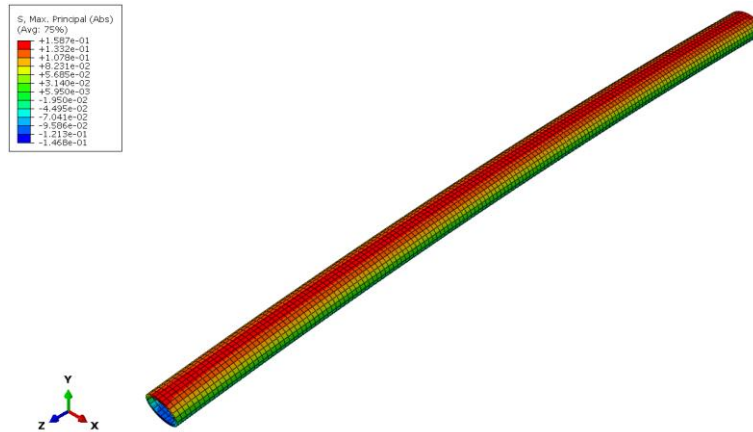


Figure 10.90 Back part with EISEOS cross-section geometry meshed and subjected to bending about X-axis

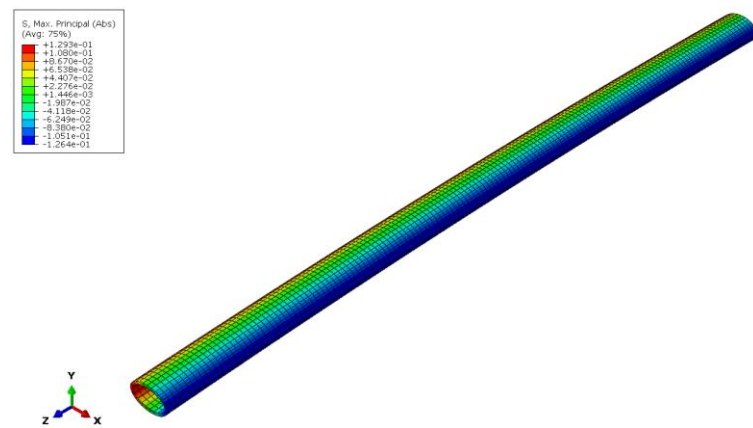


Figure 10.91 Back part with EISEOS cross-section geometry meshed and subjected to bending about Y-axis

### 10.5.4 EISCOS cross-section geometry for Back part test simulations

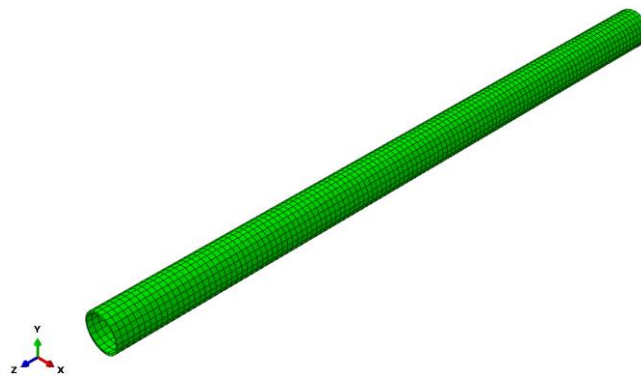


Figure 10.92 Back part with EISCOS cross-section geometry meshed at rest

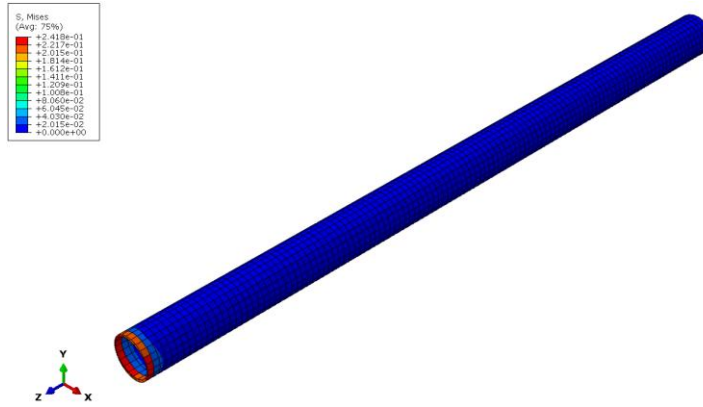


Figure 10.93 Back part with EISCOS cross-section geometry meshed and subjected to compression

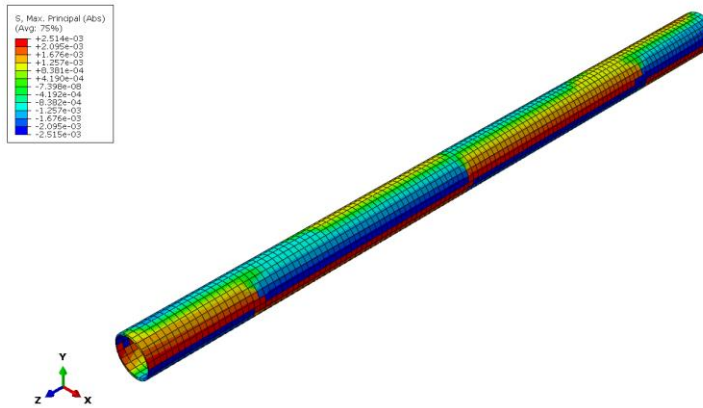


Figure 10.94 Back part with EISCOS cross-section geometry meshed and subjected to torsion

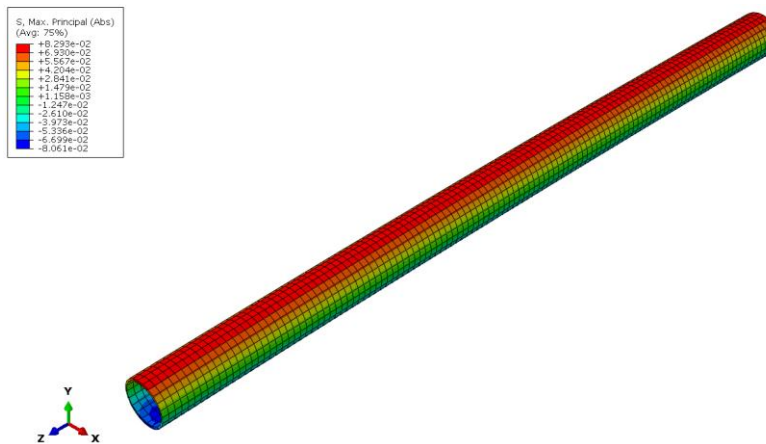


Figure 10.95 Back part with EISCOS cross-section geometry meshed and subjected to bending about X-axis

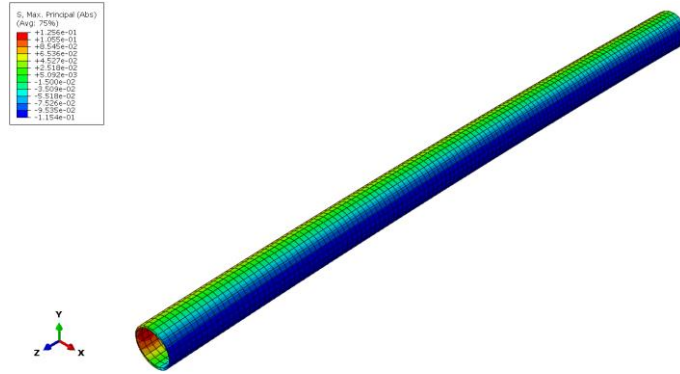


Figure 10.96 Back part with EISCOS cross-section geometry meshed and subjected to bending about Y-axis

### 10.5.5 CISEOS cross-section geometry for Back part test simulations

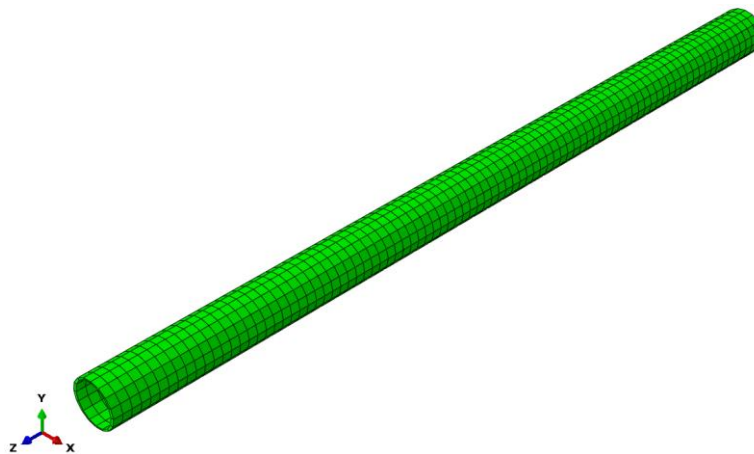


Figure 10.97 Back part with CISEOS cross-section geometry meshed at rest

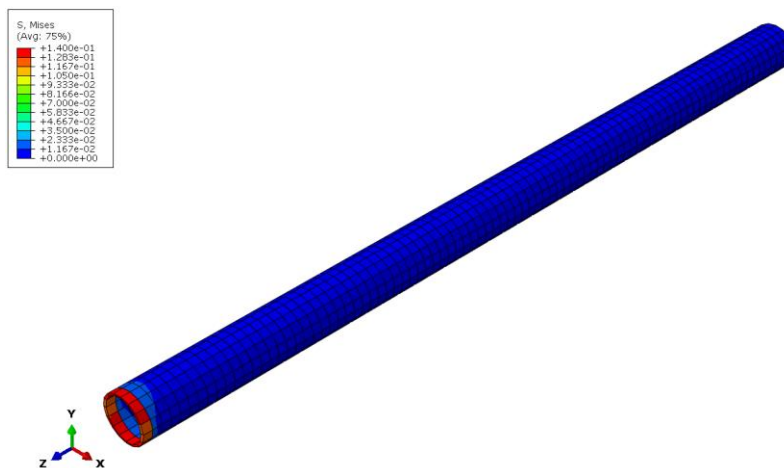


Figure 10.98 Back part with CISEOS cross-section geometry meshed and subjected to compression

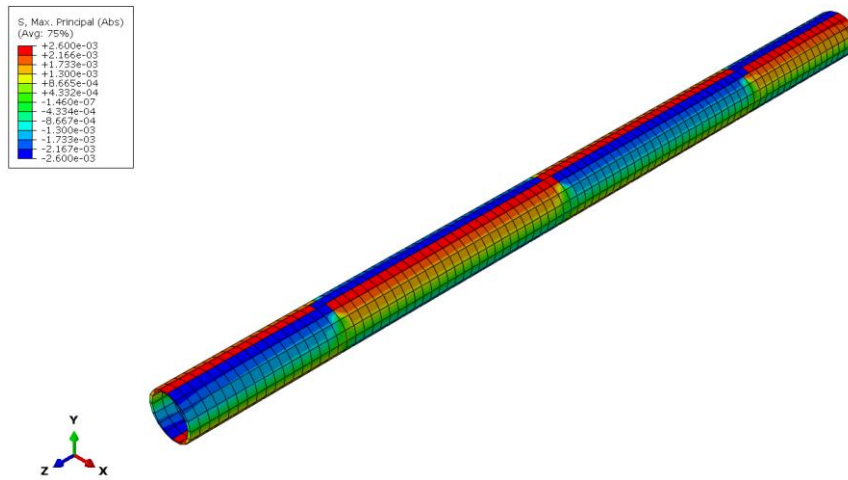


Figure 10.99 Back part with CISEOS cross-section geometry meshed and subjected to torsion

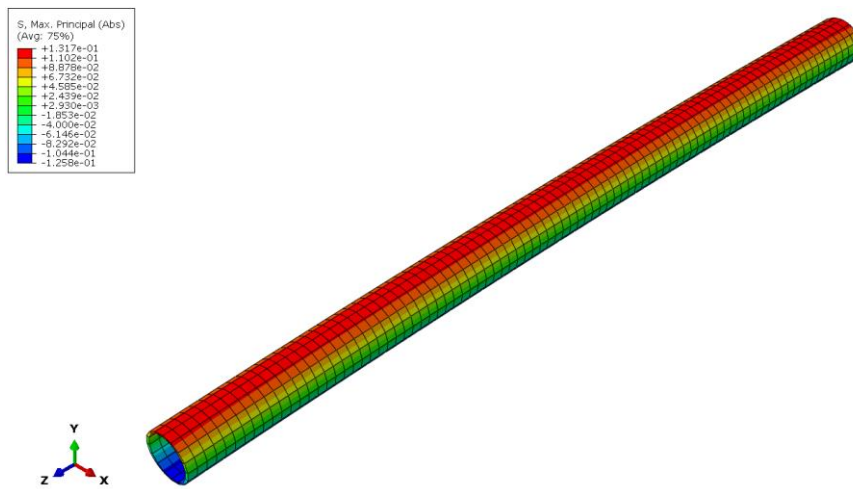


Figure 10.100 Back part with CISEOS cross-section geometry meshed and subjected to bending about X-axis

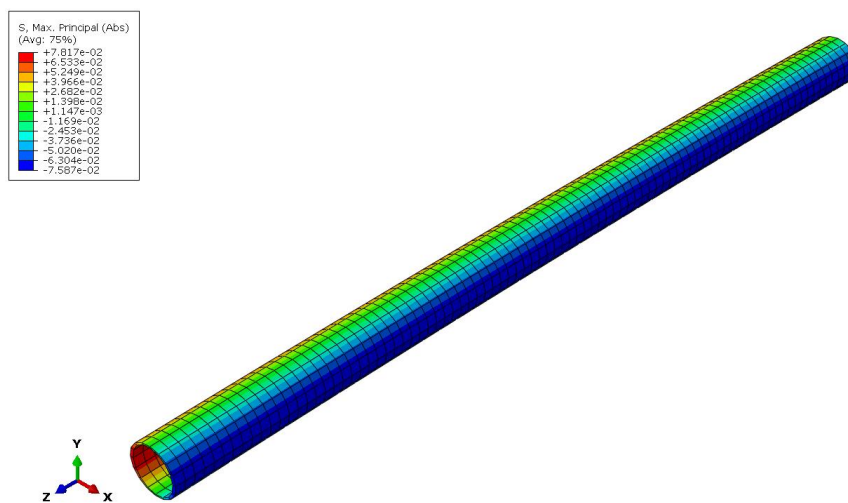


Figure 10.101 Back part with CISEOS cross-section geometry meshed and subjected to bending about Y-axis

## 10.5.6 EISROS cross-section geometry for Back part test simulations

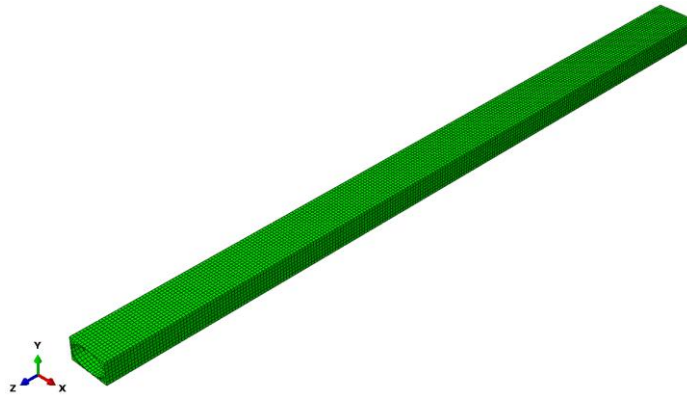


Figure 10.102 Back part with EISROS cross-section geometry meshed at rest

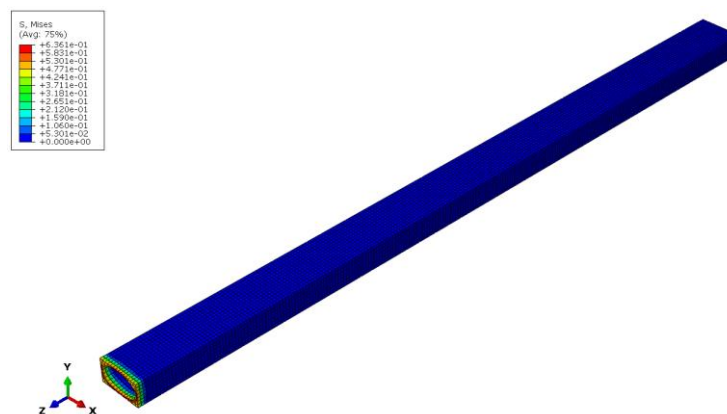


Figure 10.103 Back part with EISROS cross-section geometry meshed and subjected to compression

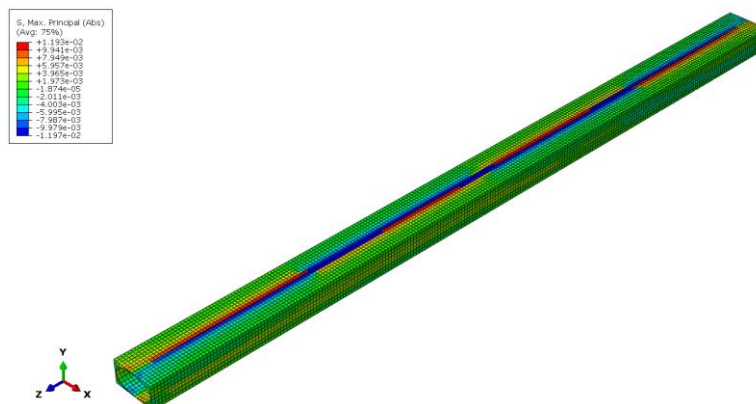


Figure 10.104 Back part with EISROS cross-section geometry meshed and subjected to torsion

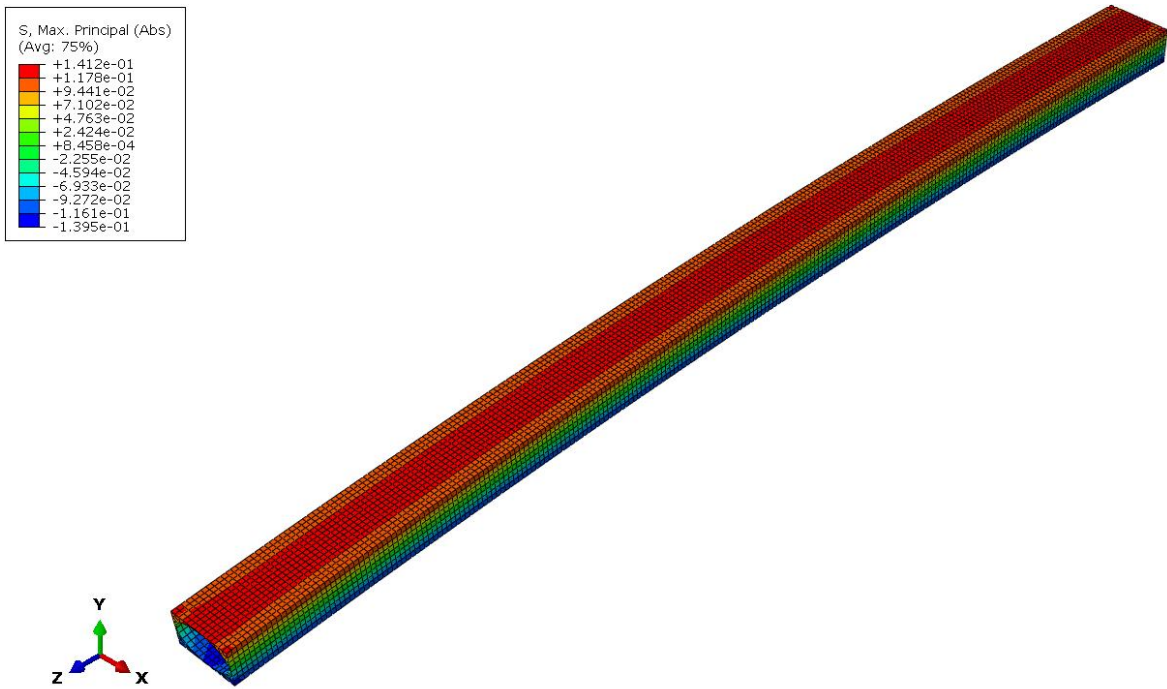


Figure 10.105 Back part with EISROS cross-section geometry meshed and subjected to bending about X-axis

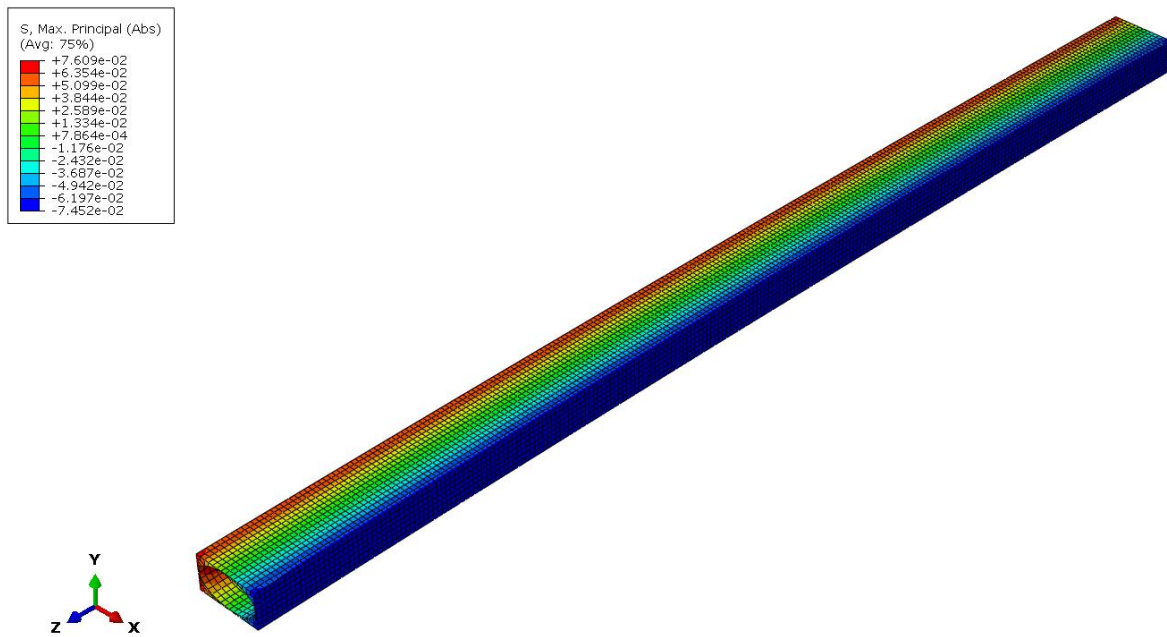


Figure 10.106 Back part with EISROS cross-section geometry meshed and subjected to bending about Y-axis

## **GRAPHICAL MATERIAL**

# METHODOLOGY OF CROSS-SECTION SELECTION OF UPPER LIMB EXOSKELETON FOR INDUSTRY APPLICATIONS

VÄLISSKELETI ÜLAJÄSEME TÖÖSTUSES KASUTAMISEKS RISTLÕIGE VAILMISE MEETODIKA

## Problem statement

- The cross-section of existing upper-body exoskeletons in the market is not the best for all conditions
- There is lack of defined methodology of the best mechanically behaving upper body exoskeleton for industry applications
- There is a lack of knowledge about the best mechanical method to test the exoskeleton parts durability

## Objective

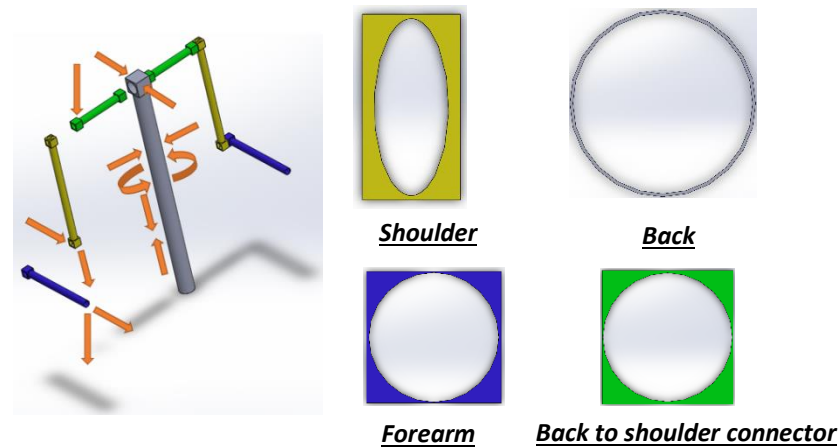
To define the methodology of selection of the parts of the upper body exoskeletons, so it will be used on commercial level with better durability

## Conclusions

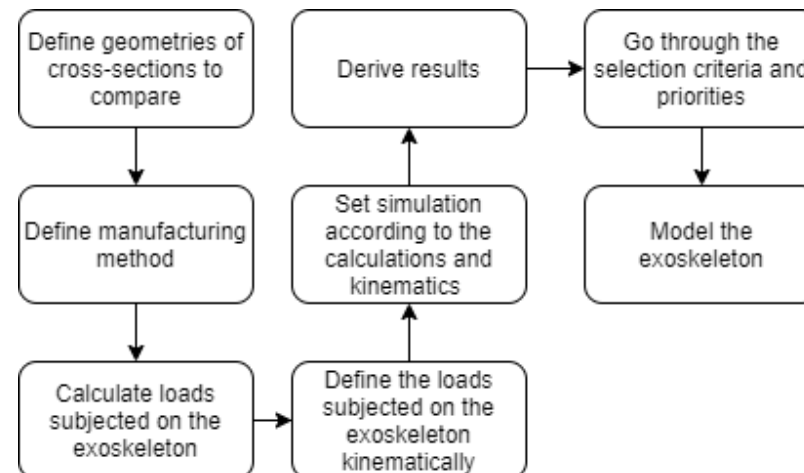
- Best cross-sections are as shown in graphical representation for a generic model.
- The methodology is successful to find better mechanically behaving cross-sections



## Graphical representation of results



## Methodology of selection



## Process Description

After following the methodology of selection, a model has been created as generic model, then the simulations have been done according to the estimated motion of the exoskeleton. For FEA simulation, Abaqus software tool was used to make the study, then the modeling of the generic model was created on SOLIDWORKS. Each part has been simulated with the shown kinematics independently, so FEA simulation would be a simulation of mechanical testing of each part.

## Results

In this generic case, the results showed that the recent market existing exoskeletons are presumably not using the best cross-section geometries for the part, as the results showed that the CISCOS (Circular Inner Shape and Circular Outer Shape) is not always the best recommendation for the part's geometry. A mix of circular, elliptical, or rectangular shapes as shown in the graphical representation of results can be the best mechanically behaving cross-sections.

